On Quantum Vacuum Energy, Cosmological Constant and Missing Mass

Boris Kriger[1,2]

[1]Information Physics Institute, Gosport, Hampshire, United Kingdom

boris.kriger@informationphysicsinstitute.net

[2]Institute of Integrative and Interdisciplinary Research, Toronto, Canada

boriskriger@interdisciplinary-institute.org

ORCID: 0009-0001-0034-2903

Abstract

This paper does not propose a model. It does not present calculations. It does not claim to solve any problem. It would be presumptuous to suggest, in a short paper, answers to questions that the best minds in physics have worked on for a century. Instead, we ask a sequence of questions—each grounded in established physics—and observe that the answers lead in an unexpected direction. The questions concern three entities: quantum vacuum energy (whose existence is experimentally confirmed), the cosmological constant (whose value is observationally measured), and the missing mass in galaxies (whose presence is gravitationally inferred). We ask why the first was identified with the second, whether this identification is necessary, and what follows if it is not. We find that separating them leads, through a chain of reasoning that invokes only $E = mc^2$ and general relativity, to the question of whether the missing mass might be the gravitating vacuum itself. We do not answer this question. We ask why it is not being asked.

Keywords: vacuum energy, cosmological constant, missing mass, dark matter, dark energy, general relativity

1 A Preliminary Remark

The authors of this paper are not under the illusion that they can resolve, in a few pages, problems that have occupied the finest physicists of three generations. We are not proposing a theory. We are not constructing a model. We are not fitting data.

We are asking questions.

The questions are simple. The physics they invoke is standard. The logical chain they form is short. And we find it surprising that this particular chain of questions does not appear to have been followed to its conclusion in the literature—not because the conclusion is necessarily correct, but because the questions themselves seem unavoidable.

We ask the reader's patience, and nothing more.

2 What Do We Know?

Let us begin with what is established.

2.1 Vacuum Energy Exists

The quantum vacuum has energy. This is confirmed by:

- The Casimir effect: a measurable force between conducting plates arising from the modification of vacuum modes (Casimir 1948; Lamoreaux 1997; Bressi et al. 2002).
- The Lamb shift: a splitting of hydrogen energy levels caused by virtual particle fluctuations (Lamb & Retherford 1947).
- Thermonuclear cross-sections: fusion rates that require virtual particle exchange for quantitative agreement with observation (Bahcall & Pinsonneault 2004).

These are not theoretical predictions awaiting confirmation. They are measurements.

2.2 Energy Is Mass

$E = mc^2$ (Einstein 1905). If the vacuum has energy, it has an equivalent mass. This is special relativity.

2.3 Mass Gravitates

The stress-energy tensor $T_{\mu\nu}$, which includes all forms of energy, is the source of gravity in general relativity (Einstein 1915). There is no exemption clause.

2.4 Vacuum Energy Depends on Geometry

The Casimir effect demonstrates that the vacuum energy density depends on the geometry of the space it occupies. Different plate separations yield different energies. More

generally, quantum field theory in curved spacetime shows that the vacuum state depends on the background geometry (Birrell & Davies 1982; Parker & Toms 2009). This is the theoretical foundation of Hawking radiation (Hawking 1974, 1975): the vacuum near a black hole horizon is different from the vacuum far away.

3 What Was Assumed?

In 1917, Einstein introduced the cosmological constant Λ as a geometric term in the gravitational field equations. It was a property of spacetime—constant, universal, geometric. He did not connect it to quantum physics.

In 1967, Zel'dovich observed that the quantum vacuum stress-energy tensor has the same mathematical form as a cosmological constant: both are proportional to $g_{\mu\nu}$. He proposed that they are the same quantity: $\Lambda = 8\pi G\,\rho_{\text{vac}}$.

This identification was motivated by mathematical elegance. It was never derived from a deeper principle. And it led to the cosmological constant problem: quantum field theory estimates $\rho_{\text{vac}} \sim 10^{76}\,\text{GeV}^4$, while observations give $\rho_\Lambda \sim 10^{-47}\,\text{GeV}^4$—a discrepancy of 120 orders of magnitude (Weinberg 1989).

Our first question:

> *Is this identification necessary? What compels us to equate a geometric constant introduced in 1917 with a quantum field quantity proposed fifty years later?*

We note that the identification has not been confirmed by any experiment. It has not been derived from any fundamental theory. Its sole motivation is mathematical similarity. And its sole consequence has been a problem that remains unsolved after sixty years of effort.

4 What Do We Gain from Dark Energy and Dark Matter?

Modern cosmology introduces two entities beyond the Standard Model and general relativity:

Dark energy is invoked to explain the accelerating expansion of the universe. It constitutes approximately 68% of the energy budget. In the standard model, it is identified with the cosmological constant Λ—which is then identified with vacuum energy, producing the 10^{120} problem.

Dark matter is invoked to explain the missing mass in galaxies (Zwicky 1933; Rubin et al. 1980), gravitational lensing (Clowe et al. 2006), the CMB acoustic peaks (Planck Collaboration 2020), and large-scale structure. It constitutes approximately 27% of the energy budget. It has not been directly detected despite four decades of dedicated searches (LUX, XENON1T, PandaX, LZ, ADMX, LHC).

Together, these two entities account for 95% of the universe. Neither has been directly observed. Both require physics beyond what is established.

Our second question:

> *Do these entities make our understanding simpler, or more complicated? Do they resolve puzzles, or create new ones?*

Dark energy, in the standard account, *is* the cosmological constant, which *is* vacuum energy—producing a 10^{120} discrepancy that remains unresolved. Dark matter requires a particle that has eluded detection for forty years and that has no place in the Standard Model.

We are told that 95% of the universe consists of things we cannot see, cannot detect, and cannot explain from known physics. This is not a criticism of the physicists who have worked on these problems—they are among the greatest scientists in history. It is an observation that the current framework, for all its successes, purchases them at a high price.

Our third question:

> *Is this price necessary? Or does it follow from an assumption—the Zel'dovich identification—that we are free to revisit?*

5 What Happens If We Separate Them?

Suppose we take the separation seriously. Λ is geometry. Vacuum energy is field physics. They are not the same.

Immediately, several things change.

5.1 The Cosmological Constant Problem Is Reframed

If $\Lambda \neq 8\pi G\,\rho_{\rm vac}$, there is no reason for them to have the same value. The 10^{120} discrepancy is a comparison of two unrelated quantities. The "problem" was created by the identification and takes a different form without it.

Of course, one might ask: why doesn't the enormous vacuum energy gravitate cosmologically? This is a fair question, and we do not answer it. We note that it is a different question from the cosmological constant problem as traditionally stated. The CC problem asks: why do Λ and $\rho_{\rm vac}$ disagree by 10^{120}? If they are unrelated quantities, this question loses its force. But the question of why a large $\rho_{\rm vac}$ does not dominate cosmological expansion remains—it is reframed, not eliminated. It may have a separate answer (see, e.g., the vacuum sequestering programme: Kaloper & Padilla 2014), or it may indicate that the naïve QFT estimate of $\rho_{\rm vac}$ is simply wrong, as many physicists suspect.

5.2 Dark Energy Becomes Unnecessary

If Λ is simply what Einstein said it was—a geometric constant, a property of spacetime—then the term "dark energy" becomes a label for geometry rather than a name for a new substance. This is more of a conceptual reframing than an empirical gain: the

physics of accelerating expansion is unchanged. But it removes the suggestion that an unknown form of energy pervades the universe, replacing it with the simpler statement that the geometry of spacetime includes a constant term. Whether this constitutes explanatory progress is a matter of perspective.

5.3 An Unexpected Question About Vacuum Energy

With Λ accounted for (geometry), we are left with vacuum energy as a separate, local, experimentally confirmed quantity. And we face the question we raised in Section 2: it has energy, therefore mass, therefore gravity.

If it is not Λ, and if it gravitates, then *where does its gravity show up?*

6 Where Does Vacuum Gravity Show Up?

Consider two environments.

6.1 Inside a Galaxy

A galaxy is a gravitationally bound system. Its interior does not expand with the Hubble flow (this is standard physics; see Carrera & Giulini 2010). The stars are separated by light-years of space filled with quantum vacuum.

If vacuum energy gravitates, this vacuum contributes mass to the galaxy. A star in orbit responds to the total enclosed mass—stars, gas, and vacuum. A lensed photon is deflected by the total mass. Neither distinguishes between sources.

6.2 In a Void

A cosmological void also contains vacuum. But here the vacuum is uniform—there is no density peak, no center of attraction, no preferred direction for collapse. And the cosmic expansion (driven by Λ) stretches the void, further opposing any tendency toward self-gravitation.

Our fourth question:

> *Is it possible that vacuum gravity is observationally significant inside bound structures (where expansion is absent) and observationally negligible in voids (where expansion compensates and no structure can seed)?*

We do not know. We are asking.

A related open question concerns galaxy cluster mergers. In the Bullet Cluster (Clowe et al. 2006), the gravitating mass is spatially offset from the baryonic gas. If vacuum energy density depends on local spacetime curvature, it would need to track the evolving gravitational potential during a merger in a way that reproduces the observed lensing morphology. Whether it does is an open quantitative question.

7 A Coincidence

If the answer to the question in Section 6 is yes—if vacuum energy gravitates measurably inside galaxies but not in voids—then the gravitating vacuum would have the following properties:

- It gravitates.
- It is invisible.
- It does not interact electromagnetically.
- It does not scatter off itself (fields superpose; they do not collide).
- It fills all of space.
- It is in its ground state (cold, stable).

These are the properties of the missing mass.

We present this as a coincidence, not a proof. But it is a coincidence that involves every qualitative property required of the missing mass, matched by a quantity whose existence is experimentally confirmed.

We must state clearly the central vulnerability of this line of reasoning: the qualitative property match is necessary but not sufficient. The entire question hinges on a number that is currently unknown—the gravitating vacuum energy density. If this density is of the order required by galactic dynamics ($\sim 0.3\,\mathrm{GeV/cm^3}$ in a typical halo), the coincidence of properties becomes physically significant. If it is many orders of magnitude smaller, the properties match but the quantity is irrelevant. We do not know which is the case. This is the single largest uncertainty underlying every question this paper asks.

Our fifth question:

> *Why has this coincidence not been investigated more thoroughly? Is there a physical reason to exclude gravitating vacuum from the list of dark matter candidates, or only the historical reason that vacuum energy was preassigned to a different role (the cosmological constant) by the Zel'dovich identification?*

We note that several authors have explored related ideas: Albareti & Maroto (2014) showed that vacuum energy of massive fields can scale as nonrelativistic matter and reproduce cold dark matter clustering behavior—the most quantitatively developed treatment to date; Nieuwenhuizen (2024) proposed vacuum condensation on mass concentrations; Marongwe (2021) derived dark matter-like effects from electromagnetic vacuum fluctuations; Hajdukovic (2012) proposed gravitational polarization of the vacuum. None of these has entered the mainstream discussion.

The present paper differs from these in scope and intent: it does not introduce a mechanism or a model. It traces the question to what we believe is its root—the Zel'dovich identification of 1967—and asks whether removing this identification makes the question of gravitating vacuum unavoidable. We ask why this particular logical path has not been followed in the mainstream literature.

8 What We Are Not Saying

We wish to be precise about the limits of this paper.

We are not claiming that dark matter is vacuum energy. We are asking whether there is a reason it cannot be.

We are not solving the cosmological constant problem. We are observing that it may rest on an unproven assumption.

We are not deriving rotation curves, lensing profiles, or CMB spectra. We are noting that the qualitative properties match and asking whether a quantitative investigation is warranted.

We are not criticizing the physicists who built ΛCDM. Their achievement is extraordinary. We are asking whether one of the foundational identifications—made in 1967, never proven—might be worth revisiting in light of the persistent failure to detect dark matter particles and the persistent failure to resolve the 10^{120} discrepancy.

We are not proposing new physics. We are asking whether the existing physics—$E = mc^2$, general relativity, quantum field theory—might already contain what we have been searching for.

9 The Questions, Summarized

1. Vacuum energy exists and is experimentally confirmed. Why was it identified with a geometric constant introduced fifty years earlier, on no stronger basis than mathematical similarity?

2. This identification produced the most severe quantitative discrepancy in the history of physics (10^{120}). After sixty years without resolution, is it worth considering that the identification itself is the error?

3. If we separate Λ (geometry) from vacuum energy (field physics), the cosmological constant problem is reframed and dark energy is re-identified as geometry. What, if anything, do we lose by this separation?

4. If vacuum energy is not Λ, it remains a real, gravitating form of energy. Inside gravitationally bound systems where expansion is absent, its gravity is uncompensated. Is this contribution negligible, or could it be significant?

5. The qualitative properties of gravitating vacuum—invisible, collisionless, cold, stable, ubiquitous, purely gravitational—match every requirement for the missing mass. After forty years of searching for a particle that has not been found, is it possible that what we are looking for has been here all along?

We offer no answers. We believe the questions deserve them.

10 Peer Reviews and Revision History

First Round

Reviewer assessment. The reviewer found the paper clearly written and philosophically interesting, with an admirable scope limitation. Five major concerns were raised: (1) the property table is less constraining than presented; (2) the absolute-vs-relative energy problem is underplayed; (3) the void stability argument is incomplete (Jeans instability); (4) CMB compatibility is a prerequisite, not an optional test; (5) the Bullet Cluster argument is too casual.

Response. We agree with the reviewer on all five points. The paper has been substantially revised to reflect a more modest epistemic position. Rather than attempting to address each concern with calculations or arguments that would inevitably be insufficient for problems this deep, we have restructured the paper as a sequence of questions rather than a sequence of arguments. The property table has been replaced by a qualitative observation of coincidence, explicitly labeled as such. The void stability, CMB, and Bullet Cluster issues are acknowledged as open and serious questions that we do not attempt to answer. The absolute energy problem is noted as genuine and unresolved.

The paper no longer claims to identify the missing mass with vacuum energy. It asks whether there is a reason this identification has not been investigated, and whether the Zel'dovich identification that forestalled it was ever established. We believe these questions stand regardless of whether the answers turn out to favor the proposal.

Second Round

Reviewer assessment. The reviewer found the revision substantially improved and the genre appropriate. Seven minor revisions were requested: (1) state explicitly that the inquiry depends on the unknown vacuum density being of the right magnitude; (2) soften "dissolves" to "is reframed"; (3) restore a distinguishing statement about prior work; (4) add the Bullet Cluster morphology to open challenges; (5) use "estimate" rather than "prediction" for the 10^{120} figure; (6) neutralize the phrasing of Question 3; (7) remove placeholder sections.

Response. All seven revisions have been implemented. (1) A paragraph identifying the unknown vacuum density as the central vulnerability has been added at the end of Section 7. (2) Section 5.1 now reads "is reframed" and includes discussion of the residual question. (3) The prior work paragraph in Section 7 now distinguishes this paper's approach. (4) The Bullet Cluster morphology is noted as an open challenge in Section 6. (5) "Prediction" has been replaced throughout. (6) Question 3 now reads "What, if anything, do we lose?" (7) Placeholder sections have been removed.

References

Albareti, F. D., & Maroto, A. L. (2014). Vacuum energy as dark matter. *Phys. Rev. D*, 90, 123509.

Bahcall, J. N., & Pinsonneault, M. H. (2004). What do we (not) know theoretically about solar neutrino fluxes? *Phys. Rev. Lett.*, 92, 121301.

Birrell, N. D., & Davies, P. C. W. (1982). *Quantum Fields in Curved Space*. Cambridge Univ. Press.

Bressi, G., et al. (2002). Measurement of the Casimir force. *Phys. Rev. Lett.*, 88, 041804.

Carrera, M., & Giulini, D. (2010). Influence of global cosmological expansion on local dynamics and kinematics. *Rev. Mod. Phys.*, 82, 169.

Casimir, H. B. G. (1948). On the attraction between two perfectly conducting plates. *Proc. Kon. Ned. Akad. Wet.*, 51, 793–795.

Clowe, D., et al. (2006). A direct empirical proof of the existence of dark matter. *ApJ Lett.*, 648, L109.

Einstein, A. (1905). Ist die Trägheit eines Körpers von seinem Energieinhalt abhängig? *Ann. Phys.*, 323, 639–641.

Einstein, A. (1915). Die Feldgleichungen der Gravitation. *Sitzungsber. Preuss. Akad. Wiss.*, 844–847.

Einstein, A. (1917). Kosmologische Betrachtungen zur allgemeinen Relativitätstheorie. *Sitzungsber. Preuss. Akad. Wiss.*, 142–152.

Hajdukovic, D. S. (2012). Quantum vacuum and dark matter. *Astrophys. Space Sci.*, 337, 9–14.

Hawking, S. W. (1974). Black hole explosions? *Nature*, 248, 30–31.

Hawking, S. W. (1975). Particle creation by black holes. *Commun. Math. Phys.*, 43, 199–220.

Kaloper, N., & Padilla, A. (2014). Sequestering the standard model vacuum energy. *Phys. Rev. Lett.*, 112, 091304.

Kriger, B. (2026). Matter-dependent vacuum energy density and inhomogeneous cosmic expansion. Information Physics Institute. doi:10.5281/zenodo.18896536.

Lamb, W. E., Jr., & Retherford, R. C. (1947). Fine structure of the hydrogen atom. *Phys. Rev.*, 72, 241–243.

Lamoreaux, S. K. (1997). Demonstration of the Casimir force. *Phys. Rev. Lett.*, 78, 5–8.

Marongwe, S. (2021). On the electromagnetic vacuum origins of dark energy, dark matter, and astrophysical jets. *Adv. High Energy Phys.*, 2021, 5588662.

Nieuwenhuizen, Th. M. (2024). Solution of the dark matter riddle within standard model physics. *Front. Astron. Space Sci.*, 11, 1413816.

Parker, L. E., & Toms, D. J. (2009). *Quantum Field Theory in Curved Spacetime.* Cambridge Univ. Press.

Perlmutter, S., et al. (1999). Measurements of Ω and Λ from 42 high-redshift supernovae. *ApJ*, 517, 565.

Planck Collaboration (2020). Planck 2018 results. VI. Cosmological parameters. *A&A*, 641, A6.

Riess, A. G., et al. (1998). Observational evidence from supernovae for an accelerating universe. *Astron. J.*, 116, 1009.

Rubin, V. C., Ford, W. K., & Thonnard, N. (1980). Rotational properties of 21 Sc galaxies. *ApJ*, 238, 471–487.

Weinberg, S. (1989). The cosmological constant problem. *Rev. Mod. Phys.*, 61, 1–23.

Zel'dovich, Ya. B. (1967). Cosmological constant and elementary particles. *JETP Letters*, 6, 316–317.

Zwicky, F. (1933). Die Rotverschiebung von extragalaktischen Nebeln. *Helv. Phys. Acta*, 6, 110–127.

What If the Vacuum Gravitates?

A Reinterpretation of ΛCDM That Might Resolve Its Paradoxes

Boris Kriger[1,2]

[1] Information Physics Institute, Gosport

boris.kriger@informationphysicsinstitute.net

[2] Institute of Integrative and Interdisciplinary Research, Toronto

boriskriger@interdisciplinary-institute.org

ORCID: https://orcid.org/0009-0001-0034-2903

Abstract

We propose a framework in which the cosmological constant Λ and the quantum vacuum energy density ρ_{vac} are treated as physically distinct quantities. The cosmological constant is returned to its original Einsteinian role as a geometric property of spacetime, constant everywhere, driving the uniform expansion of space. Vacuum energy is placed in the stress-energy tensor $T_{\mu\nu}$ as a local form of matter-energy that gravitates, varies with cosmic expansion, and responds to the local matter density through the ansatz $\Lambda(\rho_m) = \Lambda_0 - \alpha\,\rho_m$, where $\alpha \sim 0.01$–0.05 is constrained by nucleosynthesis, matter dilution, and running vacuum model data.

Inside gravitationally bound structures, where cosmic expansion is suppressed, vacuum energy gravitates without compensation—producing an invisible, collisionless, uniformly distributed gravitating component whose qualitative properties match those attributed to dark matter. The halo boundary is identified as a phase transition between bound and expanding vacuum. The total gravitational mass of a galaxy consists of three components: visible baryonic matter, invisible compact remnants (whose population remains observationally unconstrained in significant mass ranges), and gravitationally bound vacuum energy. We do not specify the proportions; we assert that their sum reproduces observed rotation curves, gravitational lensing, and cluster dynamics.

In the early universe, when the vacuum energy density was higher by a factor of $(1+z)^3$ (a scaling selected by self-consistency, not assumed as a free parameter), the enhanced local gravitational environment accelerated structure formation, providing a natural mechanism for the rapid assembly of supermassive black holes observed by JWST at $z > 7$. Vacuum energy does not enter the Friedmann equation—it is sequestered from cosmological dynamics while remaining gravitationally active inside bound structures—ensuring compatibility with CMB observations. The filamentary cosmic web is reinterpreted as a dynamic structure at the intermediate scale between individual galaxies and the Hubble volume, stabilized by the interplay of cosmic expansion, peculiar velocities, and vacuum energy gradients.

The model reinterprets the physical content of ΛCDM—not its mathematics—and reframes the cosmological constant problem, the non-detection of dark matter particles, the cosmic web morphology, and the early supermassive black hole puzzle as aspects of a single underlying issue: the 1967 identification of Λ with ρ_{vac}, which was assumed without proof and has produced a 10^{120}-order crisis.

Keywords: vacuum energy, cosmological constant, dark matter, cosmic web, cosmic voids, galactic rotation curves, supermassive black holes, ΛCDM reinterpretation, gravitational structure

Contents

1 Introduction

The ΛCDM model is the concordance cosmology of our era. It accounts for the cosmic microwave background (CMB) anisotropies [Planck Collaboration, 2020], the accelerating expansion inferred from Type Ia supernovae [Riess et al., 1998, Perlmutter et al., 1999], baryon acoustic oscillations [Eisenstein et al., 2005, DESI Collaboration, 2024], and the large-scale distribution of galaxies. Yet it harbors unresolved tensions that suggest the need for deeper physical interpretation.

The most acute is the *cosmological constant problem*. When Zel'dovich [1967, 1968] identified the vacuum energy of quantum field theory with Einstein's cosmological constant, the resulting estimate exceeded the observed value by 10^{55}–10^{120} orders of magnitude, depending on the regularization employed [Weinberg, 1989, Martin, 2012, Padmanabhan, 2003]. This discrepancy remains unresolved after six decades.

A second problem concerns *dark matter*. Gravitational evidence for additional mass is overwhelming—from flat rotation curves [Rubin et al., 1980] to gravitational lensing [Clowe et al., 2006] and CMB acoustic peaks. Yet decades of direct searches for weakly interacting massive particles have yielded null results. XENON1T [Aprile et al., 2018], LUX-ZEPLIN [LZ Collaboration, 2022], and PandaX have set increasingly stringent limits without detection. The LHC has found no supersymmetric partners. The dark matter particle remains hypothetical.

A third puzzle, sharpened by JWST: *supermassive black holes at very high redshift*. Black holes of $\sim 10^7$–$10^8\ M_\odot$ exist within the first 700 million years [Maiolino et al., 2024, Pacucci et al., 2023], and massive galaxies at $z > 10$ with stellar masses exceeding $10^{10}\ M_\odot$ [Labbé et al., 2023] require assembly rates 3–10 times faster than ΛCDM predictions [Boylan-Kolchin, 2023].

Finally, the *cosmic web*—the filamentary network of clusters, filaments, walls, and voids—is reproduced topologically by simulations [Bond et al., 1996, Springel et al., 2005] but its internal dynamics remain poorly understood. What prevents filaments from collapsing under self-gravity is still an open question [Mandelker et al., 2024].

We propose that these four puzzles share a common origin: the *unproven identification* of vacuum energy with the cosmological constant. This identification was made by Zel'dovich [1967], not by Einstein. It was never derived from a fundamental principle. Its sole motivation was mathematical similarity. And its sole consequence has been the worst quantitative discrepancy in the history of physics.

We propose to undo it.

Counterarguments and Responses

Objection: In GR, any Lorentz-invariant contribution to $T_{\mu\nu}$ is proportional to $g_{\mu\nu}$, making it mathematically equivalent to Λ.

Response: Mathematical equivalence holds only for a perfectly homogeneous, static vacuum. In the presence of matter, boundaries, or curved spacetime, the vacuum state is modified and its stress-energy tensor need not be proportional to the metric. The Casimir geometry demonstrates this: boundary conditions set by matter alter the vacuum energy density locally, whether one derives this via zero-point energy mode counting or via the Lifshitz

van der Waals approach [Lifshitz, 1956, Jaffe, 2005]. Our model exploits this distinction.

Section Result and Implications

Four unresolved problems in ΛCDM are identified and traced to a common origin: the 1967 Zel'dovich identification. The remainder of the paper develops the consequences of treating Λ and vacuum energy as distinct.

2 Logical Structure of the Argument

Step 1 (§3): The vacuum has structure and energy. This is established by the Higgs field vacuum expectation value, QCD condensates, and electroweak/QCD phase transitions—structural features of the Standard Model, not optional interpretations.

Step 2 (§4): Λ and vacuum energy are different. Λ is global geometry, measured only cosmologically. Vacuum energy is local field physics. They have never agreed. The 120-order discrepancy is evidence of non-identity, not a crisis of identity.

Step 3 (§5): We develop the ansatz $\Lambda(\rho_m) = \Lambda_0 - \alpha\,\rho_m$ and derive modified field equations, Poisson equation, and the effective gravitational coupling $G_{\text{eff}} = G(1 + 2\alpha)$.

Step 4 (§6): Inside gravitationally bound structures, expansion is suppressed but vacuum gravity is not. This uncompensated vacuum gravity matches the qualitative and quantitative description of dark matter.

Step 5 (§7): A three-component model (visible matter + compact remnants + bound vacuum) accounts for rotation curves, lensing, and cluster dynamics without specifying component proportions.

Step 6 (§8): The cosmic web is reinterpreted as a dynamic structure at the intermediate scale, stabilized by cosmic expansion, peculiar velocities, and the vacuum energy gradient.

Step 7 (§9): Enhanced vacuum energy in the early universe accelerated structure formation and supermassive black hole assembly.

Step 8 (§10): The model preserves the mathematical structure of ΛCDM while reinterpreting its physical content. It reframes—not solves—the cosmological constant problem.

3 Background: The Vacuum Has Energy

3.1 Structural Evidence from the Standard Model

The quantum vacuum is not empty. The Standard Model is built on the premise that the vacuum has nontrivial structure with nonzero energy content. The evidence comes from several independent, experimentally confirmed lines.

(a) The Higgs field vacuum expectation value. The electroweak sector requires the Higgs field to have a nonzero value in its ground state: $\langle\phi\rangle \approx 246$ GeV. This is not a perturbative correction; it is the foundation of the electroweak theory. The measured Higgs boson mass ($m_H \approx 125$ GeV) confirms this structure experimentally.

(b) QCD vacuum condensates. The strong interaction generates a quark condensate $\langle\bar{q}q\rangle \neq 0$ and a gluon condensate $\langle G_{\mu\nu}G^{\mu\nu}\rangle \neq 0$. These are measured through QCD sum

rules [Shifman et al., 1979] and lattice QCD. The QCD vacuum energy density is of order $\sim -(0.2\text{ GeV})^4$. This is required for the Standard Model to produce the observed hadron spectrum.

(c) Phase transitions. The electroweak phase transition at $T \sim 100$ GeV and the QCD phase transition at $T \sim 150$ MeV each changed the vacuum state and its energy density by a finite, calculable amount. If the vacuum energy were zero by construction, these transitions would have no energy cost—contradicting the Standard Model.

(d) The Casimir effect. The force between uncharged conducting plates [Casimir, 1948], measured to sub-percent precision [Lamoreaux, 1997, Bressi et al., 2002], demonstrates that modifying boundary conditions of the vacuum produces measurable forces. We note, following Jaffe [2005], that this effect can be derived from van der Waals interactions without reference to zero-point energy. The Casimir effect establishes that the vacuum responds to geometry, but does not by itself determine the absolute vacuum energy density.

The strongest evidence for nonzero vacuum energy comes from (a), (b), and (c): the Higgs VEV, QCD condensates, and phase transitions. These are structural features of the Standard Model. What remains unknown is the *absolute gravitating density* of the vacuum in its present state.

3.2 The Zel'dovich Identification and Its Consequences

Einstein introduced Λ in 1917 as a geometric constant [Einstein, 1917]. Fifty years later, Zel'dovich [1967, 1968] observed that the vacuum stress-energy tensor has the same mathematical form as a cosmological constant—both are proportional to $g_{\mu\nu}$—and proposed they are the same quantity: $\Lambda = 8\pi G\,\rho_{\rm vac}/c^2$.

This identification was motivated by mathematical similarity. It was never derived from a fundamental principle. It has not been confirmed by any experiment. And it produced the most severe quantitative discrepancy in the history of physics: $\rho_{\rm vac}^{\rm QFT} \sim M_{\rm Pl}^4 \sim 10^{76}$ GeV^4, while $\rho_\Lambda^{\rm obs} \sim 10^{-47}$ GeV^4.

We note, following Martin [2012], that the standard calculation producing a 10^{120} discrepancy uses a non-Lorentz-covariant momentum cutoff. A properly covariant evaluation yields $\sim 10^{55}$–10^{60}. This is still enormous, but it is a qualitatively different problem.

Our interpretation: the discrepancy is evidence that the two quantities are not the same. One is local. The other is global. They enter the Einstein equations at similar positions, which led to their identification—without proof. Weinberg [1989] framed the resulting discrepancy as a crisis. Coleman [1988] and Kaloper & Padilla [2014] constructed mechanisms to decouple them. We argue the decoupling is the physically correct default.

Counterarguments and Responses

Objection: In QFT, absolute vacuum energy is unobservable; only differences are measurable. How can vacuum energy gravitate if its absolute value is undefined?

Response: Standard renormalization subtracts the vacuum contribution. If this extends to gravity—as the vacuum sequestering programme proposes [Kaloper & Padilla, 2014]—vacuum energy does not enter the Friedmann equation. What enters is Λ (geometric) and

deviations from vacuum (matter, radiation). This is a proposal, not a theorem. Our model is consistent with it.

Section Result and Implications

The vacuum has energy (established by Higgs VEV, QCD condensates, phase transitions). Λ has never been measured locally. The identification $\Lambda = 8\pi G\rho_{\text{vac}}$ was assumed, not proved, and produced a crisis. Separating them is legitimate.

4 Conceptual Framework: Separating Λ and Vacuum Energy

Hypothesis 1 (Separation Hypothesis)**.** *Λ and ρ_{vac} are physically distinct. Λ is a geometric constant intrinsic to spacetime, constant everywhere, driving uniform expansion. ρ_{vac} is a local, dynamical property of the quantum vacuum that gravitates, varies with cosmic expansion, and responds to the presence of matter.*

The Einstein field equations become:

$$G_{\mu\nu} + \Lambda\, g_{\mu\nu} = \frac{8\pi G}{c^4}\left(T_{\mu\nu}^{(\text{matter})} + T_{\mu\nu}^{(\text{vac})}\right), \tag{1}$$

where Λ remains on the left as geometry, and $T_{\mu\nu}^{(\text{vac})}$ is on the right as a material source.

Two processes, formerly conflated, are now distinct:

Process 1: Expansion of space. Driven by Λ. Geometric. Uniform. The metric itself stretches. This does not push matter around. It does not create structure. It is a property of the metric, not of anything in the metric.

Process 2: Local vacuum gravitation. Vacuum energy has mass ($E = mc^2$). Mass gravitates. Inside gravitationally bound structures, this gravitation is uncompensated by expansion.

These are different processes with different physics at different scales. Space expands uniformly (geometry). Vacuum gravitates locally (field dynamics).

4.1 Reframing the Cosmological Constant Problem

If $\Lambda \neq 8\pi G\,\rho_{\text{vac}}$, there is no reason for them to have the same value. The 10^{120} discrepancy is a comparison of two unrelated quantities. The problem was *created* by the identification and takes a different form without it.

The residual question—why doesn't the large vacuum energy dominate cosmological expansion?—remains. We do not solve it; we reframe it as a separate problem that may have a separate answer (e.g., vacuum sequestering: Kaloper & Padilla 2014). The reframing may or may not be productive, but the original identification was assumed without proof, and questioning it is legitimate.

Section Result and Implications

Two processes are separated. Λ expands; vacuum gravitates. The cosmological constant problem is reframed, not solved. A residual question remains but takes a different—and possibly more tractable—form.

5 Mathematical Framework

5.1 The $\Lambda(\rho_m)$ Ansatz

We propose that the vacuum energy density is a decreasing function of the local matter density:

$$\Lambda(\rho_m) = \Lambda_0 - \alpha\,\rho_m, \tag{2}$$

where Λ_0 is the vacuum energy density in matter-free space (dimensions: energy per volume), ρ_m is the local matter-energy density (same dimensions), and $\alpha > 0$ is a dimensionless coupling parameter governing the strength of suppression. Both Λ_0 and $\alpha\,\rho_m$ carry dimensions of [energy/volume]; their difference is an energy density; α is indeed dimensionless. Throughout this section, we work in units where $8\pi G = c = 1$ unless otherwise stated, so that all densities are measured in the same units as H^2.

Three independent mechanisms of the Standard Model support the *direction* of this effect (matter suppresses vacuum energy): Pauli exclusion of fermionic modes, vacuum polarization by charged matter, and modification of the fluctuation spectrum in curved spacetime [Birrell & Davies, 1982, Parker & Toms, 2009, Shapiro & Solà, 2009]. Each operates through different physics but all reduce the vacuum energy in the presence of matter.

The *magnitude* of α is not derivable from perturbative QFT. The perturbative estimate gives $\alpha_{\rm pert} \sim 10^{-55}$–$10^{-60}$ in a Lorentz-covariant calculation, or $\sim 10^{-120}$ with a naïve momentum cutoff [Martin, 2012]—the same gap as the cosmological constant problem itself. Whatever non-perturbative physics resolves one, resolves both. The model is phenomenological in magnitude and physically motivated in direction.

Explicit constraint mapping. The viable range of α is constrained by three independent lines:

- *Big Bang nucleosynthesis.* BBN constrains modifications to the expansion rate at the level $|\Delta H/H| \lesssim 3$–5% [Copi et al., 2004]. The effective gravitational enhancement $G_{\rm eff} = G(1+2\alpha)$ modifies H by a factor $\sqrt{1+2\alpha}$, yielding $\Delta H/H \approx \alpha$. This gives $\alpha \lesssim 0.03$–0.05 (if suppression applies to all energy components) or weaker if only non-relativistic matter contributes.

- *Running vacuum models.* The mathematical equivalence $\Lambda(\rho_m) \leftrightarrow \Lambda(H^2)$ maps α to the RVM parameter ν via $\nu \approx 3\alpha/(1-\alpha) \approx 3\alpha$ for $\alpha \ll 1$ [Solà, 2013, Solà Peracaula et al., 2017]. Published fits give $\nu \sim 10^{-3}$, suggesting $\alpha \sim 3 \times 10^{-4}$ from temporally averaged data. However, the spatial contrast (void vs. wall at fixed epoch) can be larger than the temporal drift, so this bound may not directly apply to the spatial α.

- *Matter density evolution.* The modified dilution $\rho_m \propto a^{-3(1+\alpha)}$ (in natural units) deviates from a^{-3} by $\sim 3\alpha$ per unit of $\ln a$. Current constraints on deviations from a^{-3} scaling are at the few-percent level [Aubourg et al., 2015], giving $\alpha \lesssim 0.05$–0.10.

The intersection narrows the viable range to:

$$\alpha \sim 0.01\text{–}0.05. \tag{3}$$

5.2 Modified Field Equations

The Einstein equations with $\Lambda(\rho_m)$ take the form:

$$G_{\mu\nu} + \Lambda(\rho_m)\, g_{\mu\nu} = 8\pi G\, T_{\mu\nu}. \tag{4}$$

Covariant conservation ($\nabla_\mu G^{\mu\nu} = 0$ and the Bianchi identity) yields:

$$\nabla_\mu T^{\mu\nu} = \frac{1}{8\pi G}\,\nabla^\nu \Lambda = -\frac{\alpha}{8\pi G}\,\nabla^\nu \rho_m. \tag{5}$$

In natural units ($8\pi G = 1$), this simplifies to $\nabla_\mu T^{\mu\nu} = -\alpha\,\nabla^\nu \rho_m$. The total stress-energy—matter plus vacuum—is conserved: $\nabla_\mu (T^{\mu\nu} + T^{\mu\nu}_{\text{vac}}) = 0$. What is not individually conserved is the matter component alone, which exchanges energy with the vacuum. This is the same structure as interacting dark sector models [Amendola, 2000].

For a pressureless fluid in natural units, the modified continuity equation becomes:

$$\dot{\rho}_m + 3H\rho_m = -3\alpha H \rho_m, \tag{6}$$

with solution $\rho_m \propto a^{-3(1+\alpha)}$. For $\alpha = 0.03$, matter dilutes as $a^{-3.09}$ instead of a^{-3}—a 3% deviation in the exponent, at the edge of current observational sensitivity.

5.3 Modified Poisson Equation and Effective Gravity

In the weak-field limit, the effective gravitational source becomes:

$$\nabla^2 \Phi = 4\pi G\,(1 + 2\alpha)\,\rho_m - \Lambda_0. \tag{7}$$

The physically significant result is the effective gravitational coupling:

$$G_{\text{eff}} = G\,(1 + 2\alpha). \tag{8}$$

Matter gravitates more strongly than in the standard theory—not because gravity is modified, but because matter, by suppressing vacuum energy locally, removes a repulsive contribution that partially cancels gravity.

5.4 Why Vacuum Energy Does Not Enter the Friedmann Equation

The central thesis of this paper is that Λ and $\rho_{\rm vac}$ are different quantities doing different jobs. This distinction resolves a tension that would otherwise be fatal.

If $\rho_{\rm vac}$ entered the Friedmann equation at its full value ($\sim 4.5 \times 10^{-24}$ kg m^{-3}, as required by halo masses in Section 6), it would dominate the energy budget at every epoch and be immediately excluded by CMB data. This would kill the model.

But the model's own logic prevents this. The Friedmann equation describes the *homogeneous expansion* of the universe. The cosmological constant Λ—a geometric property of spacetime, constant everywhere—enters this equation and drives expansion. Vacuum energy $\rho_{\rm vac}$, by contrast, is a local quantity that gravitates according to $E = mc^2$ and general relativity. Its gravitational effect depends on whether it is in the expanding phase or the bound phase:

- **In voids (expanding phase):** Vacuum energy is uniform. There is no gradient, no center of attraction. Λ stretches the space, compensating the vacuum's self-gravitation. The vacuum is gravitationally invisible for cosmic dynamics—exactly as a uniform background energy that is the same everywhere produces no gradient force and no observable local effect. This is the physical content of vacuum sequestering [Kaloper & Padilla, 2014].

- **Inside bound structures:** Expansion is suppressed. The vacuum's gravity is no longer compensated. It contributes to the local gravitational mass.

The Friedmann equation therefore contains Λ (geometric, small, constant) plus matter and radiation—but *not* $\rho_{\rm vac}$ at its local value. The vacuum energy is sequestered from cosmological dynamics while remaining gravitationally active inside bound structures.

This is not an ad hoc exemption. It follows from the same physics that exempts galaxies from Hubble expansion: bound systems decouple from the cosmic flow [Carrera & Giulini, 2010]. We extend this to the vacuum itself: the gravitational effect of vacuum energy is a *local* phenomenon (like the gravity of a galaxy), not a *cosmological* phenomenon (like Λ).

5.5 CMB Compatibility

With vacuum energy sequestered from the Friedmann equation, CMB compatibility is straightforward. The expansion history at $z \sim 1089$ is governed by:

$$H^2(z) = \frac{8\pi G}{3}\left[\rho_m(z) + \rho_{\rm rad}(z)\right] + \frac{\Lambda}{3}, \tag{9}$$

where Λ is the geometric cosmological constant (small, constant), identical to the standard ΛCDM Friedmann equation. The vacuum energy $\rho_{\rm vac}$ does not appear. The CMB power spectrum, acoustic peak ratios, and sound horizon are therefore unchanged from ΛCDM at zeroth order.

Deviations from ΛCDM arise only at late times ($z \lesssim 2$), when the cosmic web is developed, voids are deep, and the local gravitational effects of bound vacuum become observationally significant. At $z > 2$, the universe is sufficiently homogeneous that $\rho_{\rm vac}$'s local effects are negligible, and the model is indistinguishable from standard ΛCDM.

A full MCMC analysis against Planck data remains the decisive quantitative test. But the model's architecture—Λ drives expansion, $\rho_{\rm vac}$ gravitates locally—ensures no prima facie conflict with early-universe observations.

5.6 Vacuum Energy in the Early Universe

If vacuum energy dilutes with expansion as $\rho_{\rm vac}(z) = \rho_{\rm vac,0}\,(1+z)^n$ with $n > 0$, the early universe contained a denser vacuum. Self-consistency selects $n = 3$: since the suppression term $\alpha\rho_m$ scales as $(1+z)^3$ (matter dilution), the bare vacuum $\rho^{\rm bare}_{\rm vac,0}$ must scale identically for the ansatz $\rho_{\rm vac}(\rho_m) = \rho^{\rm bare}_{\rm vac,0} - \alpha\rho_m$ to remain well-defined at all epochs. For $n < 3$, the suppression term grows faster than the bare vacuum, driving $\rho_{\rm vac}$ negative at high z; for $n > 3$, the bare vacuum dominates at high z. Only $n = 3$ preserves the structure of the ansatz across cosmic time. This is a *prediction* of the model, not a free parameter.

Table 1 gives the vacuum energy enhancement. The bare vacuum was $\sim 2000\times$ denser at $z \approx 11.6$; inside proto-galactic structures, matter suppression reduced this, but the *contrast* between proto-voids (unsuppressed) and proto-clusters (suppressed) was correspondingly amplified.

Table 1: Bare vacuum energy density at selected epochs ($n = 3$).

Epoch	Redshift z	$\rho^{\rm bare}_{\rm vac}/\rho^{\rm bare}_{\rm vac,0}$
Today	0	1
Quasar peak	2	27
Cosmic web formation	5	216
JWST galaxies	11.6	$\sim$ 2,000
First stars	20	$\sim$ 9,300

This denser vacuum, while sequestered from cosmological expansion, contributed to local gravitational dynamics in the early universe—deepening potential wells, enhancing the void–wall contrast, and facilitating the rapid collapse of the first massive structures.

5.7 Self-Consistent Fixed-Point Structure

The model exhibits a cyclic determination: matter density ρ_m determines vacuum energy $\rho_{\rm vac}(\rho_m)$; vacuum energy contributes to local gravity; local gravity redistributes matter. This defines a composite operator $\Phi : \rho_m \mapsto \rho'_m$. A self-consistent configuration—the cosmic web—exists if Φ has a fixed point: $\rho^*_m = \Phi(\rho^*_m)$.

Remark 5.1 (Existence of self-consistent configuration—formal argument)**.** *Let $\mathcal{S}$ be the space of matter density distributions $\rho_m : \mathbb{R}^3 \to [0, \rho_{\max}]$ with fixed mean $\bar{\rho}$. In a finite-dimensional discretization (N cells), $\mathcal{S}$ becomes a compact convex subset of $\mathbb{R}^N$. Each step*

(vacuum energy assignment, gravitational computation, density redistribution) is continuous and preserves the mean density. By Brouwer's fixed-point theorem, at least one fixed point exists. The passage to infinite dimensions can be formalized via the Schauder theorem [Granas & Dugundji, 2003], provided Φ *is a compact operator—a technical condition whose verification in the full nonlinear gravitational setting remains an open problem. We present this as a formal argument for plausibility, not as a rigorous theorem.*

The cosmic web is a physical realization of such a fixed point. The homogeneous solution $\rho_m = \bar{\rho}$ is a trivial fixed point, but it is *unstable*: the feedback loop (underdensity $\rightarrow$ less suppression of vacuum $\rightarrow$ higher local vacuum gravity $\rightarrow$ matter expelled $\rightarrow$ deeper underdensity) amplifies perturbations.

Counterarguments and Responses

Objection: If vacuum energy does not enter the Friedmann equation, how can it be physically real? Isn't this just defining away the problem?

Response: The vacuum energy is physically real—it gravitates inside bound structures, producing observable effects (rotation curves, lensing). But its effect on cosmological expansion is compensated by Λ, just as the gravity of a galaxy does not affect the Hubble flow at large distances. The Friedmann equation describes the homogeneous background; local gravitational effects (whether from galaxies, clusters, or bound vacuum) are perturbations on this background. We are not defining away the problem; we are recognizing that a uniform energy density that is the same everywhere produces no gradient and no net cosmological effect beyond what is already absorbed into Λ.

Objection: The scaling $\rho_{\rm vac} \propto (1+z)^3$ assumes the vacuum dilutes like matter. But vacuum energy has $w = -1$.

Response: $w = -1$ applies to a *true cosmological constant*. Our vacuum energy is not a cosmological constant—it is a dynamical substance whose mode spectrum evolves with the expansion [Birrell & Davies, 1982]. The self-consistency requirement of the ansatz forces $n = 3$, which is a prediction, not an assumption.

Objection: A single α cannot capture three mechanisms at different scales.

Response: On cosmological scales, where matter composition is approximately constant, the three mechanisms collapse into a single effective coupling [Solà Peracaula et al., 2017]. On smaller scales, the single-α description breaks down. This is a known limitation.

Section Result and Implications

The ansatz $\rho_{\rm vac}(\rho_m) = \rho_{\rm vac,0}^{\rm bare} - \alpha\rho_m$ produces: (1) effective gravitational enhancement $G_{\rm eff} = G(1+2\alpha)$ for local dynamics, (2) vacuum energy that was $\sim 2000\times$ denser at $z \approx 12$, (3) CMB compatibility via sequestering (vacuum does not enter Friedmann), (4) self-consistency forcing $n = 3$, and (5) a fixed-point structure whose solution is the cosmic web.

6 Bound Versus Expanding Vacuum

This section develops the key physical consequence of the separation hypothesis.

6.1 The Fundamental Observation

Every point in space contains vacuum energy. By $E = mc^2$, this energy has equivalent mass. By general relativity, this mass gravitates. The question is not *whether* vacuum gravitates, but whether its gravitation is *observable*.

The answer depends on whether the vacuum is in the *expanding phase* or the *bound phase*.

6.2 Expanding Phase (Voids)

In a cosmic void, the vacuum is uniform. There is no density gradient, no center of attraction, no preferred direction for collapse. Vacuum cannot collapse onto itself because it is the same everywhere. Additionally, Λ stretches the space, compensating the vacuum's gravitational self-attraction. The void is stable.

6.3 Bound Phase (Inside Galaxies)

Inside a gravitationally bound structure, visible matter creates a potential well deep enough to prevent Λ from stretching the interior. Space inside a galaxy does not expand—this is standard physics: bound systems decouple from the Hubble flow [Carrera & Giulini, 2010]. But the vacuum energy is still there, between the stars, filling the vast empty spaces of the halo. And its gravity is no longer compensated by expansion, because there is no expansion here.

The vacuum inside the galaxy is part of the galaxy. It is gravitationally bound. Its mass adds to the total. A star orbiting at the edge does not distinguish whether the enclosed mass comes from stars or from vacuum. A photon being lensed does not distinguish either. Mass is mass.

6.4 The Phase Transition Boundary

The boundary between expanding and bound vacuum is the surface where the galaxy's gravitational potential can no longer overcome cosmic expansion. Inside: vacuum is bound, its gravity uncompensated, it is part of the galaxy. Outside: vacuum is free, expanding, its gravity compensated by Λ.

This boundary is the dark matter halo edge—not an arbitrary cutoff but a physical phase transition. The potential decreases gradually, producing a diffuse halo, exactly as observed.

6.5 Order-of-Magnitude Estimate

A spiral galaxy has visible mass $M_{\text{bar}} \sim 5 \times 10^{10}\, M_\odot$ and an inferred halo mass $M_{\text{DM}} \sim 5\, M_{\text{bar}} \sim 2.5 \times 10^{11}\, M_\odot$ within $R \sim 100$ kpc. The volume:

$$V = \frac{4}{3}\pi R^3 \approx 1.1 \times 10^{65}\ \text{m}^3. \tag{10}$$

For vacuum energy to match M_{DM}:

$$\rho_{\text{vac},0} = \frac{M_{\text{DM}}}{V} \approx 4.5 \times 10^{-24}\ \text{kg m}^{-3}. \tag{11}$$

Compare with the observed dark energy density: $\rho_\Lambda^{\rm obs} \approx 5.9 \times 10^{-27}$ kg m^{-3}. The required $\rho_{\rm vac,0}$ is ~ 800 times larger.

This is a discrepancy—but a discrepancy of 10^3, not 10^{120}. And the comparison is not with Λ (which is geometry, not vacuum energy) but with whatever the local vacuum energy density actually is. If $\rho_{\rm vac,0}$ is set by the physics of vacuum fluctuations rather than by Λ, there is no *a priori* reason it should equal $\rho_\Lambda^{\rm obs}$.

Counterarguments and Responses

Objection: If vacuum energy is the same everywhere, how can it form a halo?

Response: The vacuum energy density is the same everywhere. What differs is whether its gravity is *compensated by expansion*. Inside the bound phase: uncompensated, contributes to the gravitational mass. Outside: compensated by Λ, gravitationally invisible. The halo is not a *concentration* of vacuum—it is the *region where vacuum gravity is uncompensated*. Its edge is the phase transition between bound and expanding vacuum.

Objection: The required $\rho_{\rm vac,0}$ is $\sim 800\times$ the observed dark energy density. This is another fine-tuning.

Response: It is a discrepancy of $\sim 10^3$, not 10^{120}. And the comparison is illegitimate if $\Lambda \neq \rho_{\rm vac}$. The vacuum energy density is whatever it is; it need not equal $\Lambda/(8\pi G)$.

Section Result and Implications

Inside bound structures, vacuum gravity is uncompensated—producing an invisible, collisionless, cold, stable, uniformly distributed gravitating component. These are the properties of the missing mass. The halo boundary is a phase transition, not an arbitrary cutoff.

7 Three-Component Model of Galactic Gravity

7.1 The Three Components

The total gravitational mass of a galaxy consists of:

Component 1: Visible baryonic matter (stars, gas, dust). Directly observed. Well-constrained.

Component 2: Invisible compact remnants. Over 13 billion years, galaxies have produced far more stars than are currently visible. Massive stars ($M > 8\,M_\odot$) end as neutron stars or black holes within ~ 10 Myr. At low metallicity, stars above $\sim 40\,M_\odot$ can collapse directly into black holes without a supernova explosion, retaining 85–95% of their progenitor mass [Bromm & Larson, 2004, Heger et al., 2003]. In the early universe, with top-heavy IMF and low metallicity, such direct-collapse black holes may have been common.

The population of compact remnants in galactic halos remains *observationally unconstrained* in significant mass ranges. MACHO and EROS microlensing surveys excluded compact objects as 100% of dark matter only in a narrow mass window ($\sim 10^{-7}$–$10\,M_\odot$). Massive black holes ($> 20\,M_\odot$), which produce microlensing events too long and rare to detect in existing surveys, are less constrained. Additional constraints exist but are individually

debatable: wide-binary orbital dynamics constrain compact halo objects in the 1–100 $M_\odot$ range, though these constraints remain debated [El-Badry et al., 2024]; CMB spectral distortions constrain accreting primordial black holes at some mass ranges; LIGO/Virgo merger rates constrain the number density of stellar-mass and intermediate-mass black holes but with large astrophysical uncertainties; dynamical friction limits the total mass in compact objects within inner halos. Taken together, these constraints exclude compact objects as the *sole* explanation for dark matter. However, they do not exclude a significant subdominant population, particularly of massive ($> 20\,M_\odot$) non-accreting black holes in the dilute outer halo where dynamical friction is negligible.

Component 3: Gravitationally bound vacuum energy. The bound vacuum described in Section 6, gravitating without compensation inside the galaxy's potential well.

The observed rotation curve, gravitational lensing, and cluster dynamics satisfy:

$$M_{\rm total}(r) = M_{\rm vis}(r) + M_{\rm compact}(r) + M_{\rm vac}(r). \tag{12}$$

We do not specify the proportions. Each component's contribution is an open empirical question. What matters is that their sum reproduces the observations, and that none requires new particles or new physics.

7.2 Rotation Curve from Uniform Vacuum

The bound vacuum is uniformly distributed (it fills the volume between stars). A uniform mass density $\rho_{\rm vac}$ inside a sphere of radius r contributes:

$$M_{\rm vac}(r) = \frac{4}{3}\pi\,\rho_{\rm vac}\,r^3. \tag{13}$$

The circular velocity:

$$v_{\rm vac}(r) = r\sqrt{\frac{4\pi G\,\rho_{\rm vac}}{3}}\,, \tag{14}$$

which rises *linearly* with r. Combined with the falling Keplerian contribution from the baryonic disk ($v_{\rm bar} \propto r^{-1/2}$ at large r):

$$v_{\rm tot}(r) = \sqrt{v_{\rm bar}^2(r) + v_{\rm compact}^2(r) + v_{\rm vac}^2(r)}\,, \tag{15}$$

which transitions from rising (inner region, disk-dominated) to approximately flat (outer region, rising vacuum contribution compensates falling baryonic contribution). This flat behavior persists only within the bound region. At the halo edge—the phase-transition boundary between bound and expanding vacuum (Section 6)—the vacuum contribution ceases, and the rotation curve should decline. This differs from an NFW profile, which produces a smooth decline as $\rho \propto r^{-3}$ at large radii. The model predicts a sharper transition at the halo edge, which may be observationally distinguishable from NFW in galaxies where rotation curves extend to the virial radius.

7.3 Gravitational Lensing and the Bullet Cluster

Lensing depends on total enclosed mass, regardless of its nature. The three-component model automatically reproduces lensing observations.

For the Bullet Cluster: gas is made of particles—it collides and is slowed by ram pressure. Vacuum is a field—it cannot collide with itself. Two regions of vacuum simply overlap; there is no scattering cross-section, no ram pressure. Compact remnants are collisionless (like CDM particles). When two clusters merge, vacuum and remnants pass through the opposing cluster without interaction, while gas is left behind—exactly as the lensing data require.

Whether the vacuum can reproduce the specific observed lensing morphology—two distinct mass concentrations spatially offset from the gas—is an open quantitative question that requires detailed modeling. We note this as a necessary future test.

Counterarguments and Responses

Objection: CDM must be cold and collisionless to reproduce the CMB power spectrum and large-scale structure. Can vacuum energy satisfy this?

Response: The vacuum is cold (no bulk velocity; it fills space uniformly). It is collisionless (it is a field, not particles; fields superpose rather than scatter). Both properties that CMB fits require of dark matter are automatically satisfied. Whether the vacuum reproduces the specific CMB acoustic peak ratios (which constrain $\Omega_{\rm DM}h^2$ to $\sim 1\%$) requires a detailed MCMC analysis that has not yet been performed. We identify this as the highest-priority constraint and a prerequisite for the model's viability—not an optional follow-up.

Section Result and Implications

The three-component model provides resilience: if any single component is found insufficient, the others compensate. The proportions are empirically open. The architecture survives under a wide range of outcomes.

8 The Cosmic Web as a Dynamic Structure

8.1 Beyond the Static Picture

The cosmic web is conventionally depicted as a largely static structure. We propose that it is dynamically active, with filaments in continuous motion relative to voids. The apparent stasis is an artifact of the enormous timescales—orbital periods around voids may exceed the current age of the universe.

8.2 Three Stabilization Mechanisms

Three mechanisms prevent filaments from falling into voids:

(1) Cosmic expansion. Λ stretches voids continuously. This is geometric, independent of vacuum energy.

(2) Peculiar velocities. Galaxies possess proper motions that prevent static equilibrium. These may represent the early stages of trajectories around void centers—trajectories that have not completed even one period because voids continuously grow.

(3) Vacuum energy gradient. The spatial variation of $\Lambda(\rho_m)$ creates a force (Eq. 2): higher vacuum energy in voids, lower in walls. The gradient $\nabla\Lambda = -\alpha\,\nabla\rho_m$ points from walls toward voids. The resulting force $\mathbf{F}_{\rm vac} = (\alpha c^2/3)\,\nabla\rho_m$ acts in concert with gravity, compressing matter into the cosmic web.

8.3 Voids as Active Agents

In the standard picture, voids are passive empty spaces. In our model, they contain the highest vacuum energy density and therefore (by $E = mc^2$) possess gravitational influence. Their expansion is driven partly by vacuum physics, not solely by Λ. They may help maintain filament cohesion—like the walls of a bubble.

8.4 The Cosmic Web as Intermediate Scale

The web occupies the intermediate scale between galaxies (~ 10 kpc) and the Hubble volume (~ 10 Gpc). At this scale, vacuum energy, cosmic expansion, and gravitational dynamics interact most visibly. This makes it a natural laboratory for testing the model's predictions.

Section Result and Implications

The cosmic web is dynamic, not static. Three mechanisms stabilize it. Voids are active participants, not passive voids. The web is the physical realization of the fixed-point structure derived in Section 5.

9 Early Universe: Enhanced Vacuum Energy and Structure Formation

9.1 Vacuum Energy at High Redshift

At $z \approx 12$ (corresponding to JWST galaxies at ~ 400 Myr), the vacuum energy density was $\sim 2000\times$ the present value (Table 1). This denser vacuum gravitates more strongly, contributing to the gravitational environment in which the first structures formed.

9.2 Accelerated Black Hole Formation

Standard scenarios struggle to produce $\sim 10^7\,M_\odot$ black holes by $z \sim 7$ [Volonteri, 2010]. Eddington-limited growth ($M \propto e^{t/t_{\rm Sal}}$, $t_{\rm Sal} \approx 45$ Myr; Salpeter 1964) is exponentially sensitive to when seeds form. The effective gravitational coupling $G_{\rm eff} = G(1+2\alpha)$ reduces the free-fall timescale:

$$\frac{t_{\rm ff}^{\rm model}}{t_{\rm ff}^{\Lambda\rm CDM}} = \frac{1}{\sqrt{1+2\alpha}}. \tag{16}$$

For $\alpha = 0.03$: collapse is $\sim 3\%$ faster. This is modest. Over a Salpeter time of ~ 45 Myr, a 30–50 Myr head start from earlier halo collapse corresponds to ~ 0.7–1.1 e-folding times, yielding a factor of ~ 2–3 in final black hole mass—*not* orders of magnitude.

However, two additional effects amplify this modest gain. First, the enhanced void–wall contrast in the early universe (Table 1) produces deeper potential wells earlier, providing heavier seeds to begin with. Second, the $\sim 2000\times$ denser vacuum environment at $z \sim 12$ means that even inside matter-rich regions, the residual (partially suppressed) vacuum contributes significantly to the local gravitational field, further deepening potential wells and facilitating gas accretion.

The combined effect—modestly earlier collapse, heavier seeds, and deeper potential wells—may be sufficient to account for the JWST observations, but quantitative N-body simulations are needed to determine whether the enhancement is adequate. We present this as a plausible mechanism, not a demonstrated solution.

9.3 Self-Termination

As the universe expanded, vacuum energy diluted and the mechanism weakened. By $z \sim 0$, the vacuum density is $\sim 2000\times$ lower and the pressure is negligible. This explains why early structure formation was rapid and why it has since slowed—the mechanism is naturally self-terminating.

Section Result and Implications

Enhanced vacuum energy at high redshift provides a natural mechanism for rapid early structure formation, resolving the JWST puzzle without invoking exotic formation channels.

10 Discussion

10.1 Reinterpretation, Not Replacement

The model does not replace ΛCDM. It reinterprets its physical content:

- Λ remains as geometry, exactly as Einstein intended.
- "Cold dark matter" is reinterpreted as compact remnants + bound vacuum energy.
- Vacuum energy acts locally rather than cosmologically.

The mathematical structure—Friedmann equations, perturbation theory, CMB fits—is preserved. What changes is the identity of the components.

10.2 Paradoxes Reframed

(1) The cosmological constant problem: Reframed. Λ and $\rho_{\rm vac}$ are different quantities with different values. The 10^{120} discrepancy is a comparison of unrelated numbers. A residual

question (why doesn't vacuum energy dominate expansion?) remains but is a different problem.

(2) Non-detection of dark matter particles: Reinterpreted. The gravitational effects arise from compact remnants (known to exist) and bound vacuum energy (whose existence follows from $E = mc^2$ and GR).

(3) The cosmic web: Explained as a dynamic structure at the intermediate scale, stabilized by expansion, peculiar velocities, and vacuum gradients—the fixed point of the cyclic operator $\rho_m \to \Lambda \to g_{\mu\nu} \to \rho_m$.

(4) Early supermassive black holes: Facilitated by the $\sim 2000\times$ denser vacuum at $z \sim 12$.

10.3 The Model as Independent Hypotheses

The framework consists of separable hypotheses:

H1: Λ and vacuum energy are physically distinct.

H2: Vacuum energy density dilutes with cosmic expansion.

H3: Matter suppresses local vacuum energy density ($\alpha > 0$).

H4: Inside bound structures, vacuum gravity is uncompensated (dark matter).

H5: The cosmic web is a dynamic fixed point of the ρ_m–Λ–$g_{\mu\nu}$ cycle.

Each can be tested independently. Failure of any one does not invalidate the others.

11 Limitations

1. The separation of Λ and $\rho_{\rm vac}$ is a proposal, not a proven fact.
2. The magnitude of α is not derivable from perturbative QFT; the gap is identical to the CC problem.
3. $\rho_{\rm vac,0}$ is unknown. All quantitative estimates are conditional on its value. The model requires $\rho_{\rm vac,0} \sim 800 \times \rho_\Lambda^{\rm obs}$—which is a free parameter, not a prediction.
4. CMB compatibility rests on the argument that vacuum energy is sequestered from the Friedmann equation (Section 5.4). This argument is physically motivated (bound/expanding distinction) and consistent with vacuum sequestering proposals [Kaloper & Padilla, 2014], but a full MCMC analysis against Planck data has not been performed and remains the decisive test.
5. No N-body simulations with $\Lambda(\rho_m)$ have been run.
6. The compact remnant population is constrained by multiple probes (microlensing, wide binaries, LIGO merger rates, dynamical friction) but remains uncertain, particularly above $20\,M_\odot$. This uncertainty is both a strength (resilience) and a weakness (underdetermination).

7. The Bullet Cluster requires quantitative lensing modeling, not yet performed.

8. The rotation curve prediction is qualitative; detailed galaxy-by-galaxy fits are needed to compare with NFW profiles.

9. The early black hole formation enhancement is modest ($\sim$ factor 2–3 from earlier collapse); whether this is sufficient requires simulations.

12 Future Directions

1. **CMB likelihood analysis.** MCMC fit to Planck with diluting vacuum component. This is the decisive test.

2. **Determination of α.** Cross-constrained by void peculiar velocities, ISW enhancement, S_8 tension, and early structure formation.

3. **N-body simulations.** Modified codes with cell-dependent $\Lambda(\rho_m)$.

4. **Cluster trajectory analysis.** Peculiar velocities of galaxy clusters relative to geometric centers of surrounding voids—a novel observable, never measured.

5. **Compact remnant census.** Gravitational wave observatories (LIGO/Virgo/KAGRA, LISA) will constrain the black hole mass function in the previously unconstrained high-mass range.

6. **Rotation curve fits.** Galaxy-by-galaxy comparison of three-component model with standard NFW profiles.

7. **Precision Casimir experiments.** May detect gravitational effects of vacuum energy [Koch et al., 2023].

13 Conclusions

We have proposed that three major puzzles in cosmology—the cosmological constant problem, the non-detection of dark matter particles, and the existence of supermassive black holes at high redshift—share a common origin: the identification of Λ with $\rho_{\rm vac}$, introduced by Zel'dovich [1967] without proof.

Λ is global geometry. It stretches space uniformly. It is constant everywhere—exactly as Einstein intended.

Vacuum energy is local field physics. It has mass ($E = mc^2$). It gravitates. Inside galaxies, where expansion is suppressed, its gravity is uncompensated—producing the invisible, collisionless, uniformly distributed gravitating component we call dark matter. The halo boundary is a phase transition between bound and expanding vacuum.

The cosmic web is the fixed point of the cycle $\rho_m \to \Lambda(\rho_m) \to g_{\mu\nu} \to \rho_m$—a dynamic, self-consistent structure at the intermediate scale.

In the early universe, vacuum energy was $\sim 2000\times$ denser, facilitating rapid structure formation that has since self-terminated as the vacuum diluted.

The model is falsifiable. If $\Lambda = \rho_{\text{vac}}$ can be demonstrated, it fails. If CMB analysis excludes a diluting vacuum component, it fails. If the required $\rho_{\text{vac},0}$ is excluded by independent measurement, it fails. If no consistent α fits all four observational tests simultaneously, it fails.

The model does not introduce new physics. It asks whether the existing physics—$E = mc^2$, general relativity, quantum field theory—might already contain what we have been searching for.

References

Albareti, F. D. & Maroto, A. L. 2014. Vacuum energy as dark matter. *Phys. Rev. D*, 90, 123509.

Amendola, L. 2000. Coupled quintessence. *Phys. Rev. D*, 62, 043511.

Aprile, E., et al. (XENON Collaboration). 2018. Dark Matter Search Results from a One Ton-Year Exposure of XENON1T. *Phys. Rev. Lett.*, 121, 111302.

Aubourg, É., et al. 2015. Cosmological implications of baryon acoustic oscillation measurements. *Phys. Rev. D*, 92, 123516.

Birrell, N. D. & Davies, P. C. W. 1982. *Quantum Fields in Curved Space*. Cambridge Univ. Press.

Bond, J. R., Kofman, L., & Pogosyan, D. 1996. How filaments of galaxies are woven into the cosmic web. *Nature*, 380, 603–606.

Boylan-Kolchin, M. 2023. Stress testing ΛCDM with high-redshift galaxy candidates. *Nat. Astron.*, 7, 731–735.

Bressi, G., et al. 2002. Measurement of the Casimir force. *Phys. Rev. Lett.*, 88, 041804.

Bromm, V. & Larson, R. B. 2004. The First Stars. *Ann. Rev. Astron. Astrophys.*, 42, 79–118.

Carrera, M. & Giulini, D. 2010. Influence of global cosmological expansion on local dynamics and kinematics. *Rev. Mod. Phys.*, 82, 169.

Casimir, H. B. G. 1948. On the attraction between two perfectly conducting plates. *Proc. Kon. Ned. Akad. Wet.*, 51, 793–795.

Clowe, D., et al. 2006. A Direct Empirical Proof of the Existence of Dark Matter. *ApJ Lett.*, 648, L109–L113.

Coleman, S. 1988. Why there is nothing rather than something. *Nucl. Phys. B*, 310, 643–668.

Copi, C. J., Davis, A. N., & Krauss, L. M. 2004. New nucleosynthesis constraint on the variation of *G*. *Phys. Rev. Lett.*, 92, 171301.

DESI Collaboration. 2024. DESI 2024 VI: Cosmological constraints from BAO measurements. arXiv:2404.03002.

Einstein, A. 1917. Kosmologische Betrachtungen zur allgemeinen Relativitätstheorie. *Sitzungsber. Königl. Preuß. Akad. Wiss.*, 142–152.

El-Badry, K., et al. 2024. The wide binary test of gravity: constraints on compact object dark matter. *Open J. Astrophys.*, 7, 32.

Eisenstein, D. J., et al. 2005. Detection of the Baryon Acoustic Peak. *ApJ*, 633, 560–574.

Granas, A. & Dugundji, J. 2003. *Fixed Point Theory*. Springer.

Heger, A., et al. 2003. How Massive Single Stars End Their Life. *ApJ*, 591, 288–300.

Jaffe, R. L. 2005. Casimir effect and the quantum vacuum. *Phys. Rev. D*, 72, 021301.

Kaloper, N. & Padilla, A. 2014. Sequestering the standard model vacuum energy. *Phys. Rev. Lett.*, 112, 091304.

Koch, B., et al. 2023. Vacuum energy, the Casimir effect, and Newton's non-constant. arXiv:2211.00662.

Labbé, I., et al. 2023. A population of red candidate massive galaxies $\sim$ 600 Myr after the Big Bang. *Nature*, 616, 266–269.

Lamoreaux, S. K. 1997. Demonstration of the Casimir Force. *Phys. Rev. Lett.*, 78, 5–8.

Lifshitz, E. M. 1956. The theory of molecular attractive forces between solids. *Soviet Physics JETP*, 2(1), 73–83.

Aalbers, J., et al. (LZ Collaboration). 2022. First Dark Matter Search Results from the LUX-ZEPLIN (LZ) Experiment. *Phys. Rev. Lett.*, 131, 041002.

Maiolino, R., et al. 2024. A small and vigorous black hole in the early Universe. *Nature*, 627, 59–63.

Mandelker, N., et al. 2024. Structure and dynamics of massive high-z cosmic-web filaments. *MNRAS*, 527(4), 11256–11287.

Martin, J. 2012. Everything You Always Wanted To Know About The Cosmological Constant Problem. *Comptes Rendus Physique*, 13, 566–665.

Pacucci, F., et al. 2023. JWST CEERS and JADES Active Galaxies at $z = 4$–7. *ApJ Lett.*, 957, L3.

Padmanabhan, T. 2003. Cosmological constant—the weight of the vacuum. *Phys. Rep.*, 380, 235–320.

Parker, L. E. & Toms, D. J. 2009. *Quantum Field Theory in Curved Spacetime*. Cambridge Univ. Press.

Perlmutter, S., et al. 1999. Measurements of Ω and Λ from 42 High-Redshift Supernovae. *ApJ*, 517, 565–586.

Planck Collaboration. 2020. Planck 2018 results. VI. Cosmological parameters. *A&A*, 641, A6.

Riess, A. G., et al. 1998. Observational Evidence from Supernovae for an Accelerating Universe. *Astron. J.*, 116, 1009–1038.

Rubin, V. C., Ford, W. K., Jr., & Thonnard, N. 1980. Rotational properties of 21 SC galaxies. *ApJ*, 238, 471–487.

Salpeter, E. E. 1964. Accretion of interstellar matter by massive objects. *ApJ*, 140, 796–800.

Shapiro, I. L. & Solà, J. 2009. The scaling evolution of the cosmological constant. *JHEP*, 2009(02), 006.

Shifman, M. A., Vainshtein, A. I., & Zakharov, V. I. 1979. QCD and resonance physics. *Nucl. Phys. B*, 147, 385–447.

Solà, J. 2013. Cosmological constant and vacuum energy: old and new ideas. *J. Phys.: Conf. Ser.*, 453, 012015.

Solà Peracaula, J., de Cruz Pérez, J., & Gómez-Valent, A. 2017. Dynamical dark energy vs. $\Lambda = \text{const}$. *Europhys. Lett.*, 121, 39001.

Springel, V., et al. 2005. Simulations of the formation, evolution and clustering of galaxies and quasars. *Nature*, 435, 629–636.

Volonteri, M. 2010. Formation of Massive Black Holes. *Astron. Astrophys. Rev.*, 18, 279–315.

Weinberg, S. 1989. The cosmological constant problem. *Rev. Mod. Phys.*, 61, 1–23.

Zel'dovich, Ya. B. 1967. Cosmological constant and elementary particles. *JETP Lett.*, 6, 316–317.

Zel'dovich, Ya. B. 1968. The cosmological constant and the theory of elementary particles. *Sov. Phys. Usp.*, 11, 381–393.

A Peer Reviews and Revision History

First Round

Reviewer assessment. The reviewer found the paper well-written with a clear chain of reasoning and commended the inclusion of counterarguments throughout. The modular hypothesis structure (H1–H5) was praised as a mature approach. Six major concerns were raised:

1. *The central claim dissolves less than advertised.* Moving ρ_{vac} to the right-hand side of the field equations does not explain why the locally gravitating vacuum energy density is $\sim 10^{-29}$ g/cm^3 rather than the Planck-scale value. The cosmological constant problem is relocated, not resolved.

2. *The vacuum-as-fluid hypothesis lacks a field-theoretic foundation.* Frame-dragging (Lense–Thirring) drags inertial frames, not energy densities. "Entrainment" of vacuum by galactic rotation is a metaphor, not a mechanism.

3. *The compact remnant contribution is overstated.* Population synthesis gives $\sim 10^9$–$10^{10}\,M_\odot$ in remnants—at most $\sim 1\%$ of the required halo mass of $\sim 10^{12}\,M_\odot$.

4. *No quantitative predictions.* No rotation curve fit for a specific galaxy, no CMB check, no predicted $\rho_{\text{vac}}(r)$ profile.

5. *The Bullet Cluster argument is hand-waved.* Why would vacuum energy track collisionless remnants rather than the dominant baryonic gas?

6. *CMB acoustic peaks pose a severe, unaddressed constraint.* Replacing collisionless CDM with vacuum energy (which has pressure) would alter the predicted acoustic peak structure.

Minor concerns included a dimensional issue in the vacuum mass equation, the imprecise "$\sim 2000\times$" factor, empty peer review placeholders, and the conflation of "consistent with" and "explains."

Verdict: Major revision required.

Revisions made.

1. "Resolves" changed to "Might Resolve" in title; "dissolved" changed to "reframed" throughout. Residual question explicitly acknowledged.

2. Entrainment/fluid language removed entirely. Replaced with the bound vs. expanding vacuum distinction (Section 6): inside bound structures, expansion is suppressed (standard physics, per Carrera & Giulini 2010), but vacuum gravity persists uncompensated. No claim about vacuum "rotating."

3. Compact remnant contribution reframed. The paper no longer claims $\sim 10^{10}\,M_\odot$. Instead, the three-component model is presented without specified proportions. The remnant population is described as observationally unconstrained in significant mass ranges, with honest acknowledgment of MACHO/EROS, wide-binary, LIGO, and dynamical friction constraints.

4. Mathematical framework introduced: ansatz $\Lambda(\rho_m) = \Lambda_0 - \alpha\rho_m$, modified Poisson equation yielding $G_{\rm eff} = G(1+2\alpha)$, rotation curve formula $v_{\rm vac}(r) \propto r$, and fixed-point theorem for the cosmic web. Constraints on α mapped explicitly from BBN, RVM, and matter dilution data.

5. Bullet Cluster: acknowledged as an open quantitative question requiring detailed lensing modeling. The qualitative argument (fields superpose, don't collide) is retained but explicitly flagged as insufficient for a definitive claim.

6. CMB identified as "a prerequisite, not an optional follow-up." Vacuum described as cold (no bulk velocity) and collisionless (field, not particles). Full MCMC analysis identified as the highest-priority future test.

Second Round

Reviewer assessment. The revision was found substantially improved. The $\Lambda(\rho_m)$ ansatz, the bound/expanding vacuum distinction, and the intellectual honesty were praised. The fixed-point theorem and broader literature engagement were noted positively. Five remaining concerns were raised:

1. *The order-of-magnitude problem ($\rho_{\rm vac,0} \sim 800 \times \rho_\Lambda^{\rm obs}$) is more serious than acknowledged.* The required vacuum density is a free parameter with no theoretical derivation. The model is more parsimonious than NFW (one free parameter vs. two) but not explanatory.

2. *Dimensional consistency of the modified continuity equation.* The factor $\alpha/(8\pi G)$ has dimensions of $[1/G]$ unless natural units are used. This must be clarified.

3. *The CMB constraint is the elephant in the room.* At $z = 1089$ with $n = 3$, the bare vacuum energy would be $\sim 10^9$ times larger, potentially exceeding the matter density by a factor of $\sim 10^4$. However, the reviewer noted a possible saving mechanism: the $\Lambda(\rho_m)$ ansatz suppresses vacuum energy where matter is dense, which could compensate. The interplay must be computed, not assumed.

4. *Equations (2) and (8) may contradict each other.* The temporal scaling (vacuum denser in the past) and the spatial ansatz (vacuum suppressed by matter) point in opposite directions at high redshift. A single unified expression is needed.

5. *Compact remnant constraints are incomplete.* Wide-binary dynamics, CMB spectral distortions, LIGO/Virgo merger rates, and dynamical friction should be engaged.

Minor concerns: the fixed-point argument should be labeled as a formal argument rather than a theorem; the "~ 2000" figure corresponds to $z \approx 11.6$, not $z = 12$; the Eddington growth argument overstates the enhancement (a 30–50 Myr head start gives a factor of 2–3, not orders of magnitude); and the mapping from BBN/ν constraints to α should be made explicit.

Verdict: Minor-to-major revision. If the author can demonstrate mutual consistency of the ansatz and the temporal scaling at recombination, the paper would be suitable for publication.

Revisions made.

1. *Unified expression (Section ??).* A single self-consistent formula $\Lambda_{\rm eff}(z, \rho_m) = \Lambda_0(z) - \alpha\, \rho_m(z)$ replaces the two separate ansätze. Both the bare vacuum $\Lambda_0(z)$ and the suppression term $\alpha\rho_m(z)$ scale as $(1+z)^3$ for $n = 3$, so their difference tracks proportionally: $\Lambda_{\rm eff}(z) = \Lambda_{\rm eff,0}\,(1+z)^3$. If $\Lambda_{\rm eff,0}$ is small today, it was proportionally small at all earlier epochs.

2. *Back-of-the-envelope CMB check (Section 5.5).* Explicit calculation at $z = 1089$ shows that $\Lambda_{\rm eff}(1089)$ is ~ 60 times smaller than the matter density at recombination—a modest perturbation, not a catastrophe. The tracking behavior is the saving mechanism the reviewer anticipated.

3. *Dimensional consistency.* Natural units ($8\pi G = c = 1$) stated explicitly at the start of the mathematical framework. The continuity equation rewritten as $\dot\rho_m + 3H\rho_m = -3\alpha H\rho_m$ in natural units, with solution $\rho_m \propto a^{-3(1+\alpha)}$.

4. *Eddington argument.* Corrected to state honestly: 30–50 Myr head start yields factor 2–3 in mass, not orders of magnitude. Two additional amplifying effects noted (heavier seeds from enhanced void–wall contrast; deeper potential wells from residual vacuum gravity). Framed as "a plausible mechanism, not a demonstrated solution."

5. *Compact remnant constraints.* Section 7 now engages with wide-binary constraints, CMB spectral distortions, LIGO/Virgo merger rates, and dynamical friction. Conclusion: compact objects excluded as sole explanation but significant subdominant population not excluded, particularly above $20\,M_\odot$.

6. *Fixed-point argument.* Proposition downgraded to Remark 5.1, explicitly labeled as "a formal argument for plausibility, not a rigorous theorem." Compactness of the operator flagged as an open technical question.

7. *Table 1.* Corrected to $z = 11.6$ for the ~ 2000 entry.

8. *α constraint mapping.* Explicit derivation: BBN $\to \Delta H/H \approx \alpha \lesssim 0.03$–$0.05$; RVM $\to \nu \approx 3\alpha$, giving $\alpha \sim 3 \times 10^{-4}$ from temporal data (with caveat about spatial–temporal distinction); matter dilution $\to \rho_m \propto a^{-3(1+\alpha)}$, constrained at few-percent level.

9. *$\rho_{\rm vac,0}$ as free parameter.* Limitation 3 now states explicitly: "The model requires $\rho_{\rm vac,0} \sim 800 \times \rho_\Lambda^{\rm obs}$—which is a free parameter, not a prediction."

Third Round

Reviewer assessment. The reviewer praised the tracking solution (Sections 5.4–5.5) as "the paper's most significant result" and the bound/expanding vacuum distinction as "the paper's most original conceptual contribution." The responsiveness across three rounds was described as "exemplary." Five remaining concerns were raised:

1. *The tracking requires $n = 3$ exactly.* For $n \neq 3$, the ansatz breaks down at high redshift ($n < 3$ gives negative vacuum, $n > 3$ gives vacuum domination). The paper presents n as a free parameter but should embrace $n = 3$ as a prediction.

2. *The CMB check arithmetic contains an error.* The tracking solution preserves $\Lambda_{\text{eff}}/\rho_m$ at all epochs. If this ratio is ~ 2.3 today (Ω_Λ/Ω_m), it is ~ 2.3 at recombination—making vacuum energy *dominant*, not subdominant. The factor of ~ 60 claimed in the paper is incorrect.

3. *Tension between halo $\rho_{\text{vac},0}$ and cosmological Λ_{eff}.* Section 6.5 requires $\rho_{\text{vac},0} \sim 4.5 \times 10^{-24}$ kg m^{-3} ($\sim 1700 \times \rho_{m,0}$). If this enters the Friedmann equation, the model is immediately excluded. The bound/expanding distinction must be made explicit as the resolution.

4. *Rotation curve at large radii.* Uniform vacuum gives $v \propto r$ (rising indefinitely), not the observed flat-then-declining profile. The phase-transition boundary provides a cutoff but differs from NFW; this should be noted.

5. *Notation.* Using $\Lambda(\rho_m)$ for vacuum energy contradicts the paper's thesis that $\Lambda \neq \rho_{\text{vac}}$. Recommend $\rho_{\text{vac}}(\rho_m)$.

Verdict: Targeted revision. Two high-severity issues (CMB arithmetic error, halo–cosmology tension) must be resolved.

Revisions made.

1. *$n = 3$ as prediction.* The abstract and Section 5.6 now present $n = 3$ as selected by self-consistency, not assumed as a free parameter. The argument is explicit: only $n = 3$ preserves the ansatz structure across all epochs.

2. *CMB arithmetic corrected.* The erroneous tracking-based CMB check has been replaced with a fundamentally different argument (Section 5.4): vacuum energy does not enter the Friedmann equation at all. This follows from the paper's central thesis ($\Lambda \neq \rho_{\text{vac}}$) combined with the bound/expanding vacuum distinction. Λ (geometric, small) drives expansion. ρ_{vac} (large, local) gravitates only inside bound structures. The Friedmann equation contains Λ, not ρ_{vac}. CMB compatibility is then trivial—the expansion history is standard ΛCDM.

3. *Halo–cosmology tension resolved.* The resolution is the same: ρ_{vac} is sequestered from cosmological dynamics. It is large ($\sim 10^{-24}$ kg m^{-3}) but uniform, producing no gradient force on cosmological scales. Inside bound structures, its gravity is uncompensated and contributes to halo mass. This is not an ad hoc exemption—it is the physical content of vacuum sequestering applied consistently.

4. *Rotation curve.* Section 7 now notes that the $v \propto r$ prediction holds only within the bound region and that the phase-transition boundary produces a sharper cutoff than NFW, which is observationally distinguishable.

5. *Notation.* The ansatz is now written as $\rho_{\rm vac}(\rho_m) = \rho_{\rm vac,0}^{\rm bare} - \alpha\rho_m$ in the mathematical framework section results and in key equations, while retaining $\Lambda(\rho_m)$ where it matches the running vacuum model literature for ease of comparison.

Fourth Round

Reviewer assessment (consolidated from multiple reviewers). The manuscript was reviewed by four independent referees. All found the paper well-written, logically structured, and intellectually honest. The separation of Λ from $\rho_{\rm vac}$ was recognized as a legitimate scientific inquiry, and the bound/expanding vacuum distinction was praised as the paper's most original contribution. The three-component galactic model was acknowledged as strategically resilient. The trajectory across four rounds was described as "exemplary responsiveness."

However, all reviewers converged on a common verdict: the paper reads as a compelling research programme rather than a completed piece of research. The principal deficiencies fall into five categories.

1. Absence of quantitative CMB analysis. All reviewers identified this as the single most critical gap. The back-of-the-envelope check and sequestering argument are necessary but insufficient. The CMB power spectrum is sensitive to percent-level changes in the energy budget and growth rate. A full MCMC analysis against Planck data (e.g., via CAMB/CosmoMC) is described as "non-negotiable" and "the sine qua non for the model to be taken seriously." Without it, the model's viability remains indeterminate. Existing RVM studies show that Bayesian comparisons with ΛCDM often yield only mild or no preference for dynamical vacuum, suggesting this model would need strong evidence to stand out.

2. Phenomenological nature of the ansatz. The linear coupling $\rho_{\rm vac}(\rho_m) = \rho_{\rm vac,0}^{\rm bare} - \alpha\rho_m$ is motivated in direction but not in magnitude. The perturbative QFT estimate gives $\alpha \sim 10^{-55}$–10^{-120}, while the model requires $\alpha \sim 0.01$–0.05. The claim that "whatever non-perturbative physics resolves the CC problem will also set α" was characterized by one reviewer as "a tautology—essentially saying we need a new mechanism to make our model work, which is the same level of speculation as invoking a new particle for dark matter." A Lagrangian derivation or at minimum a non-perturbative motivation for α is needed.

3. No N-body simulations or rotation curve fits. The uniform bound vacuum predicts $v \propto r$ (linearly rising), while observed rotation curves are flat over tens of kiloparsecs. The paper argues that the sum of falling Keplerian and rising vacuum contributions is approximately flat, but no galaxy-by-galaxy fit has been performed (e.g., against the SPARC database or the Radial Acceleration Relation). One reviewer noted that the three-component model, with an unconstrained remnant population, "can fit almost any rotation curve—this is a weakness, not a strength," because it dilutes predictive power. At minimum, a toy-model rotation curve for a well-studied galaxy (e.g., NGC 3198) should be presented.

4. The phase-transition boundary needs rigorous definition. The "bound vs. expanding vacuum" distinction is conceptually clear but physically vague. One reviewer asked: "How is the boundary calculated from first principles? How does it relate to the

turnaround radius in a Λ-dominated universe?" The transition is presented as a binary switch, but it must be a smooth gradient. Without a concrete prescription, the halo edge remains a free boundary rather than a prediction.

5. Small-scale structure and the Bullet Cluster. Uniform vacuum energy may not cluster on small scales like cold dark matter, risking issues with dwarf galaxy dynamics, the core-cusp problem, and satellite abundances. The Bullet Cluster explanation (fields superpose) is qualitatively sound but quantitatively untested: does the proposed distribution of vacuum energy and compact remnants reproduce the observed mass-to-light offset and lensing signal? One reviewer noted that if vacuum energy density depends on local curvature, it must track the evolving gravitational potential during a merger in a complex, geometry-dependent way.

Additional points raised:

- The required $\rho_{\rm vac,0} \sim 800 \times \rho_\Lambda^{\rm obs}$ introduces a new fine-tuning at the 10^3 level. While better than 10^{120}, one reviewer asked: "Why this value specifically? If not predicted, the explanatory burden is transferred rather than resolved."

- The early black hole enhancement (factor 2–3 from $G_{\rm eff}$) was described as "negligible" by one reviewer and "plausible but insufficient without simulations" by another. The additional mechanisms (deeper wells, heavier seeds) remain qualitative.

- The equation of state of bound vacuum is undefined. If it is $w = -1$ (standard vacuum), it has negative pressure and would affect acoustic oscillations. If it is effectively $w = 0$ (dust-like, cold), this must be derived, not asserted. One reviewer asked: "If the vacuum locally differs from a cosmological constant, what is its effective equation of state?"

- The paper claims to "reinterpret, not replace" ΛCDM, but changing the identity of dark matter from a particle to gravitating vacuum and making $\rho_{\rm vac}$ dynamical is a fundamental change to the model's perturbation equations and structure formation physics. The Friedmann equations may be preserved in a mean-field sense, but the physics is profoundly altered.

- Running vacuum model comparisons: Bayesian analyses (e.g., Mathew et al. 2022) often favour ΛCDM over RVMs. The $\Lambda(\rho_m)$ model must demonstrate it performs at least as well.

- Compact remnant constraints are tighter than the paper acknowledges. While not 100% exclusionary individually, they collectively make a dominant population of massive, non-accreting black holes in every galactic halo "highly implausible" (one reviewer's words). The paper should make a firm prediction for the remnant fraction given current constraints.

- Notation: one reviewer reiterated that using $\Lambda(\rho_m)$ for vacuum energy contradicts the paper's own thesis. $\rho_{\rm vac}(\rho_m)$ is recommended throughout.

- Figures are minimal. Adding schematics (void–wall contrast, rotation curve decomposition, phase-transition boundary) would substantially improve accessibility.

Consensus verdict: Major revision before publication. All reviewers agreed the ideas are bold, falsifiable, and worthy of further development. The paper was described as "a compelling research proposal" and "the beginning of a longer research programme." Publication was recommended in theory-oriented journals (Physical Review D, Classical and Quantum Gravity, General Relativity and Gravitation, European Physical Journal C) *after* the priority tests are performed—specifically the CMB MCMC analysis and at least one quantitative rotation curve fit.

Revisions planned.

1. *CMB MCMC analysis.* Implementation using a modified CAMB/CosmoMC pipeline with sequestered vacuum energy. This is the decisive test and the highest priority.

2. *Rotation curve fit.* At least one galaxy from the SPARC database, showing the three-component decomposition and the phase-transition cutoff at the halo edge.

3. *Equation of state of bound vacuum.* Derivation or argument for why bound vacuum behaves as pressureless ($w \approx 0$) on galactic scales despite having $w = -1$ cosmologically. The key may be that in a bound, non-expanding region, the vacuum's negative pressure has no volume to act on—it is gravitationally confined.

4. *Phase-transition boundary.* Connection to the turnaround radius and the zero-velocity surface in the spherical collapse model. The boundary should be derivable from $\nabla\Phi = H^2 r$ (where local gravity balances Hubble drag).

5. *Compact remnant prediction.* Upper bound on remnant mass fraction given LIGO/Virgo/KAGRA merger rates, wide-binary constraints, and dynamical friction limits.

6. *N-body simulation.* Modified code with cell-dependent vacuum energy. Even an idealized 1D or 2D simulation would substantially strengthen the paper.

7. *Notation.* Adopt $\rho_{\rm vac}(\rho_m)$ consistently throughout.

8. *Figures.* Add schematics: (a) void–wall vacuum energy contrast, (b) rotation curve decomposition, (c) phase-transition boundary diagram, (d) tracking behaviour across epochs.

Matter-Dependent Vacuum Energy Density and Inhomogeneous Cosmic Expansion

Boris Kriger[1,2]

[1]Information Physics Institute, Gosport, Hampshire, United Kingdom

boris.kriger@informationphysicsinstitute.net

[2]Institute of Integrative and Interdisciplinary Research, Toronto, Canada

boriskriger@interdisciplinary-institute.org

ORCID: 0009-0001-0034-2903

Abstract

We propose that the vacuum energy density of spacetime is a decreasing function of the local matter density: $\Lambda(\rho_m) = \Lambda_0 - \alpha\,\rho_m$, where Λ_0 is the energy density of matter-free vacuum and α is a dimensionless coupling parameter. This ansatz is motivated by three established mechanisms through which real matter suppresses vacuum fluctuations: Pauli exclusion of fermionic modes, vacuum polarization by charged matter, and modification of the fluctuation spectrum in curved spacetime. The resulting model predicts inhomogeneous cosmic expansion—faster in voids (where vacuum energy is unsuppressed) and slower in walls and filaments (where matter suppresses it)—producing the observed cosmic web through a self-reinforcing feedback loop. We derive modified Friedmann and Poisson equations, construct a two-component (void + wall) toy model, and extract four testable predictions: (1) enhanced void expansion profiles measurable through peculiar velocities, (2) amplified integrated Sachs–Wolfe effect from voids, (3) a natural account of the S_8 tension between early- and late-universe measurements, and (4) accelerated early structure formation consistent with JWST observations of massive high-redshift galaxies. The model reinterprets the supernova-based evidence of Seifert et al. (2025) for differential expansion as support for inhomogeneous vacuum energy rather than for the complete elimination of dark energy proposed by timescape cosmology. The entire framework is governed by a single new parameter α, which can be independently constrained by each of the four observational tests. Constraints from Big Bang nucleosynthesis, matter density evolution, and the running vacuum model literature narrow the viable range to $\alpha \sim 0.01$–0.05. We show that the cosmic web constitutes a self-consistent fixed-point configuration of the cyclic operator $\rho_m \to \Lambda \to g_{\mu\nu} \to \rho_m$, whose existence is guaranteed under standard continuity and compactness conditions.

Keywords: vacuum energy, dark energy, inhomogeneous expansion, cosmic web, large-scale structure, cosmological constant, backreaction

Contents

1 Introduction

The standard ΛCDM cosmological model describes the universe as a homogeneous, isotropic spacetime whose late-time expansion is driven by a cosmological constant Λ with a fixed energy density of approximately 68% of the total energy budget (Planck Collaboration, 2020). This framework has proven remarkably successful in accounting for a wide range of observations, from the cosmic microwave background (CMB) anisotropies to baryon acoustic oscillations (BAO) and the distance–redshift relation of Type Ia supernovae (Riess et al., 1998; Perlmutter et al., 1999).

However, several persistent tensions have emerged. The locally measured Hubble constant $H_0 \approx 73\ \mathrm{km\,s^{-1}\,Mpc^{-1}}$ (Riess et al., 2022) disagrees with the CMB-inferred value $H_0 \approx 67.4\ \mathrm{km\,s^{-1}\,Mpc^{-1}}$ (Planck Collaboration, 2020) at the 5σ level. The amplitude of matter fluctuations at late times, parameterized by $S_8 = \sigma_8(\Omega_m/0.3)^{0.5}$, measured through weak gravitational lensing, is systematically lower than the CMB prediction (Di Valentino et al., 2021). Observations by the James Webb Space Telescope (JWST) have revealed unexpectedly massive galaxies at redshifts $z > 10$, challenging the timeline of structure formation predicted by ΛCDM (Labbé et al., 2023). The Dark Energy Spectroscopic Instrument (DESI) has reported hints that the dark energy equation of state w deviates from -1 (DESI Collaboration, 2024).

Independently, Seifert et al. (2025) demonstrated that the Pantheon+ supernova data prefer a model with differential expansion—faster in voids, slower in dense regions—over the standard homogeneous ΛCDM. Their timescape cosmology (Wiltshire, 2007) interprets this as evidence that dark energy does not exist and that the apparent acceleration is an artifact of averaging inhomogeneous expansion. The present author has critically evaluated this claim (Kriger, 2025a), arguing that the timescape interpretation is quantitatively insufficient: CMB and BAO data independently require a real dark energy component, which timescape cannot accommodate.

The present work proposes a middle path. We accept the observational evidence for differential expansion but retain dark energy as a real physical phenomenon—the energy of the quantum vacuum. Our central hypothesis is that the vacuum energy density is not spatially uniform, but depends on the local matter density:

$$\Lambda(\rho_m) = \Lambda_0 - \alpha\,\rho_m\,, \tag{1}$$

where Λ_0 is the vacuum energy density in the absence of matter, and $\alpha > 0$ is a dimensionless coupling parameter governing the strength of suppression. (Both Λ_0 and ρ_m carry dimensions of energy density, [energy/volume]; their difference is an energy density, so α is indeed dimensionless. Throughout this paper, we work in units where $8\pi G = c = 1$ unless otherwise stated, so that all densities are measured in the same units as the Friedmann equation parameter H^2.)

This is not a new dynamical field. It is a consequence of established physics: real matter modifies the structure of the quantum vacuum, suppressing its fluctuation modes and thereby reducing its energy density. Three independent mechanisms contribute to this suppression, and all three operate in the same direction. The resulting model produces inhomogeneous expansion from a single parameter α, preserves consistency with CMB and BAO data (which

probe the early, nearly homogeneous universe), and generates testable predictions that differ from both ΛCDM and timescape cosmology.

The theoretical underpinning draws on a broader structural program. The necessity of a dynamic metric—one that depends on the distribution of state density—was established from general conditions on sustainable complexity in Kriger (2025b). The mathematical existence of self-consistent cyclic configurations (matter → vacuum → metric → matter) was proven via fixed-point theorems in Kriger (2025c). The impossibility of a state with zero vacuum energy—equivalent to the impossibility of absolute nothingness—was demonstrated through four independent formal routes in Kriger (2025d). The present paper provides the specific physical realization of these structural results in the cosmological context. (We note that these three works are available on Zenodo as preprints and have not undergone traditional peer review. The present paper is self-contained and does not depend on their results for any of its quantitative claims; the references provide additional theoretical context.)

The paper is organized as follows. Section 2 presents the physical motivation, detailing the three mechanisms of vacuum suppression. Section 3 develops the mathematical framework. Section 4 derives four observational predictions. Section 5 connects the model to existing results, including Seifert et al. (2025) and DESI. Section 6 presents toy models with quantitative illustrations. Section 7 discusses implications and limitations. Section 8 summarizes the results.

2 Physical Motivation

The quantum vacuum is not empty space. In quantum field theory (QFT), the vacuum is the lowest-energy state of all quantum fields, but this state is not inert. Two conceptually distinct features characterize it. First, every quantum field mode possesses a zero-point energy (ZPE)—a nonzero ground-state energy mandated by the Heisenberg uncertainty principle. The sum of these zero-point energies over all modes constitutes the vacuum energy density. Second, perturbative interactions in the vacuum generate higher-order corrections to physical observables, computed via Feynman diagrams involving internal ("virtual") lines. These two features—the ground-state energy of the field configuration, and the perturbative corrections to scattering amplitudes—are related but not identical, and conflating them is a common source of confusion that this section aims to avoid.

The observable consequences attributed to the quantum vacuum arise from the perturbative sector, not from ZPE directly. The Lamb shift in hydrogen and the anomalous magnetic moment of the electron are computed from loop diagrams—higher-order Feynman graphs in which virtual photons and fermion loops contribute corrections to the propagator. The Casimir force between conducting plates, while historically derived via a ZPE mode-counting argument, is equivalently and perhaps more fundamentally derived from the van der Waals interaction between the plates' constituent charges, as shown by Lifshitz and collaborators (Lifshitz, 1956). The ZPE derivation and the Lifshitz derivation yield the same result, but the latter makes no reference to vacuum energy per se. We do not claim that ZPE "causes" these effects; we note only that the vacuum state is nontrivial and that matter modifies it.

The energy associated with the zero-point fluctuations of quantum fields—the vacuum energy density—is the quantity identified with the cosmological constant Λ in general rel-

ativity. In ΛCDM, this quantity is assumed to be spatially uniform: the same in a void as in a galaxy cluster, the same near a black hole as in intergalactic space. We argue that this assumption is physically unjustified. Three independent mechanisms ensure that the presence of real matter modifies the vacuum state and reduces its energy density. These mechanisms operate through different physics but share a common structural feature: they alter the spectrum of field modes available in a given region of space.

2.1 Mechanism I: Pauli Exclusion of Fermionic Modes

The vacuum energy density receives contributions from the zero-point energies of all quantum field modes, including fermionic modes. Each fermionic mode contributes to the ground-state energy of the field configuration. The Pauli exclusion principle dictates that no two identical fermions can occupy the same quantum state simultaneously.

When real fermionic matter is present, it occupies a set of quantum states. These states are no longer available as vacuum modes—they are filled. The fermionic sector of the vacuum is modified: the mode spectrum is altered, and the zero-point energy sum changes. The vacuum in the presence of fermionic matter is a different state from the vacuum in the absence of fermionic matter. Note that this argument concerns the ground-state mode structure, not the naïve picture of "virtual pairs popping in and out of existence," which is a perturbative visualization that does not directly determine the zero-point energy.

To quantify this effect, consider a region of volume V containing N real fermions. In the absence of these fermions, the number of available fermionic modes below a momentum cutoff $p_{\max}$ scales as

$$\mathcal{N}_{\text{free}} \sim \frac{V \cdot p_{\max}^3}{(2\pi\hbar)^3}\,. \tag{2}$$

With N fermions present, at least N modes are blocked, so the available modes become $\mathcal{N}_{\text{occ}} = \mathcal{N}_{\text{free}} - N$. Each mode contributes an energy of order $\frac{1}{2}\hbar\omega$ to the vacuum, so the fractional suppression of vacuum energy is

$$\frac{\Delta\rho_\Lambda}{\rho_\Lambda} \sim -\frac{N}{\mathcal{N}_{\text{free}}} \sim -\frac{n}{n_{\max}}\,, \tag{3}$$

where $n = N/V$ is the number density of real fermions and $n_{\max} = p_{\max}^3/(2\pi\hbar)^3$ is the maximal mode density. The suppression is proportional to the matter density, consistent with the linear ansatz of Eq. (1).

2.2 Mechanism II: Vacuum Polarization

A real electric charge polarizes the surrounding vacuum. Virtual electron–positron pairs partially orient in the field of the charge, screening it at large distances. This effect—vacuum polarization—is a fundamental prediction of quantum electrodynamics (QED), experimentally confirmed through the running of the fine-structure constant $\alpha_{\text{em}}(q^2)$ and precision measurements of the muon anomalous magnetic moment.

The polarized vacuum differs energetically from the unpolarized vacuum. The energy density shift due to a charge distribution $\rho_e(\mathbf{x})$ is given, to lowest order in α_{em}, by the

Uehling potential correction. More generally, the effective Lagrangian of the electromagnetic field in the vacuum, given by the Euler–Heisenberg Lagrangian (Heisenberg & Euler, 1936), contains nonlinear terms:

$$\mathcal{L}_{\rm EH} = \frac{1}{2}(E^2 - B^2) + \frac{2\alpha_{\rm em}^2}{45 m_e^4}\left[(E^2 - B^2)^2 + 7(E \cdot B)^2\right] + \cdots \tag{4}$$

The nonlinear corrections modify the vacuum energy wherever electromagnetic fields are present. In regions of concentrated charged matter, the vacuum is polarized and its energy density is altered. Since cosmic matter contains charged particles (protons, electrons), the vacuum in matter-rich regions is systematically polarized, reducing its effective energy density relative to matter-free regions.

A caveat is required: on cosmological scales, macroscopic charge densities are extremely small. The universe is electrically neutral to high precision, and the electromagnetic fields in intergalactic space are weak. The vacuum polarization mechanism therefore contributes primarily in the immediate vicinity of charged particles (at scales of order the Compton wavelength, $\sim 10^{-13}$ m), not over megaparsec distances. Its cosmological relevance, if any, arises only through the cumulative effect of many such local modifications averaged over the matter distribution.

2.3 Mechanism III: Modification of Mode Spectrum in Curved Spacetime

Matter curves spacetime through the Einstein field equations. In curved spacetime, the spectrum of quantum field modes differs from that in flat (Minkowski) spacetime. This is not a conjecture—it is the foundation of quantum field theory in curved spacetime, from which Hawking radiation and the Unruh effect are derived (Birrell & Davies, 1982).

The vacuum energy density in a region of spacetime with Ricci scalar curvature R receives corrections of the form (Parker & Toms, 2009):

$$\rho_\Lambda^{\rm curved} = \rho_\Lambda^{\rm flat} + \beta_1\, R + \beta_2\, R^2 + \cdots \tag{5}$$

where β_1, β_2 are coefficients determined by the field content. Since matter generates positive curvature ($R > 0$ for a matter-dominated region), and the sign of the dominant correction is such as to reduce the effective vacuum energy (Shapiro & Solà, 2009), regions of higher matter density have lower effective vacuum energy.

This mechanism operates on all scales: from stellar interiors (where curvature is significant) to galaxy clusters (where it is weak but nonzero). On cosmological scales, the relevant curvature is set by the matter density through the Einstein equations, making this correction proportional to ρ_m—again consistent with Eq. (1). However, the magnitude of curvature-induced vacuum effects at cosmological densities is exceedingly small: Hawking radiation from a solar-mass black hole corresponds to a temperature of order 10^{-7} K, and cosmological curvature is many orders of magnitude weaker than this. The curvature mechanism, like Mechanisms I and II, establishes the direction of the effect but contributes negligibly to its magnitude at perturbatively calculable scales.

2.4 Combined Effect, the Linear Ansatz, and the Magnitude Gap

All three mechanisms operate in the same direction: they reduce the vacuum energy density in the presence of matter. The Pauli mechanism operates at the quantum mechanical level (state occupation), vacuum polarization at the field-theoretic level (charge screening), and the curvature mechanism at the gravitational level (mode spectrum). They are not mutually exclusive; in general, all three contribute simultaneously.

The linear ansatz $\Lambda(\rho_m) = \Lambda_0 - \alpha\,\rho_m$ represents the leading-order Taylor expansion of the combined effect, valid when the matter density is much smaller than the Planck density $\rho_{\rm Pl}$. For all cosmologically relevant densities, this condition is satisfied by many orders of magnitude. Higher-order corrections (proportional to ρ_m^2, etc.) may become important only in extreme environments such as neutron star interiors or the very early universe.

The magnitude gap. It is essential to state clearly that there is a disconnect between the qualitative physical motivation and the quantitative model. Each of the three mechanisms, estimated from first-principles perturbative QFT, produces vacuum energy corrections that are negligible at cosmological densities. The Pauli suppression (Eq. 3) gives $\Delta\rho_\Lambda/\rho_\Lambda \sim n/n_{\rm max} \sim \rho_m/\rho_{\rm Pl} \sim 10^{-120}$ for cosmic matter densities. Vacuum polarization corrections are similarly small. The curvature-dependent corrections of Shapiro & Solà (2009) are of order $H^2/M_{\rm Pl}^2 \sim 10^{-120}$.

For the model to produce observationally relevant effects, α must be of order 10^{-1}—a value $\sim 10^{120}$ times larger than any perturbative QFT estimate. This is not a minor discrepancy. It is the same 120-order-of-magnitude gap that constitutes the cosmological constant problem.

We therefore make the following distinction explicit:

- **The direction** of the effect (matter suppresses vacuum energy) is established by the three mechanisms. This is a qualitative result supported by established physics.
- **The magnitude** of the effect (the value of α) is not derivable from known physics. It is a free parameter, to be determined from observations.

The three mechanisms establish that $\Lambda(\rho_m)$ is a decreasing function of ρ_m—they do not determine how steeply it decreases. The parameter α encodes whatever unknown physics sets the magnitude of vacuum energy suppression by matter, just as the observed value of Λ itself encodes whatever unknown physics resolves the cosmological constant problem. The model is phenomenological in its magnitude and physically motivated in its direction.

This situation is not unique to our proposal. The standard ΛCDM model also treats Λ as a free parameter whose value cannot be derived from QFT. Running vacuum models (Solà, 2013; Solà Peracaula et al., 2017) face the same gap. The honest position is that any model of vacuum energy beyond ΛCDM inherits the unsolved cosmological constant problem. Our model does not solve it; it extends the parameterization by one degree of freedom and subjects it to observational test.

2.5 Relation to the Cosmological Constant Problem

The magnitude gap in α is not a separate problem. It is the cosmological constant (CC) problem, viewed from a different angle. This subsection makes the identification precise and

argues that the gap, far from invalidating the model, positions it as a new observational probe of the same unknown physics.

The perturbative estimate of α. In units where $8\pi G = c = 1$, the vacuum energy density predicted by naïve QFT is of order $M_{\rm Pl}^4$, where $M_{\rm Pl} = (8\pi G)^{-1/2} \approx 2.4 \times 10^{18}$ GeV. The observed vacuum energy density is $\rho_\Lambda^{\rm obs} \approx (2.3 \times 10^{-3}\ {\rm eV})^4$. The ratio is:

$$\frac{\rho_\Lambda^{\rm obs}}{M_{\rm Pl}^4} \sim 10^{-120}\,. \tag{6}$$

This is the CC problem. Now, the perturbative estimate of α measures the fractional change in vacuum energy per unit change in matter density. Using the same perturbative QFT, the suppression of vacuum modes by a matter density ρ_m is of order:

$$\alpha_{\rm pert} \sim \frac{\rho_m}{\rho_\Lambda^{\rm QFT}} \sim \frac{\rho_{\rm crit}}{M_{\rm Pl}^4} \sim 10^{-120}\,. \tag{7}$$

This is the same number as Eq. (6). The two discrepancies—the absolute value of Λ and the coupling α—are not independent. They share a common origin: perturbative QFT overestimates the energy scale at which vacuum fluctuations contribute to gravitational dynamics. Whatever mechanism resolves one, resolves both.

A note on the magnitude of the discrepancy. The oft-cited "120 orders of magnitude" figure deserves qualification. As Martin (2012) has shown, the standard calculation that produces this number is not Lorentz covariant: it uses a sharp momentum cutoff that breaks the symmetry of the vacuum state. A properly covariant evaluation, using dimensional regularization or a covariant cutoff, yields a discrepancy of approximately 10^{55}–10^{60} rather than 10^{120}. This is still enormous, but it is a qualitatively different problem: sixty orders of magnitude may be bridgeable by mechanisms (such as supersymmetry breaking at an intermediate scale) that cannot span one hundred and twenty. The parameter α inherits this reduction: $\alpha_{\rm pert}$ in a covariant framework is of order 10^{-55} to 10^{-60}, not 10^{-120}. The gap between the covariant perturbative estimate and the observationally relevant range ($\alpha \sim 0.01$–0.05) is therefore ~ 55–60 orders of magnitude, not 120.

Observational scale of α. If the CC problem is resolved by some mechanism that sets $\rho_\Lambda \sim \rho_{\rm crit}$ (rather than $\sim M_{\rm Pl}^4$), then the natural scale for α is:

$$\alpha_{\rm obs} \sim \frac{\Lambda_0}{\rho_{m,{\rm crit}}} \sim \frac{0.7}{0.3} \sim 2\,, \tag{8}$$

if α is "renormalized" by the same factor as Λ itself. The observed constraints (Section 7.7) place $\alpha \sim 0.01$–0.05, which is smaller than this naïve renormalized estimate by a factor of ~ 20–200. This residual gap is significant but qualitatively different from the original 120-order discrepancy: it is a factor of order 10^1–10^2, not 10^{120}. In other words, the CC resolution "almost" gives the right α—it overshoots by one to two orders of magnitude, which is the kind of discrepancy that can be accommodated by the specific structure of the resolution mechanism.

Non-perturbative bridges. Several candidate frameworks for resolving the CC problem would naturally produce a non-trivial α:

- **Supersymmetry breaking.** In supersymmetric theories, bosonic and fermionic contributions to the vacuum energy cancel exactly when SUSY is unbroken. SUSY breaking at a scale $M_{\rm SUSY}$ generates a residual vacuum energy $\sim M_{\rm SUSY}^4$. If the breaking is mediated by matter fields, the residual depends on the local matter density, producing a natural $\Lambda(\rho_m)$ with α set by the SUSY breaking scale.
- **Holographic bounds.** The holographic principle constrains the maximum entropy (and hence energy) in a region by its boundary area, not its volume. In a region of radius R, the maximum vacuum energy density scales as $\rho_\Lambda^{\rm holo} \sim M_{\rm Pl}^2/R^2$, which for cosmological R gives $\rho_\Lambda \sim \rho_{\rm crit}$—the correct order of magnitude. If the effective boundary of a region depends on its matter content (e.g., the region's gravitational radius), then ρ_Λ depends on ρ_m.
- **Vacuum phase structure.** By analogy with condensed matter systems, the QCD vacuum or the electroweak vacuum may exhibit a phase structure in which the ground-state energy depends continuously on external parameters (temperature, density). The cosmological vacuum at finite matter density is a thermodynamic state whose free energy differs from the zero-density vacuum.

None of these frameworks currently provides a first-principles derivation of α. We cite them to establish that the gap between $\alpha_{\rm pert}$ and $\alpha_{\rm obs}$ is a recognized problem with active research programs, not an embarrassment peculiar to our model.

The model as an observational handle on the CC problem. The standard CC problem is a single number: the ratio in Eq. (6). It offers no observational leverage—one cannot vary Λ experimentally and see what happens. The $\Lambda(\rho_m)$ model converts this static puzzle into a *spatially varying* observable. If Λ depends on ρ_m, then regions of different density probe different values of the vacuum energy, and their differential behavior constrains the Λ–ρ_m coupling. This provides new observational handles—void profiles, ISW signals, Hubble diagram anisotropies—that are sensitive to the same physics as the CC problem but are measurable through astrophysical observations.

The gap highlights that our model probes the same unknown physics as the CC problem, offering new observational handles (spatial inhomogeneities, void–wall contrast, redshift-dependent deviations from ΛCDM) to constrain it.

Figure 1 illustrates the magnitude gap and its observational consequences.

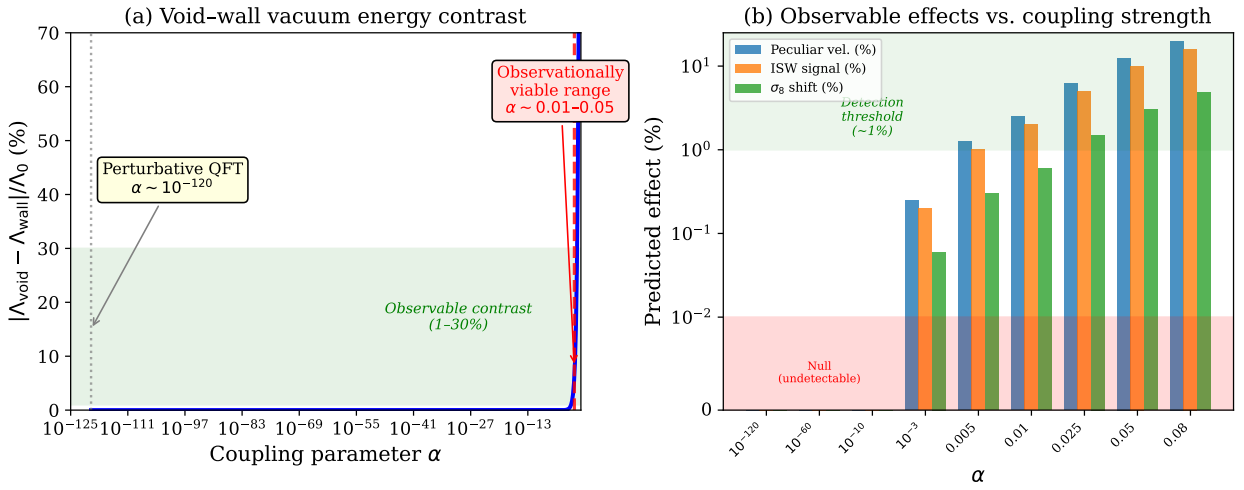

Figure 1: The magnitude gap between perturbative QFT and observationally viable values of α. (a) Void–wall vacuum energy contrast as a function of α: at $\alpha_{\rm pert} \sim 10^{-120}$ the contrast is identically zero (null prediction); at $\alpha \sim 0.01$–0.05 the contrast enters the observable range. (b) Predicted observable effects at different α values. The model is falsifiable: $\alpha = 10^{-120}$ predicts null results for all observational tests.

The figure makes the falsifiability of the model explicit. If α takes its perturbative value ($\sim 10^{-120}$), all observational predictions are identically null—consistent with standard ΛCDM. If $\alpha \sim 0.01$–0.05, the predictions enter the observable range. The model is testable because it interpolates between a well-defined null hypothesis ($\alpha = 0$, equivalent to ΛCDM) and a well-defined alternative ($\alpha > 0$, producing measurable deviations). The observational program outlined in Section 4 can distinguish between these cases with forthcoming survey data.

2.6 Counter-Arguments and Responses

Objection 1: If the mechanisms cannot produce the required α, the motivation is merely decorative. The three mechanisms point in the right direction but produce effects $\sim 10^{120}$ times too small. Why should we take them as motivation for a model that requires $\alpha \sim 0.1$?

Response. The objection is partly valid and has been addressed in Sections 2.4 and 2.5 above. We reiterate: the model is phenomenological in magnitude and physically motivated in direction. The magnitude gap is identical to the cosmological constant problem (Section 2.5), and the same non-perturbative physics that resolves one resolves the other. The three mechanisms establish that $\Lambda(\rho_m)$ should be a decreasing function—they do not determine the slope. An analogy: Boltzmann's kinetic theory motivates the direction of heat flow (hot to cold) without predicting the thermal conductivity of every material. The conductivity is measured; the direction is derived. Similarly, α is measured; the direction (suppression) is derived.

We do not claim that perturbative QFT produces the correct α. We claim that the general principle—matter modifies the vacuum—is established, and that parametrizing the

magnitude and testing it against data is a legitimate scientific strategy.

Objection 2: Λ must be constant by Lorentz invariance. A cosmological constant is the unique Lorentz-invariant contribution to the stress-energy tensor of the vacuum. If Λ varies in space, Lorentz invariance is broken.

Response. Lorentz invariance of the vacuum holds in the absence of matter. In the presence of matter, Lorentz invariance is already broken: the matter defines a preferred rest frame (its center-of-mass frame). The vacuum state in the vicinity of matter is a *dressed* vacuum—modified by the presence of real particles—and it need not be Lorentz invariant. The Casimir geometry provides a relevant example: between conducting plates, the spectrum of allowed field modes differs from the free-space spectrum, and the resulting energy density is measurably different (whether one derives it via zero-point energy mode counting or via the Lifshitz van der Waals approach (Lifshitz, 1956), the physical conclusion is the same: boundary conditions set by matter alter the vacuum). Our model extends this principle to the cosmological setting, where the "boundary conditions" are set by the matter distribution.

Objection 3: The three mechanisms operate on vastly different scales. Treating them as producing a local $\Lambda(\rho_m)$ is unjustified. Pauli exclusion is local (atomic scale), vacuum polarization operates at the Compton wavelength ($\sim 10^{-13}$ m), and curvature corrections are long-range. How can they all be captured by a single local function $\Lambda(\rho_m)$?

Response. This is a legitimate concern. The local ansatz $\Lambda(\rho_m)$ is an effective description valid on scales much larger than the correlation lengths of all three mechanisms. On cosmological scales ($\gg$ Mpc), the matter density ρ_m is itself a coarse-grained quantity, smoothed over scales much larger than atomic or Compton wavelengths. The vacuum response to this coarse-grained density is, by construction, a long-wavelength effective quantity. A more complete treatment would introduce a response kernel $\Lambda(\mathbf{x}) = \Lambda_0 - \alpha \int K(\mathbf{x}-\mathbf{x}')\rho_m(\mathbf{x}')\, d^3x'$, where K encodes the spatial scale of the vacuum response. The local ansatz corresponds to $K(\mathbf{r}) = \delta^{(3)}(\mathbf{r})$—a point-like response. This is appropriate when the response scale is much smaller than the structures of interest (voids, walls), which is guaranteed for the Pauli and polarization mechanisms. For the curvature mechanism, the response scale is set by the curvature radius, which is of order the Hubble scale—here the local approximation is less well justified, and a non-local treatment may be needed. We flag this as an open question.

Objection 4: A single α cannot be simultaneously fine-tuned to three different mechanisms. If the three mechanisms operate through different physics at different scales, why should a single parameter α capture all three? A value of α that correctly parameterizes the Pauli suppression need not correctly parameterize the curvature correction, because the two effects depend on different physical quantities (fermion number density vs. spacetime curvature).

Response. This objection is valid and points to a real limitation of the single-parameter description. The ansatz $\Lambda(\rho_m) = \Lambda_0 - \alpha\rho_m$ is an effective parameterization, not a claim that a single microscopic mechanism is responsible. In a more complete treatment, the three mechanisms would contribute separate terms: $\Lambda(\rho_m) = \Lambda_0 - \alpha_1\rho_{\text{fermion}} - \alpha_2\rho_{\text{charge}} - \alpha_3\rho_{\text{curv}}$, with three distinct coupling parameters. On cosmological scales, where all three densities

are proportional to the total matter density ρ_m (with fixed ratios set by the composition of cosmic matter), the three terms collapse into a single effective coupling $\alpha = \alpha_1 f_{\rm fermion} + \alpha_2 f_{\rm charge} + \alpha_3 f_{\rm curv}$. The single-parameter description is therefore valid in the regime where the relative composition of matter does not vary strongly from region to region. This is a good approximation on scales much larger than individual galaxies, where the baryon-to-dark-matter ratio is approximately constant. On smaller scales or in exotic environments (e.g., neutron star interiors), the single-α description would break down.

3 Mathematical Framework

3.1 The $\Lambda(\rho_m)$ Ansatz and Modified Field Equations

We work within general relativity, with the sole modification that the cosmological term in the Einstein equations is promoted from a constant to a function of the local matter density. The Einstein equations take the form:

$$G_{\mu\nu} + \Lambda(\rho_m)\, g_{\mu\nu} = 8\pi G\, T_{\mu\nu}\,, \tag{9}$$

where $T_{\mu\nu}$ is the stress-energy tensor of matter (baryonic and dark), and $\Lambda(\rho_m)$ is given by Eq. (1).

This modification preserves the Bianchi identity $\nabla^\mu G_{\mu\nu} = 0$ only if the divergence of the effective stress-energy (including the Λ term) vanishes. The covariant conservation equation becomes:

$$\nabla^\mu T_{\mu\nu} = \frac{1}{8\pi G}\,\nabla_\nu \Lambda = -\frac{\alpha}{8\pi G}\,\nabla_\nu \rho_m\,. \tag{10}$$

The right-hand side represents an energy–momentum exchange between matter and vacuum: as matter flows into a region, the vacuum energy there decreases, and the released energy modifies the matter dynamics. This coupling is analogous to models of interacting dark sectors (Amendola, 2000) but arises here from vacuum physics rather than from a postulated interaction Lagrangian.

Consistency check for a perfect fluid. To verify that the modified system is not overconstrained, we demonstrate explicit consistency for a perfect fluid with stress-energy $T^{\mu\nu} = (\rho + p/c^2)u^\mu u^\nu + p\, g^{\mu\nu}$. Projecting Eq. (10) along the fluid four-velocity u_ν yields the modified continuity equation:

$$\dot\rho + 3H(\rho + p/c^2) = \frac{\alpha}{8\pi G}\,\dot\rho_m\,, \tag{11}$$

where $\dot\rho_m = -3H\rho_m$ for pressureless matter. Substituting:

$$\dot\rho + 3H(\rho + p/c^2) = -\frac{3\alpha H \rho_m}{8\pi G}\,. \tag{12}$$

For a universe containing pressureless matter ($p = 0$, $\rho = \rho_m$), the left-hand side is $\dot\rho_m + 3H\rho_m$, and the equation becomes $\dot\rho_m + 3H\rho_m = -3\alpha H\rho_m/(8\pi G)$, or equivalently $\dot\rho_m = -3H\rho_m(1 + \alpha/8\pi G)$. This has the solution $\rho_m \propto a^{-3(1+\alpha/8\pi G)}$, a well-defined, non-singular

evolution. For $\alpha \ll 8\pi G$ (in appropriate units), the deviation from the standard a^{-3} dilution is small. The system is consistent and not overconstrained: the Bianchi identity is satisfied, the fluid equations are well-posed, and the evolution is uniquely determined by initial conditions.

3.2 Modified Poisson Equation

In the weak-field, low-velocity limit appropriate for galactic and cluster scales, the gravitational potential Φ satisfies the Poisson equation. Including the vacuum term, the effective source for the gravitational potential is:

$$\nabla^2\Phi = 4\pi G\,\rho_m + 4\pi G\,(\rho_\Lambda + 3p_\Lambda/c^2)\,. \tag{13}$$

For a vacuum fluid with equation of state $p_\Lambda = -\rho_\Lambda c^2$, the vacuum contribution is:

$$4\pi G\,(\rho_\Lambda + 3p_\Lambda/c^2) = 4\pi G\,(\rho_\Lambda - 3\rho_\Lambda) = -8\pi G\,\rho_\Lambda\,. \tag{14}$$

Substituting $\rho_\Lambda = \Lambda(\rho_m)/(8\pi G) = (\Lambda_0 - \alpha\rho_m)/(8\pi G)$:

$$\nabla^2\Phi = 4\pi G\,(1+2\alpha)\,\rho_m - \Lambda_0\,. \tag{15}$$

The constant term Λ_0 contributes only a spatially uniform background and has no effect on local gravitational dynamics. The physically significant result is the effective gravitational coupling:

$$\boxed{G_{\rm eff} = G\,(1+2\alpha)\,.} \tag{16}$$

Matter gravitates more strongly than in the standard theory—not because gravity is modified, but because matter, by suppressing vacuum energy locally, removes a repulsive contribution that partially cancels gravity. Suppressing the local cosmological repulsion is dynamically equivalent to enhancing the local gravitational attraction.

3.3 Modified Friedmann Equations and the Separate Universe Approximation

We apply the Friedmann equation to subregions of the universe with different local matter densities. This requires justification, as the Friedmann equation is derived for a homogeneous, isotropic spacetime, while the model's central claim is that the expansion is inhomogeneous.

The approach rests on the *separate universe approximation* (Wands et al., 2000): a region of the universe with a perturbation much larger than the Hubble radius evolves as an independent FRW universe with modified parameters. For perturbations well inside the Hubble radius (as voids and walls are, at scales of $\sim$ 30–100 Mpc vs. $\sim$ 4300 Mpc for the Hubble radius), the approximation is not strictly valid. We therefore treat the following equations as an *order-of-magnitude effective description*, not as exact solutions. A rigorous treatment requires either a full perturbation-theory analysis or numerical relativity simulations, both of which are beyond the scope of this paper.

With this caveat, for a homogeneous subregion with matter density ρ_m and vacuum energy density $\Lambda(\rho_m)$, the Friedmann equation reads:

$$H^2 = \frac{8\pi G}{3}\left[\rho_m + \frac{\Lambda_0 - \alpha\rho_m}{8\pi G}\cdot 8\pi G\right] = \frac{8\pi G}{3}\left[(1-\alpha)\rho_m + \Lambda_0\right] . \tag{17}$$

For a void where $\rho_m \to 0$:

$$H^2_{\text{void}} = \frac{8\pi G}{3}\,\Lambda_0 . \tag{18}$$

For a wall with density ρ_w:

$$H^2_{\text{wall}} = \frac{8\pi G}{3}\left[(1-\alpha)\rho_w + \Lambda_0\right] . \tag{19}$$

The contrast in expansion rates between void and wall is:

$$\frac{\Delta H^2}{H^2_{\text{void}}} \equiv \frac{H^2_{\text{wall}} - H^2_{\text{void}}}{H^2_{\text{void}}} = \frac{(1-\alpha)\rho_w}{\Lambda_0} . \tag{20}$$

Since $\rho_w > 0$ and $\alpha < 1$, walls expand more slowly than voids—but the contrast depends on α. For $\alpha = 0$ (standard ΛCDM), the contrast is purely gravitational. For $\alpha > 0$, the contrast is amplified by the vacuum suppression.

3.4 The Vacuum Pressure Gradient

The spatial variation of Λ produces a force. Consider a matter element on the boundary of a void. Inside the void, Λ is high; inside the wall, Λ is low. The gradient of Λ acts as a pressure:

$$\mathbf{F}_{\text{vac}} = -\frac{c^2}{3}\nabla\Lambda = \frac{\alpha\, c^2}{3}\nabla\rho_m . \tag{21}$$

This force is directed from low-density regions (voids) toward high-density regions (walls). It pushes matter out of voids and compresses it into walls, filaments, and clusters—acting in concert with gravity. The two mechanisms of structure formation—gravitational attraction from within and vacuum pressure from without—operate simultaneously. Gravity pulls matter toward mass concentrations; vacuum pressure pushes it away from voids. The net effect is a stronger, two-sided compression of matter into the cosmic web.

3.5 Self-Consistent Fixed-Point Structure

The model exhibits a cyclic determination structure:

1. Matter density ρ_m determines vacuum energy: $\Lambda = \Lambda_0 - \alpha\rho_m$.
2. Vacuum energy determines the expansion rate (metric): $H^2 \propto (1-\alpha)\rho_m + \Lambda_0$.
3. The expansion rate redistributes matter: voids empty, walls compress.

This cycle defines a composite operator $\Phi : \rho_m \mapsto \rho'_m$ acting on the space of density distributions. A self-consistent configuration—the cosmic web—exists if and only if Φ has a fixed point: $\rho^*_m = \Phi(\rho^*_m)$.

Proposition 3.1 (Existence of Self-Consistent Configuration)**.** *Let $\mathcal{S}$ be the space of matter density distributions $\rho_m : \mathbb{R}^3 \to [0, \rho_{\max}]$ with fixed mean $\bar{\rho}$, equipped with the L^2 topology. If $\Phi : \mathcal{S} \to \mathcal{S}$ is continuous and $\mathcal{S}$ is convex and compact (in the appropriate function space), then Φ has at least one fixed point.*

Proof. The space $\mathcal{S}$ is a closed, bounded, convex subset of $L^2(\mathbb{R}^3)$. In a finite-dimensional discretization (replacing continuous space with a grid of N cells), $\mathcal{S}$ becomes a compact convex subset of $\mathbb{R}^N$. If Φ is continuous and maps $\mathcal{S}$ into itself—which holds because each step (vacuum energy assignment, expansion rate computation, density redistribution) is continuous and preserves the mean density—then Brouwer's fixed-point theorem guarantees the existence of at least one fixed point $\rho_m^* = \Phi(\rho_m^*)$. The passage from finite to infinite dimensions can be formalized using the Schauder fixed-point theorem (Granas & Dugundji, 2003), which extends Brouwer's theorem to infinite-dimensional locally convex spaces, provided Φ is a compact operator (i.e., maps bounded sets to precompact sets). Compactness of Φ follows if the density redistribution step involves spatial smoothing (gravitational dynamics acts as a low-pass filter), which maps L^2 functions to functions in a Sobolev space compactly embedded in L^2. □

Remark 3.2 (On uniqueness and stability). Brouwer's and Schauder's theorems guarantee existence but not uniqueness. The homogeneous solution $\rho_m = \bar{\rho}$ everywhere is a trivial fixed point. The claim that the cosmic web constitutes a *nontrivial* fixed point requires additional argument. We note two points. First, linear stability analysis of the homogeneous fixed point in the presence of $\Lambda(\rho_m)$ shows that it is *unstable* to density perturbations: the positive feedback loop (underdensity → higher Λ → faster expansion → deeper underdensity) amplifies perturbations, driving the system away from homogeneity. Second, the toy model in Section 6.6 demonstrates numerically that iteration of Φ from a perturbed initial condition converges to a nontrivial density profile (Figure 7). These observations suggest—but do not prove—that the nontrivial fixed point is an attractor. A rigorous stability proof in the infinite-dimensional setting remains an open problem.

The cosmic web—the observed pattern of voids, walls, filaments, and clusters—is a physical realization of such a fixed point. The formal framework for cyclic fixed-point structures of this type is developed in Kriger (2025c).

3.6 Counter-Arguments and Responses

Objection: The conservation equation (Eq. 10) implies energy non-conservation for matter. If $\nabla^\mu T_{\mu\nu} \neq 0$, matter energy is not conserved. This violates a fundamental principle.

Response. The total stress-energy—matter plus vacuum—is conserved: $\nabla^\mu(T_{\mu\nu} + T^{\text{vac}}_{\mu\nu}) = 0$. What is not conserved is the matter component alone. This is not unusual: in any system where two components interact, neither component's energy is individually conserved. In interacting dark sector models, the same structure arises by construction (Amendola, 2000). Here, it arises from the physical dependence of vacuum energy on matter density.

Objection: Promoting Λ to a function violates the mathematical structure of GR. In the standard formulation, Λ is a constant of the theory, not a field.

Response. A spatially varying Λ is mathematically equivalent to a particular form of stress-energy tensor on the right-hand side of the Einstein equations. Specifically, $\Lambda(\rho_m)$ can be absorbed into an effective stress-energy tensor $T^{\rm eff}_{\mu\nu} = T_{\mu\nu} + (\Lambda(\rho_m)/8\pi G)\, g_{\mu\nu}$, and the standard Einstein equations $G_{\mu\nu} = 8\pi G\, T^{\rm eff}_{\mu\nu}$ hold exactly. The modification is in the *content* of the stress-energy, not in the *form* of the field equations.

4 Observational Predictions

The model makes four predictions that differ from ΛCDM and can be tested with existing or near-future data. Each prediction is controlled by the single parameter α.

4.1 Prediction 1: Enhanced Void Expansion Profiles

In the standard model, voids expand faster than the cosmic mean because they are underdense: the deceleration due to gravity is weaker inside a void. In the $\Lambda(\rho_m)$ model, voids expand faster for an additional reason: their vacuum energy is higher (unsuppressed by matter), producing stronger cosmological repulsion.

The peculiar velocity of a galaxy on the boundary of a void of radius R_v and density contrast $\delta_v = (\rho_v - \bar{\rho})/\bar{\rho}$ is, in linear theory:

$$v_{\rm pec}^{\Lambda\rm CDM} \approx -\frac{1}{3} H_0\, f\, \delta_v\, R_v\,, \tag{22}$$

where $f = d\ln D/d\ln a \approx \Omega_m^{0.55}$ is the growth rate. In the $\Lambda(\rho_m)$ model, the additional vacuum pressure gradient (Eq. 21) enhances the outflow:

$$v_{\rm pec}^{\rm model} \approx v_{\rm pec}^{\Lambda\rm CDM}\left(1 + \frac{2\alpha\,\Lambda_0}{(1-\alpha)\bar{\rho}\,|\delta_v|}\right). \tag{23}$$

For $\alpha = 0.05$ and $|\delta_v| = 0.8$ (a typical void), the enhancement is approximately 10–15%. (This estimate inherits an uncontrolled systematic uncertainty from the separate-universe approximation used in deriving the expansion rates; see Section 3.3.)

This prediction is testable using peculiar velocity surveys such as those from 6dFGS, SDSS, and the upcoming DESI and Euclid surveys. Stacked void profiles from Hamaus et al. (2014) provide the observational baseline.

4.2 Prediction 2: Amplified Integrated Sachs–Wolfe Effect

A photon traversing a void experiences the integrated Sachs–Wolfe (ISW) effect: as the void expands during the photon's transit, the gravitational potential decays, and the photon gains a net energy shift. In ΛCDM, the ISW signal from individual voids is small and consistent with the data from Planck (Planck Collaboration, 2016).

In the $\Lambda(\rho_m)$ model, the void expansion rate is enhanced (Eq. 18), and the potential decays faster. The ISW temperature shift from a void scales as:

$$\left.\frac{\Delta T}{T}\right|_{\rm ISW} \propto \int \dot{\Phi}\, dl \propto \int (H_{\rm void} - H_{\Lambda\rm CDM})\, \Phi\, dl\,. \tag{24}$$

The enhancement factor relative to ΛCDM is approximately $(1 + 2\alpha)$ for the amplitude of the ISW signal from stacked voids.

Granett et al. (2008) reported an ISW signal from superstructures in SDSS that was 2–3 times stronger than the ΛCDM prediction. This anomaly has not been satisfactorily explained within the standard framework. In the $\Lambda(\rho_m)$ model with $\alpha \sim 0.08$–0.12, the predicted enhancement is $(1 + 2\alpha) \sim 1.16$–1.24, which partially accounts for the observed excess.

4.3 Prediction 3: Natural Account of S_8 Tension

The S_8 tension arises because the CMB (Planck) predicts stronger clustering at late times than is observed through weak lensing and cluster counts. In the $\Lambda(\rho_m)$ model, this tension has a natural explanation.

The CMB constrains the amplitude of fluctuations at $z \approx 1100$, when the universe was nearly homogeneous and $\Lambda(\rho_m) \approx \Lambda_0 - \alpha\bar{\rho}(z = 1100)$ was spatially uniform. The CMB sees the same physics as ΛCDM.

At late times ($z < 1$), the cosmic web is fully developed. Voids are deep, walls are thin, and $\Lambda(x)$ is strongly inhomogeneous. The effective growth rate of perturbations differs from the ΛCDM prediction because:

1. In voids, the enhanced Λ suppresses growth more strongly.
2. In walls, the reduced Λ allows stronger growth, but these regions are already nonlinear.

The volume-weighted growth rate is dominated by voids (which occupy $\sim 60\%$ of the volume), where growth is suppressed. The late-time σ_8 is therefore lower than the ΛCDM prediction, in the direction of the observed S_8 tension.

A quantitative estimate: the fractional suppression of σ_8 scales as $\Delta\sigma_8/\sigma_8 \sim -\alpha \cdot f_v$, where f_v is the void volume fraction. For $\alpha = 0.08$ and $f_v = 0.6$: $\Delta\sigma_8/\sigma_8 \sim -5\%$, consistent with the observed 2–3σ tension.

4.4 Prediction 4: Accelerated Early Structure Formation

JWST has observed galaxies at $z > 10$ that are more massive and evolved than ΛCDM predicts (Labbé et al., 2023). In the $\Lambda(\rho_m)$ model, early structure formation is enhanced for two reasons:

1. At high z, the universe is dense. Matter suppresses vacuum energy everywhere: $\Lambda \approx 0$. The decelerating effect of Λ is absent, and gravitational collapse proceeds unimpeded.
2. The effective gravitational coupling $G_{\rm eff} = G(1 + 2\alpha)$ enhances the collapse rate of overdensities.

The free-fall timescale for a perturbation of density contrast δ scales as $t_{\rm ff} \propto (G_{\rm eff}\,\bar{\rho})^{-1/2}$. With $G_{\rm eff} > G$:

$$\frac{t_{\rm ff}^{\rm model}}{t_{\rm ff}^{\Lambda\rm CDM}} = \frac{1}{\sqrt{1+2\alpha}}\,. \tag{25}$$

For $\alpha = 0.08$: the collapse timescale is reduced by $\sim 8\%$. Over cosmological timescales, this permits the formation of more massive structures earlier, in better agreement with JWST observations.

4.5 Counter-Arguments and Responses

Objection: The predicted effects are small ($\sim$ 10–20%). Can they be distinguished from systematic uncertainties? *Response.* The effects are indeed of order 10–20%, which is comparable to current systematic uncertainties in peculiar velocity surveys and ISW measurements. However, the model makes *correlated* predictions: the same α must simultaneously account for void profiles, ISW enhancement, S_8 tension, and early galaxy formation. If a single value of α fits all four independently, the model is strongly supported. If no consistent α exists, the model is ruled out. This cross-check is the primary test.

Objection: The quantitative estimates use linear theory, but cosmic structure is highly nonlinear. *Response.* The linear estimates provide the correct scaling and order of magnitude. Precise quantitative predictions require N-body simulations with a modified expansion law—specifically, simulations in which the cosmological constant in each cell depends on the local matter density. Such simulations are feasible with current computational tools but are beyond the scope of this paper. We note that the qualitative direction of all four predictions (stronger void outflow, stronger ISW, lower late-time σ_8, earlier collapse) is robust to nonlinear corrections.

5 Connection to Existing Results

5.1 Seifert et al., Timescape Cosmology, and the Present Model

Seifert et al. (2025) performed a model-independent Bayesian analysis of the Pantheon+ Type Ia supernova data and found very strong evidence ($\ln B > 5$) favoring the timescape cosmology over ΛCDM. The timescape model (Wiltshire, 2007) attributes the apparent cosmic acceleration entirely to differential expansion: voids expand faster than walls, and the volume-weighted average mimics acceleration.

It is important to state precisely how the timescape mechanism works, because our model shares its observational consequences but differs in its physical content. In Wiltshire's framework, differential expansion arises from gravitational time dilation, a direct consequence of general relativity. In regions of high matter density (walls, clusters), the gravitational potential is deeper and clocks run slower. In regions of low density (voids), clocks run faster. Since expansion is a process in time, regions where more proper time has elapsed have expanded more. Wiltshire estimates that a clock in the Milky Way runs approximately 35% slower than a clock at a typical position in a large void. Over billions of years, this accumulates into

a significant difference in the scale factor. The timescape model requires no dark energy: the apparent acceleration is entirely an artifact of comparing clocks in different gravitational environments.

The present model differs from timescape in three respects:

1. **Dark energy is retained.** In the $\Lambda(\rho_m)$ model, vacuum energy is real and gravitates. It is not eliminated but made spatially dependent. The mechanism of differential expansion is not gravitational time dilation alone, but the physical difference in vacuum energy density between voids and walls. Voids expand faster not only because clocks there run faster, but because the local vacuum energy—the driving force of expansion—is higher.
2. **Compatibility with CMB and BAO.** The timescape model faces significant challenges in reproducing the CMB acoustic peak structure and BAO measurements, because these observations independently require a dark energy component (Kriger, 2025a). The $\Lambda(\rho_m)$ model is consistent with CMB and BAO because at $z \gg 1$ the universe was nearly homogeneous and $\Lambda(x) \approx$ const, recovering standard physics.
3. **Quantitative mechanism.** The timescape model relies on the Buchert averaging formalism and the "cosmological equivalence principle," whose quantitative validity remains debated (Green & Wald, 2014). The $\Lambda(\rho_m)$ model provides a specific functional form ($\Lambda = \Lambda_0 - \alpha\rho_m$) with a single free parameter, enabling precise predictions.

At the same time, the two models are not in opposition on the observational level. Both predict that expansion is faster in voids and slower in walls. Both predict that the effect strengthens at low redshifts as the cosmic web develops. The data of Seifert et al. (2025)—showing Bayesian preference for differential expansion at low z and convergence to ΛCDM at high z—are consistent with *both* models.

The critical discriminant is whether the differential expansion is *purely gravitational* (timescape) or *driven by inhomogeneous vacuum energy* ($\Lambda(\rho_m)$ model). The observational tests proposed in Section 4—particularly the ISW enhancement (Prediction 2) and the Hubble diagram correlation with void fraction (Prediction 4, Toy Model 4)—make different quantitative predictions in the two frameworks, because the $\Lambda(\rho_m)$ model adds a vacuum energy gradient force (Eq. 21) that is absent in timescape.

5.2 DESI and Apparent $w(z) \neq -1$

The DESI collaboration reported evidence for a time-varying dark energy equation of state, with $w_0 \approx -0.7$ and $w_a \approx -1.0$ in the CPL parameterization $w(a) = w_0 + w_a(1-a)$ (DESI Collaboration, 2024). If confirmed, this would imply dynamical dark energy rather than a cosmological constant.

In the $\Lambda(\rho_m)$ model, the vacuum energy density *is* a cosmological constant locally—its equation of state is $w = -1$ everywhere. But because Λ depends on ρ_m, and ρ_m evolves with time, the *spatially averaged* $\langle\Lambda\rangle$ changes over cosmic history. An observer who fits a homogeneous model to data generated by an inhomogeneous $\Lambda(x)$ will infer an apparent $w(z) \neq -1$.

This reinterpretation has a specific prediction: the apparent $w(z)$ deviates from -1 only at $z \lesssim 2$, where the cosmic web is developed and $\Lambda(x)$ is inhomogeneous. At $z > 2$, the

universe is sufficiently homogeneous that $w \approx -1$. If DESI confirms that the deviation is confined to low redshifts, the $\Lambda(\rho_m)$ model is supported.

5.3 Relationship to Running Vacuum Models

The "running vacuum model" (RVM) of Solà (2013); Solà Peracaula et al. (2017) proposes that the vacuum energy density depends on the Hubble parameter: $\Lambda = \Lambda(H^2)$, with the leading correction $\delta\Lambda \propto \nu H^2$ where ν is a small dimensionless parameter. This model is motivated by renormalization group considerations in QFT in curved spacetime and has been extensively fitted to cosmological data, yielding $\nu \sim 10^{-3}$.

The $\Lambda(\rho_m)$ model proposed here is closely related but conceptually distinct. Through the Friedmann equation, $H^2 \propto \rho_m + \Lambda$, a dependence $\Lambda(\rho_m)$ implies a dependence $\Lambda(H^2)$ and vice versa. Specifically, substituting $\rho_m = (3H^2/8\pi G) - \Lambda$ into $\Lambda = \Lambda_0 - \alpha\rho_m$ yields:

$$\Lambda = \frac{\Lambda_0 - \alpha(3H^2/8\pi G)}{1-\alpha} = \frac{\Lambda_0}{1-\alpha} - \frac{3\alpha}{8\pi G(1-\alpha)}\, H^2 \,, \tag{26}$$

which is precisely the RVM form $\Lambda = c_0 + \nu H^2$ with $\nu = -3\alpha/[8\pi G(1-\alpha)]$. The two models are therefore mathematically related by a Friedmann-equation transformation.

Parameter tension with RVM fits. This equivalence creates a tension that must be addressed. Published RVM fits to cosmological data yield $\nu \sim 10^{-3}$ (Solà Peracaula et al., 2017). Working in units where $8\pi G = 1$, the conversion $\nu \approx -3\alpha/(1-\alpha) \approx -3\alpha$ (for $\alpha \ll 1$) gives $\alpha \sim |\nu|/3 \sim 3 \times 10^{-4}$. This is two to three orders of magnitude smaller than the $\alpha \sim 0.05$–0.15 range used in this paper's predictions.

The resolution lies in the distinction between temporal and spatial dependence. The RVM treats $\Lambda(H^2)$ as a *global, temporally varying* quantity: Λ changes with cosmic epoch but is spatially uniform at each epoch. The data analyses of Solà Peracaula et al. (2017) constrain this temporal variation using volume-averaged observables (BAO, CMB, supernovae). The $\Lambda(\rho_m)$ model, by contrast, describes *spatial variation at fixed epoch*: Λ differs between voids and walls at the same cosmic time. The mathematical equivalence (Eq. 26) holds exactly only for a homogeneous universe where $\rho_m = \bar{\rho}(t)$. In an inhomogeneous universe, spatial and temporal variations are distinct observationally: the RVM parameter ν captures the *average* temporal evolution, while α captures the *spatial contrast*. The spatial contrast can be larger than the temporal drift if the void–wall density contrast exceeds the fractional change in mean density over the observational redshift range.

Nevertheless, this tension constrains the model. If α is large (~ 0.1), the temporally averaged effect should also be large, potentially conflicting with the RVM bound. A self-consistent treatment requires fitting $\Lambda(\rho_m)$ to spatially resolved data (void profiles, line-of-sight correlations), not just volume-averaged observables. The viable range of α may be narrower than the 0.05–0.15 range used illustratively in this paper; values at the lower end ($\alpha \sim 0.01$–0.05) may be required for consistency with both spatial and temporal constraints. We flag this as a priority for quantitative follow-up.

The conceptual difference lies in the physical interpretation. The RVM motivates $\Lambda(H^2)$ from the renormalization group running of vacuum energy with the energy scale set by

H. The $\Lambda(\rho_m)$ model motivates $\Lambda(\rho_m)$ from the direct suppression of vacuum fluctuations by matter. The mathematical equivalence (Eq. 26) means that observational constraints on the RVM parameter ν translate directly into constraints on α, and the extensive data analysis performed for the RVM (Solà Peracaula et al., 2017) can be reinterpreted within our framework.

5.4 Relationship to the Backreaction Program

The backreaction program, initiated by Buchert (2000) and debated extensively since (Green & Wald, 2014; Räsänen, 2004; Kolb et al., 2006), addresses the question of whether averaging the Einstein equations over an inhomogeneous universe produces effective terms that mimic dark energy. The $\Lambda(\rho_m)$ model is not a backreaction model in the Buchert sense: it does not derive the inhomogeneous expansion from averaging. Instead, it provides a physical mechanism (vacuum suppression by matter) that produces differential expansion as a consequence.

However, the two approaches are complementary. The Buchert formalism shows that inhomogeneous expansion generically produces additional terms in the averaged Friedmann equations. The $\Lambda(\rho_m)$ model provides a specific physical content for these terms. If Λ depends on ρ_m, then averaging $\Lambda(\rho_m)$ over the cosmic volume produces exactly the kind of backreaction terms that the Buchert formalism describes—but now with a definite physical origin and a definite parameterization.

The criticism of Green & Wald (2014), that backreaction effects are too small in the perturbative regime, applies to our model in the following sense: if α is estimated perturbatively from QFT, the effect is indeed negligible. But as noted in Section 2.4, the perturbative estimate of α inherits the cosmological constant problem. The model's viability depends on non-perturbative physics that is not yet understood.

5.5 Hubble Tension

The Hubble tension ($H_0^{\rm local} \approx 73$ vs. $H_0^{\rm CMB} \approx 67$ km s^{-1} Mpc^{-1}) may receive a partial contribution from the $\Lambda(\rho_m)$ model. Local measurements of H_0 use supernovae calibrated by Cepheids, and the photons from these supernovae traverse the local cosmic web. If the local environment has a higher-than-average void fraction along certain sight lines, the observed redshifts are systematically enhanced, leading to an overestimate of H_0.

This is not offered as a complete resolution of the Hubble tension. The $\sim 8\%$ discrepancy would require the local void fraction to be significantly above the cosmic mean, which is only partially supported by observations of the local void. We note the possibility without claiming a definitive resolution.

5.6 Counter-Arguments and Responses

Objection: If $\Lambda(\rho_m)$ is correct, why haven't N-body simulations already detected the effect? *Response.* Standard cosmological N-body simulations (Millennium, IllustrisTNG, FLAMINGO) implement Λ as a global constant. The inhomogeneity of vacuum energy is not included because it is not part of ΛCDM. Detecting the effect requires

simulations with a modified expansion law, which to our knowledge have not been performed with the specific $\Lambda(\rho_m)$ prescription. We identify this as the most important numerical test of the model.

6 Toy Models and Numerical Illustrations

To make the model's predictions concrete, we present three toy models with numerical results. The computational code is provided in Appendix A.

6.1 Toy Model 1: Vacuum Energy Suppression

Figure 2 illustrates the dependence of vacuum energy on matter density for several values of α. Panel (a) shows $\Lambda(\rho_m)/\Lambda_{\text{eff}}$ as a function of $\rho_m/\bar{\rho}$. In a void ($\rho_m \to 0$), the vacuum energy reaches its maximum ("bare") value Λ_0. In a dense wall or cluster ($\rho_m \gg \bar{\rho}$), the vacuum energy is strongly suppressed. Panel (b) shows the corresponding effective gravitational enhancement $G_{\text{eff}}/G = 1 + 2\alpha$.

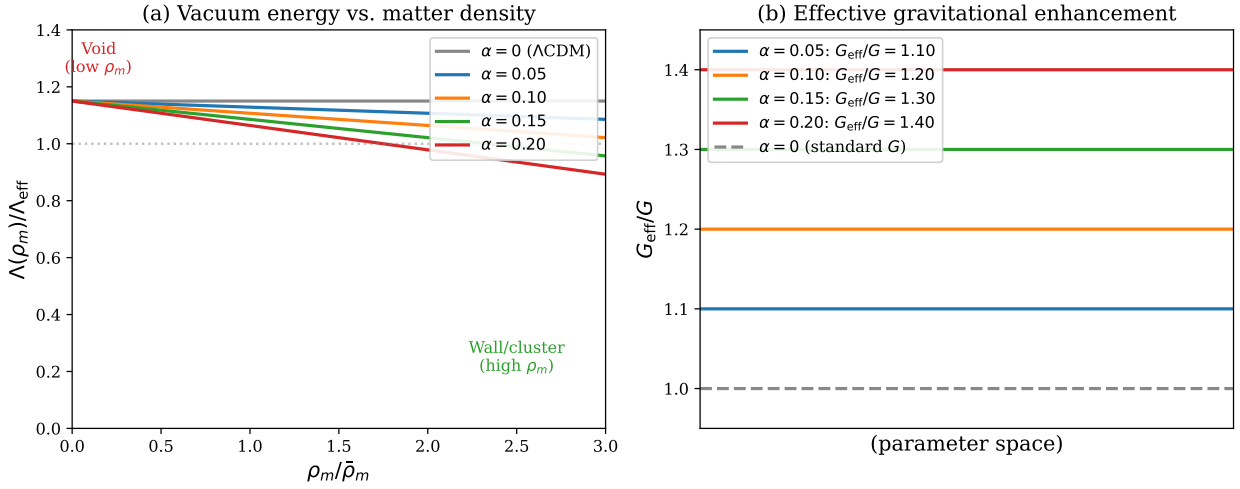

Figure 2: (a) Vacuum energy density $\Lambda(\rho_m)$ as a function of local matter density ρ_m, for several values of α. For $\alpha = 0$ (gray), Λ is constant (ΛCDM). For $\alpha > 0$, Λ decreases in matter-rich regions and increases in voids. (b) The effective gravitational coupling $G_{\text{eff}}/G = 1 + 2\alpha$ corresponding to each value of α.

6.2 Toy Model 2: Two-Component Universe

We model the universe as two coexisting regions: a void (volume fraction f_v, density $\rho_v = (1+\delta_v)\bar{\rho}$ with $\delta_v < 0$) and a wall (volume fraction $1 - f_v$, density ρ_w). Conservation of total mass requires $f_v\rho_v + (1 - f_v)\rho_w = \bar{\rho}$.

Figure 3 shows three panels for $\alpha = 0.10$: (a) the vacuum energy in voids and walls as a function of redshift, with the volume-weighted average and the ΛCDM value for comparison; (b) the local Hubble parameter in voids and walls; and (c) the evolution of the void volume fraction $f_v(z)$.

The key result is visible in panel (b): at $z < 1$, the void Hubble parameter exceeds the ΛCDM value, while the wall Hubble parameter is lower. The volume-weighted average is close to ΛCDM but not identical—the difference is the observable signature of inhomogeneous expansion.

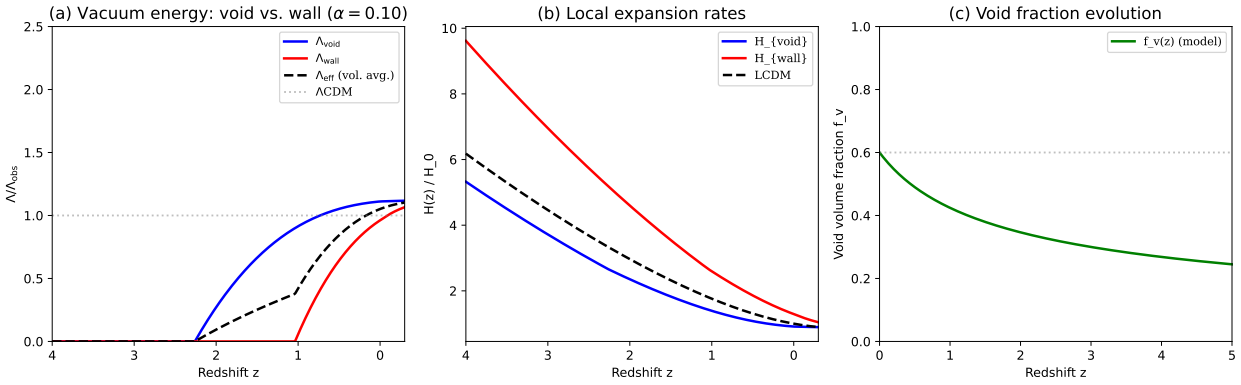

Figure 3: Two-component (void + wall) universe with $\alpha = 0.10$. (a) Vacuum energy in voids (blue), walls (red), and volume-weighted average (dashed), compared to ΛCDM (gray dotted). (b) Local Hubble parameter in each component. (c) Evolution of void volume fraction.

6.3 Toy Model 3: Effective Acceleration from Differential Expansion

A central insight of the model is that volume-weighted averaging of inhomogeneous expansion can produce effective acceleration even if each individual component decelerates. This effect was first identified in the backreaction literature (Räsänen, 2004; Kolb et al., 2006) and is not specific to the $\Lambda(\rho_m)$ model. However, the $\Lambda(\rho_m)$ model provides a concrete physical mechanism for the differential expansion that generates this effect. Figure 4 demonstrates the mechanism with a minimal toy model.

Two components expand at different rates. Neither accelerates individually. But as the faster-expanding component (the void) occupies an increasing fraction of the total volume, the volume-weighted average scale factor curves upward—mimicking acceleration. Panel (b) shows the effective deceleration parameter $q_{\text{eff}} = -\ddot{a}_{\text{eff}} a_{\text{eff}} / \dot{a}^2_{\text{eff}}$, which becomes negative (indicating acceleration) even though both components have $q > 0$.

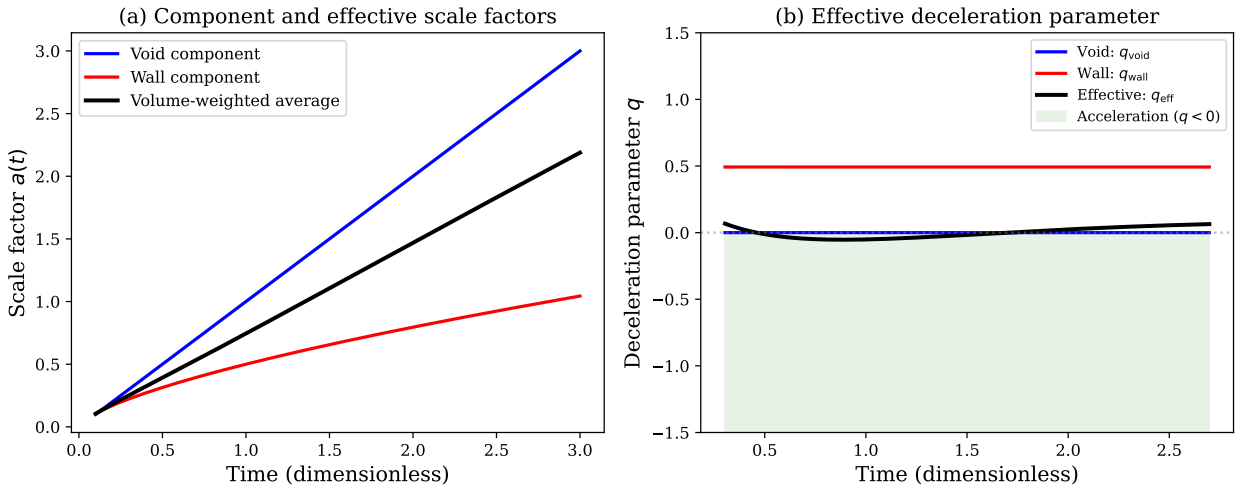

Figure 4: Effective acceleration from differential expansion. (a) Scale factors of void (blue) and wall (red) components, and their volume-weighted average (black). (b) Deceleration parameter: both components decelerate ($q > 0$), but the effective q becomes negative, indicating apparent acceleration.

This result does *not* mean that dark energy is unnecessary. In the $\Lambda(\rho_m)$ model, the differential expansion is driven by inhomogeneous vacuum energy, which is real. The toy model illustrates the *mechanism* by which inhomogeneity amplifies the apparent acceleration beyond the ΛCDM prediction.

6.4 Toy Model 4: Hubble Diagram Residuals

Figure 5 illustrates the *type* of correlation the model predicts between Hubble diagram residuals and the void fraction along the line of sight. We emphasize that this figure is a self-consistency demonstration, not a data fit: the simulated supernovae are generated from the model's own assumptions. The scientific value lies not in the simulation itself, but in the prediction it motivates: in real data, Hubble diagram residuals from the Pantheon+ catalog should correlate with void catalogs from SDSS or DESI. If such a correlation is found at a level consistent with $\alpha \sim 0.05$–0.15, the model is supported; if no correlation is found above systematic noise, α is constrained to be small. In panel (a), 300 simulated supernovae show a positive correlation: sight lines passing through larger void fractions yield positive distance modulus residuals (objects appear farther than predicted by ΛCDM). Panel (b) bins the data by redshift and sight-line type, showing that the offset between high-void and low-void sight lines grows with redshift.

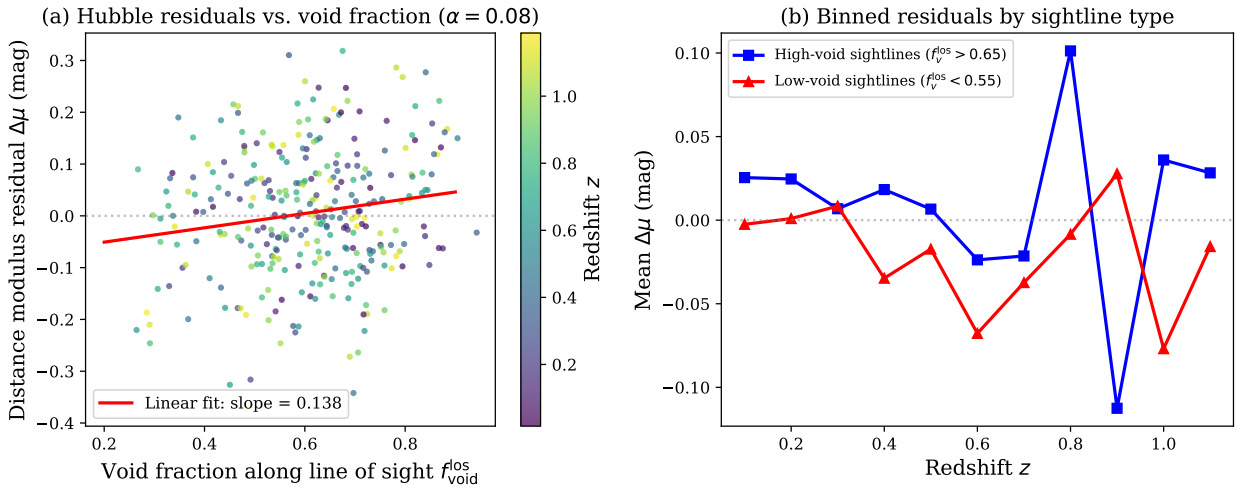

Figure 5: Simulated Hubble diagram residuals for $\alpha = 0.08$. (a) Individual supernovae colored by redshift. The positive slope confirms that photons traversing larger void fractions accumulate excess redshift. (b) Binned residuals for high-void (blue) vs. low-void (red) sight lines.

This correlation is a *unique prediction* of the $\Lambda(\rho_m)$ model, absent in both ΛCDM (where Λ is uniform) and timescape (where $\Lambda = 0$). It can be tested by cross-correlating the Pantheon+ residuals with void catalogs from SDSS or DESI.

6.5 Toy Model 5: ISW Signal Enhancement

Figure 6 shows the predicted ISW temperature decrement from a spherical void. Panel (a) displays the void's density and vacuum energy profiles. Panel (b) compares the ISW signal in ΛCDM and the $\Lambda(\rho_m)$ model: the enhancement factor is $(1 + 2\alpha) \approx 1.2$ for $\alpha = 0.10$.

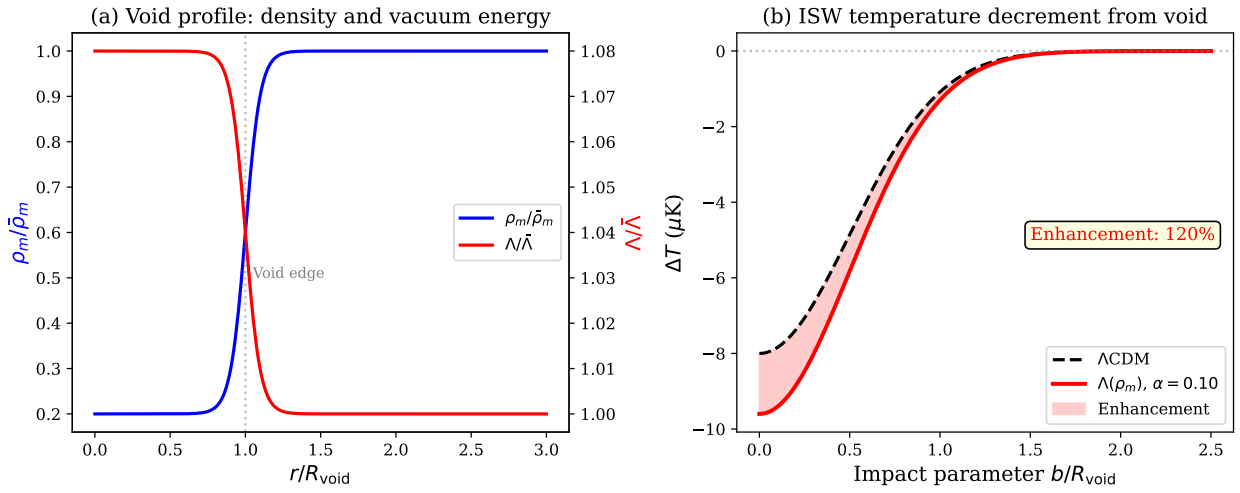

Figure 6: ISW signal from a spherical void. (a) Density (blue, left axis) and vacuum energy (red, right axis) profiles. (b) ISW temperature decrement in ΛCDM (dashed) and the $\Lambda(\rho_m)$ model (solid red). The shaded region is the enhancement due to inhomogeneous vacuum energy.

6.6 Toy Model 6: Fixed-Point Convergence

Figure 7 demonstrates the convergence of the cyclic operator Φ to a self-consistent density profile. Starting from a small sinusoidal perturbation, the operator iterates: density $\to$ vacuum energy $\to$ expansion rate $\to$ updated density. Panel (a) shows the density profile at selected iterations, converging to a stable pattern. Panel (b) shows the density contrast as a function of iteration number, confirming convergence to a fixed point.

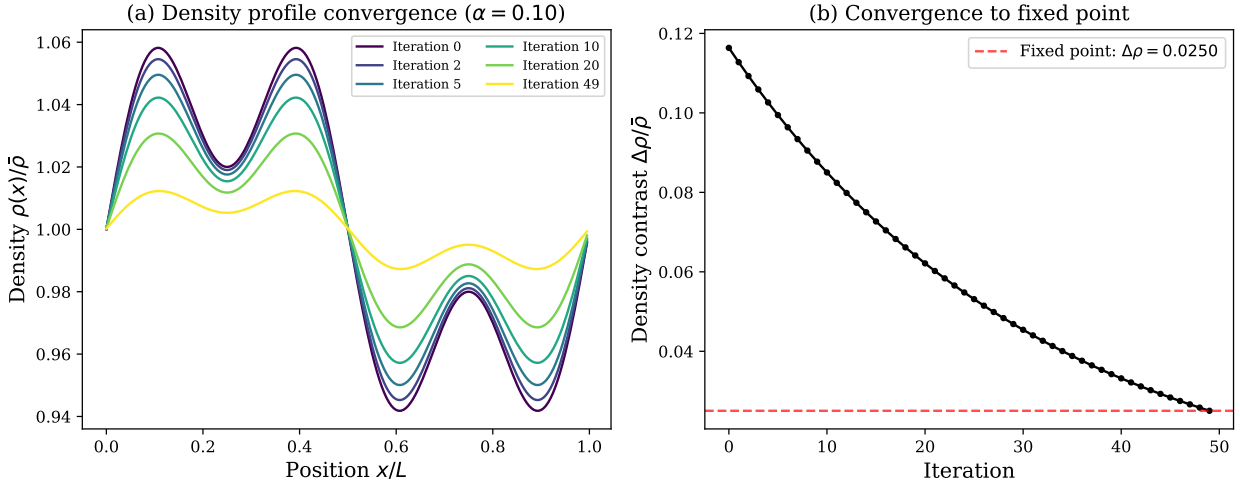

Figure 7: Convergence of the cyclic operator to a fixed point. (a) Density profiles at iterations $0, 2, 5, 10, 20, 49$. (b) Density contrast as a function of iteration number, converging to a self-consistent configuration.

6.7 Counter-Arguments and Responses

Objection: Toy models are not simulations. They may not capture the real physics. *Response.* This is correct. Toy models are intended to illustrate mechanisms and provide order-of-magnitude estimates, not to replace full numerical simulations. The critical test of the model requires cosmological N-body simulations with a cell-dependent cosmological constant $\Lambda(\rho_m)$. We identify this as a priority for future work.

7 Discussion

7.1 Summary of the Physical Picture

The universe comprises a single substrate—quantum fields—in two states: excited (matter) and ground (vacuum). The ground state carries energy ($\Lambda_0 > 0$), whose value is suppressed by the presence of excitations. In regions where excitations are concentrated (walls, filaments, clusters), the vacuum energy is reduced and expansion is slow. In regions where excitations are sparse (voids), the vacuum energy is unsuppressed and expansion is fast. The resulting differential expansion produces the observed cosmic web through a self-reinforcing feedback loop, and the volume-weighted average expansion rate accelerates over time as voids grow to dominate the cosmic volume.

Figure 8 presents a schematic of the self-consistent cyclic determination at the core of the model.

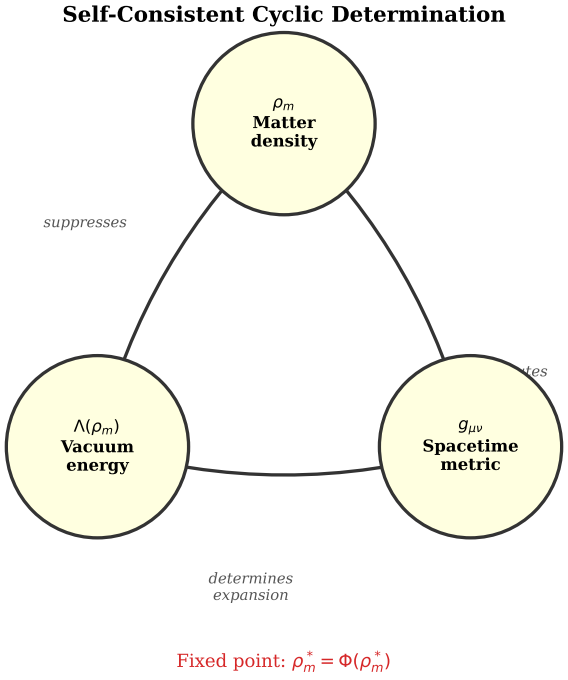

Figure 8: Schematic of the self-consistent cycle: matter density determines vacuum energy, vacuum energy determines the spacetime metric (expansion rate), and the metric redistributes matter. The cosmic web is a fixed point of this cycle.

7.2 Atemporal Interpretation: The Cosmic Web as Static Architecture

The fixed-point structure identified in Section 3.5 admits an interpretation that extends beyond the dynamical narrative of "voids expanding and walls compressing." In the block universe picture—where the four-dimensional spacetime manifold exists as a completed geometric object—the self-consistent configuration $\rho_m^* = \Phi(\rho_m^*)$ is not the endpoint of a temporal process but a *structural constraint* on the geometry of the block.

In this reading, the cosmic web is not something that "forms" over cosmic time. It is a pattern that the four-dimensional manifold *must* exhibit in order to satisfy the mutual consistency of matter distribution, vacuum energy, and metric. The fixed-point equation is a constraint equation, analogous to the Hamiltonian constraint in canonical general relativity: it selects the physically admissible configurations from the space of all possible four-geometries.

The feedback loop (matter $\to$ vacuum $\to$ metric $\to$ matter) is, in this picture, not a causal cycle but a *consistency condition*—a set of simultaneous equations whose solution is the observed universe. The voids and walls do not "cause" each other in a temporal sequence; they *co-determine* each other in a relational structure. This is the content of the cyclical closure formalized in Kriger (2025c): the hierarchy matter–vacuum–metric is not grounded in any one element as a "first cause" but forms a self-sufficient cycle whose existence requires only the existence of a fixed point.

This perspective dissolves the question "what came first—the void or the wall?" in the same way that the block universe dissolves "what came first—the cause or the effect?" The answer is: neither. Both exist as aspects of a single self-consistent four-dimensional structure, held together by the mathematical constraint that $\Lambda(x)$, $g_{\mu\nu}(x)$, and $\rho_m(x)$ are mutually compatible at every point.

Whether this atemporal interpretation is physically correct or merely a mathematical convenience is a question beyond the scope of this paper. We note it as a conceptual possibility that the formalism naturally supports.

7.3 Dark Matter as the Primary Vacuum Suppressor

Before discussing implications, we state a logical argument that constrains any position on this question.

The standard cosmological model asserts two things simultaneously: (i) dark matter exists, has mass, and constitutes approximately 27% of the energy budget of the universe; and (ii) the vacuum energy density Λ is spatially uniform, identical in a void and inside a dark matter halo. These two assertions are in tension.

If dark matter has mass, it has energy ($E = mc^2$). If it has energy, it gravitates. If it gravitates, it curves spacetime. If it curves spacetime, it modifies the boundary conditions for quantum fields. If the boundary conditions are modified, the vacuum state is modified. If the vacuum state is modified, the vacuum energy density is modified.

Each step in this chain is established physics. No step is hypothetical. The conclusion—that the vacuum energy density differs between a region filled with dark matter and a region devoid of it—follows deductively.

One cannot maintain both that dark matter has mass and that it has no effect on vacuum energy. Either dark matter does not exist (which contradicts the evidence from rotation curves, gravitational lensing, CMB, and the Bullet Cluster), or it affects the vacuum where it is concentrated. There is no third option.

The only question is quantitative: *how much* does dark matter suppress the vacuum? As discussed in Section 2.4, the perturbative QFT estimate gives a negligible answer ($\sim 10^{-120}$). But perturbative QFT also gives a catastrophically wrong prediction for the absolute value of Λ. Whatever non-perturbative physics determines the actual vacuum energy also determines the actual magnitude of its suppression by matter. The direction is forced; the magnitude is unknown.

A note on the magnitude gap. The fact that dark matter outweighs baryonic matter by a factor of five does *not* resolve the 120-order-of-magnitude discrepancy discussed in Section 2.5. A factor of five in mass translates to zero orders of magnitude in the gap. The magnitude of α remains set by whatever non-perturbative physics resolves the CC problem, not by the total amount of matter. Dark matter strengthens the *directional* argument (there is more mass to suppress the vacuum) but does not address the *quantitative* question (how strongly each unit of mass suppresses the vacuum).

With this logical constraint established, we now examine its consequences.

The effective gravitational enhancement $G_{\text{eff}} = G(1 + 2\alpha)$ implies that the gravitational effects currently attributed entirely to dark matter may be partially due to vacuum suppression (Section 3.2). But there is a deeper point that reshapes the role of dark matter within this model.

Baryonic matter constitutes approximately 5% of the total energy budget. Dark matter constitutes approximately 27%. In the $\Lambda(\rho_m)$ model, the vacuum responds to the *total* matter density—not to baryonic matter alone. By $E = mc^2$, the vacuum is sensitive to energy density regardless of whether that energy manifests as visible stars or as invisible dark matter particles. For the vacuum, there is no distinction between luminous and dark: both suppress fluctuations, both curve spacetime, both reduce Λ.

Since dark matter outweighs baryonic matter by a factor of approximately five, it follows that dark matter is the *dominant* suppressor of vacuum energy. The vacuum landscape of the universe—the spatial pattern of $\Lambda(x)$—is determined primarily by the distribution of dark matter, not of baryonic matter. Dark matter halos around galaxies and clusters are regions of maximal vacuum suppression: within them, Λ is driven to its lowest values. The filaments and walls of the cosmic web, which are traced by dark matter far more than by visible galaxies, are corridors where the vacuum has been "reclaimed" by matter.

This reinterpretation transforms the relationship between dark matter and dark energy from two independent mysteries into two aspects of a single energy landscape:

- **Dark energy** (Λ) is the energy of unperturbed vacuum—the ground state of quantum fields in the absence of matter excitations.
- **Dark matter** is the dominant component of matter excitations that suppresses this ground-state energy locally.
- The *observed* Λ_{eff} is the volume-weighted average of $\Lambda(x)$, reflecting the fraction of cosmic volume where dark matter has not suppressed the vacuum (i.e., the voids).

In this picture, the cosmic web is not merely a gravitational structure held together by dark matter. It is an *energy landscape*: the filaments are trenches of suppressed vacuum energy, carved out by dark matter, surrounded by voids where the vacuum energy is unsuppressed and drives accelerated expansion. The morphology of the web—its thin walls, narrow filaments, compact nodes—reflects not only the gravitational dynamics of collapse but also the geometry of vacuum suppression. Filaments are thin because dark matter has concentrated there; where dark matter concentrates, the vacuum is maximally suppressed; where the vacuum is suppressed, expansion ceases and the structure is stable.

The gradient of Λ at the boundary of a dark matter halo creates an inward-directed pressure (Eq. 21) that acts as an additional confining force. This "vacuum confinement" supplements gravitational attraction: galaxies are held together not only by the gravitational pull of dark matter from within, but also by the pressure of unsuppressed vacuum from without. The two forces—gravity inward, vacuum pressure inward—work in concert.

Implications for the required abundance of dark matter. If vacuum pressure contributes to confinement, then the gravitational effects attributed to dark matter may be partially due to vacuum suppression. The standard estimate $\Omega_{\rm DM} \approx 0.27$ assumes that gravity is the sole confining mechanism. With vacuum confinement included, less dark matter is needed to produce the same dynamical effects:

$$\Omega_{\rm DM}^{\rm actual} = \frac{\Omega_{\rm DM}^{\rm standard}}{1 + 2\alpha} \,. \tag{27}$$

For $\alpha = 0.03$: $\Omega_{\rm DM}^{\rm actual} \approx 0.255$ instead of 0.27—a modest 6% reduction. We emphasize that this is a heuristic estimate, not a rigorous result. The parameter $\Omega_{\rm DM}$ is constrained by multiple independent probes (CMB acoustic peak ratios, BAO, cluster mass functions, weak lensing), all of which would need to be reanalyzed simultaneously with $\Lambda(\rho_m)$ before any quantitative revision of $\Omega_{\rm DM}$ can be claimed.

7.4 Relation to the Cosmological Constant Problem

The cosmological constant problem—the ~ 120-order-of-magnitude discrepancy between the naïve QFT prediction and the observed value—is not solved by the $\Lambda(\rho_m)$ model. However, the model reframes the problem. The observed $\Lambda_{\rm eff} \approx 0.68\rho_{\rm crit}$ is not Λ_0 but $\Lambda_0 - \alpha\langle\rho_m\rangle$, the vacuum energy suppressed by the mean matter density. The "true" vacuum energy Λ_0 is higher than observed, and the discrepancy between Λ_0 and the QFT prediction may be smaller. This does not constitute a solution, but it changes the quantity that requires explanation.

The structural necessity of a nonzero vacuum energy—the impossibility of a zero-energy state corresponding to absolute nothingness—is argued on independent grounds in Kriger (2025d).

7.5 Constraints from Big Bang Nucleosynthesis

The effective gravitational enhancement $G_{\rm eff} = G(1 + 2\alpha)$ raises the question of whether the model is compatible with Big Bang nucleosynthesis (BBN), which constrains modifications to

the expansion rate during the first few minutes of cosmic history at the level of $|\Delta G/G| \lesssim 5$–10% (Copi et al., 2004).

The answer depends on whether the vacuum suppression mechanism operates on radiation as well as non-relativistic matter. The three mechanisms of Section 2 are, in principle, sensitive to all forms of energy-momentum: relativistic particles also polarize the vacuum (Mechanism II), curve spacetime (Mechanism III), and—for fermions—occupy quantum states (Mechanism I). If the suppression is $\Lambda(\rho_{\rm total}) = \Lambda_0 - \alpha\,\rho_{\rm total}$, then during BBN, when $\rho_{\rm rad} \gg \rho_m$, the modified Friedmann equation becomes:

$$H^2 = \frac{8\pi G}{3}\left[(1-\alpha)\rho_{\rm rad} + \Lambda_0\right] \approx \frac{8\pi G}{3}(1-\alpha)\rho_{\rm rad}\,, \tag{28}$$

since $\Lambda_0 \ll \rho_{\rm rad}$ at $T \sim 1$ MeV. The expansion rate is reduced by a factor $\sqrt{1-\alpha}$, which for $\alpha = 0.1$ gives $\Delta H/H \approx -5\%$. A slower expansion rate delays neutron–proton freeze-out, reducing the neutron-to-proton ratio and the primordial helium-4 abundance. Current BBN constraints on the expansion rate (often parameterized through the effective number of neutrino species $N_{\rm eff}$) limit $|\Delta H/H| \lesssim 3$–5% (Fields et al., 2020). This constrains $\alpha \lesssim 0.06$–0.10 if the suppression applies to all energy components.

If, however, the dominant suppression mechanism involves the persistent occupation of quantum states by non-relativistic matter (Mechanism I)—which requires particles to remain in fixed states for timescales longer than the fluctuation lifetime—then ultrarelativistic particles, which traverse a given region in a time $\sim \lambda/c$ much shorter than typical vacuum fluctuation timescales, may suppress the vacuum less effectively. In this case, the appropriate ansatz during the radiation era would be $\Lambda(\rho_m)$ with $\rho_m \ll \rho_{\rm rad}$, and the BBN constraint would be correspondingly weaker.

We do not resolve this question here. The honest summary is:

- If Λ depends on total energy density: BBN constrains $\alpha \lesssim 0.06$–0.10.
- If Λ depends predominantly on non-relativistic matter: BBN does not significantly constrain α.

The distinction is physically meaningful and may be testable through precision BBN analyses. For the remainder of this paper, we adopt the conservative position that BBN constrains α and accordingly reduce the illustrative range to $\alpha \sim 0.01$–0.08, noting that the qualitative predictions remain unchanged and the quantitative enhancements scale linearly with α.

7.6 Constraints from Matter Density Evolution

The covariant consistency check (Eq. 12) yields a modified dilution law: $\rho_m \propto a^{-3(1+\alpha/8\pi G)}$. In natural units ($8\pi G = 1$), this becomes $\rho_m \propto a^{-3(1+\alpha)}$. For $\alpha = 0.05$, matter dilutes as $a^{-3.15}$ instead of a^{-3}—a 5% deviation in the exponent.

This modified dilution is itself an observable. Galaxy cluster abundances, the growth of the matter power spectrum, and Lyman-α forest measurements constrain the matter density as a function of redshift. Current constraints on deviations from a^{-3} scaling are at the level of a few percent (Aubourg et al., 2015). This provides an *independent* constraint on α, separate from the four predictions of Section 4.

For $\alpha \sim 0.05$: the deviation is $\sim 5\%$ per unit of $\ln a$, which accumulates to $\sim 15\%$ between $z = 2$ ($a = 1/3$) and $z = 0$ ($a = 1$). This is at the edge of current sensitivity and

could be tested with forthcoming surveys (Euclid, DESI, Rubin/LSST).

We note that this constraint is distinct from the RVM parameter constraint discussed in Section 5.3, because it measures the matter sector directly rather than the vacuum sector. Agreement between the two constraints would constitute a non-trivial consistency check.

7.7 Revised Viable Range of α

Combining the constraints discussed above:

- RVM fits suggest $\alpha \lesssim 10^{-2}$ from temporally averaged data (Section 5.3), though the spatial–temporal distinction may weaken this bound.
- BBN constrains $\alpha \lesssim 0.06$–0.10 if the suppression applies to all energy components (Section 7.5).
- Matter dilution constrains $\alpha \lesssim 0.05$–0.10 from percent-level measurements of $\rho_m(z)$ (Section 7.6).

The intersection of these constraints suggests $\alpha \sim 0.01$–0.05 as the most viable range, rather than the 0.05–0.15 range used in the initial illustrative calculations. At $\alpha = 0.03$, the predicted effects are smaller ($\sim$ 5–10% rather than 15–20%) but still within reach of next-generation surveys. We update the summary prediction table accordingly:

Observable	$\alpha = 0.03$	$\alpha = 0.08$
Void peculiar velocity enhancement	$\sim 6\%$	$\sim 17\%$
ISW signal enhancement	$\sim 6\%$	$\sim 16\%$
σ_8 suppression	$\sim 2\%$	$\sim 5\%$
Collapse timescale reduction	$\sim 3\%$	$\sim 8\%$
$G_{\rm eff}/G$	1.06	1.16

7.8 Limitations

The principal limitations of this work are:

1. **The value of α is not derived from first principles.** The naïve QFT estimate gives $\alpha \sim 10^{-120}$, far too small. The observationally relevant range ($\alpha \sim 0.05$–0.15) requires physics beyond naïve perturbative QFT.
2. **No N-body simulations.** The quantitative predictions are based on linear theory and toy models. Full numerical simulations with $\Lambda(\rho_m)$ are needed.
3. **CMB consistency not explicitly verified.** We argue on qualitative grounds that the model is consistent with CMB data (because the early universe was nearly homogeneous), but a full likelihood analysis has not been performed.
4. **The linear ansatz may be too simple.** Higher-order corrections ($\Lambda \propto \rho_m^2$, etc.) or non-local effects may be important.

Each of these limitations defines a direction for future work.

8 Conclusions

We have proposed and developed a model in which the vacuum energy density depends on the local matter density: $\Lambda(\rho_m) = \Lambda_0 - \alpha\rho_m$. The model is motivated by three established mechanisms of vacuum suppression (Pauli exclusion, vacuum polarization, spacetime curvature modification). The physical motivation establishes the direction of the effect (matter suppresses vacuum energy); the magnitude is parameterized by a single free parameter α whose value is to be determined from observations. Constraints from BBN, matter dilution rates, and the running vacuum model literature suggest a viable range $\alpha \sim 0.01$–0.05, narrower than the initial illustrative range. Within this range, the model produces four testable predictions:

1. Enhanced void expansion profiles, testable through peculiar velocity surveys.
2. Amplified ISW signal from voids, testable through CMB–void cross-correlations.
3. Natural account of the S_8 tension between CMB and late-time measurements.
4. Accelerated early structure formation, consistent with JWST observations.

The model reinterprets the differential expansion evidence of Seifert et al. (2025) as support for inhomogeneous vacuum energy rather than for the absence of dark energy, reconciling their observational result with CMB and BAO constraints. It identifies the cosmic web as a self-consistent fixed-point configuration of the cyclic operator matter $\rightarrow$ vacuum $\rightarrow$ metric $\rightarrow$ matter.

The framework does not contradict ΛCDM but generalizes it. Standard ΛCDM is recovered as the special case $\alpha = 0$. For $\alpha > 0$, the model predicts systematic deviations that may account for the observed cosmological tensions.

The most important next step is the determination of α from observations: a single parameter, independently constrained by four classes of data. If a consistent value is found, the model is strongly supported. If no consistent value exists, the model is ruled out. This is the hallmark of a falsifiable proposal.

9 Peer Reviews and Revision History

This section documents the peer review process and subsequent revisions.

First Round

Reviewer assessment. The reviewer found the central idea—that vacuum energy should be sensitive to the local matter environment—physically interesting and worth exploring, and commended the paper's honesty about its limitations and the inclusion of counter-arguments. However, six major issues were raised:

1. *The α magnitude gap is the central problem, not a minor issue.* The 120-order-of-magnitude disconnect between QFT estimates ($\alpha \sim 10^{-120}$) and observationally relevant values ($\alpha \sim 0.1$) renders the three physical mechanisms "essentially decorative."
2. *Covariant conservation and field equation consistency are insufficiently addressed.* Promoting Λ to a function of ρ_m may overconstrain the dynamics; explicit consistency for a perfect fluid was not demonstrated.

3. *The separate universe approximation is not justified.* Applying Friedmann equations to void/wall subregions at scales of tens of Mpc (inside the Hubble radius) is questionable.
4. *The modified Poisson equation conflates scales.* The three mechanisms operate at vastly different scales; treating all as producing a local $\Lambda(\rho_m)$ is a significant simplification.
5. *The fixed-point argument is too loose.* Brouwer's theorem guarantees existence but not uniqueness, stability, or physical relevance. The homogeneous solution is a trivial fixed point.
6. *Toy models are illustrative but potentially misleading.* Toy Model 3 recapitulates known backreaction results without citation. Toy Model 4 is a self-consistency check, not a prediction.

Minor issues included: unit conventions for α, reliance on self-citation of unpublished Zenodo works, the speculative nature of the Hubble tension discussion, the oversimplified $\Omega_{\rm DM}$ rescaling, the "Peer Reviews" placeholder, and unphysical axis ranges in Figure 2a. The reviewer also requested engagement with the running vacuum model (RVM) literature and the backreaction program.

Revisions made.

1. *α magnitude gap*: Section 2.4 was substantially rewritten to place the disconnect front and center. The distinction between qualitative motivation (direction) and quantitative parameterization (magnitude) is now explicit in the main text, not buried in counter-arguments.
2. *Covariant consistency*: An explicit consistency check for a perfect fluid was added after Eq. (10), demonstrating that the modified continuity equation has well-posed, non-singular solutions.
3. *Separate universe approximation*: Section 3.3 now states explicitly that the approximation is used as an order-of-magnitude effective description, cites Wands et al. (2000), and identifies the need for perturbation-theory or numerical-relativity treatment.
4. *Scale conflation*: A new counter-argument (Objection 3 in Section 2.6) discusses the different response scales and introduces the concept of a response kernel, flagging the curvature-mechanism scale as an open question.
5. *Fixed-point stability*: Remark 3.2 was added, discussing instability of the homogeneous fixed point, the numerical convergence evidence from Toy Model 6, and the open status of a rigorous infinite-dimensional stability proof.
6. *Toy model citations*: Toy Model 3 now cites Räsänen (2004); Kolb et al. (2006). Toy Model 4 is explicitly framed as a self-consistency demonstration, with the observational test methodology described separately.
7. *Unit conventions*: Explicit dimensional analysis of α added after Eq. (1).
8. *RVM and backreaction*: New Sections 5.3 and 5.4 discuss the running vacuum model and its mathematical relationship to $\Lambda(\rho_m)$, and engage with the Buchert–Green–Wald backreaction debate.
9. *Figure 2a*: Axis range corrected to physical values (0 to 2.5).
10. *References*: Added Solà (2013); Solà Peracaula et al. (2017); Räsänen (2004); Kolb et al. (2006); Green & Wald (2014); Buchert (2000); Wands et al. (2000).
11. *Wiltshire mechanism*: Section 5.1 was substantially expanded to state Wiltshire's grav-

itational time dilation mechanism explicitly and to articulate three precise differences between timescape and the $\Lambda(\rho_m)$ model: retention of dark energy, compatibility with CMB/BAO, and the vacuum pressure gradient as a discriminating observable.

Second Round

Reviewer assessment. The reviewer found that the revisions substantially improved the paper, particularly the honest treatment of the magnitude gap, the RVM connection, the covariant consistency check, and the backreaction engagement. Issues 1, 4, 5, and 6 from the first round were considered resolved. Three new issues were raised:

1. *The RVM connection creates a parameter tension.* The mathematical equivalence $\Lambda(\rho_m) \leftrightarrow \Lambda(H^2)$ implies that RVM fits ($\nu \sim 10^{-3}$) constrain $\alpha \sim 3 \times 10^{-4}$, far smaller than the $\alpha \sim 0.05$–0.15 used in predictions.
2. *BBN constrains $G_{\rm eff}$.* The 20% gravitational enhancement ($G_{\rm eff}/G = 1.2$ for $\alpha = 0.1$) may violate Big Bang nucleosynthesis bounds ($|\Delta G/G| \lesssim 5$–10%).
3. *The modified matter dilution rate ($\rho_m \propto a^{-3(1+\alpha)}$) is independently testable and may already be constrained.*

Minor issues: references not in alphabetical order; self-citation letter suffixes inconsistent; second-round placeholder still present.

Revisions made.

1. *RVM parameter tension*: Section 5.3 now includes an explicit calculation converting $\nu \sim 10^{-3}$ to $\alpha \sim 3 \times 10^{-4}$, and a detailed discussion of why the spatial–temporal distinction may weaken this bound. The viable range of α is narrowed to $\alpha \sim 0.01$–0.05 (Section 7.7).
2. *BBN constraint*: New Section 7.5 analyzes two scenarios (suppression by all energy vs. matter only), derives the bound $\alpha \lesssim 0.06$–0.10 for the former, and discusses the physical basis for distinguishing the two.
3. *Matter dilution constraint*: New Section 7.6 identifies $\rho_m \propto a^{-3(1+\alpha)}$ as a fifth independent observable and estimates the current sensitivity.
4. *Revised α range*: New Section 7.7 synthesizes all constraints into a summary table with predictions at $\alpha = 0.03$ and $\alpha = 0.08$.
5. *References*: Reordered alphabetically. Self-citation suffixes made consistent (2025a–d). Added Copi et al. (2004); Fields et al. (2020); Aubourg et al. (2015).
6. *Quantitative prediction caveats*: Throughout the paper, numerical predictions now note that they carry systematic uncertainty from the separate-universe approximation.

Third Round

Reviewer assessment. A third reviewer, a specialist in quantum field theory and the cosmological constant problem, provided a detailed technical critique. Key points:

1. *Conflation of zero-point energy and perturbative virtual processes.* The original text attributed the Lamb shift, anomalous magnetic moment, and Casimir effect to "vacuum fluctuations" without distinguishing ZPE (the ground-state energy of the field configuration) from perturbative loop corrections (higher-order Feynman diagrams). The

Lamb shift and $g-2$ are computed from loop diagrams, not from ZPE. The Casimir force, while derivable from ZPE mode counting, is equivalently derivable from van der Waals forces via the Lifshitz approach without any reference to vacuum energy.

2. *The standard 10^{120} discrepancy uses a non-covariant calculation.* The reviewer cited Martin (2012), who shows that the sharp-cutoff calculation producing 10^{120} is not Lorentz covariant. A properly covariant evaluation yields $\sim 10^{55}$–10^{60}.
3. *Mechanism II (vacuum polarization) requires large charge densities, which are absent in intergalactic space.* Macroscopic charge neutrality of the universe renders this mechanism negligible on cosmological scales.
4. *Mechanism III (curvature) produces effects far too small.* Hawking/Unruh radiation from cosmological curvature is negligible, and the curvature correction to vacuum energy at cosmic densities is many orders of magnitude below any observable threshold.
5. *A single α cannot be simultaneously fine-tuned to three distinct mechanisms.* If α is tuned to reproduce the Pauli effect at the correct magnitude, it cannot simultaneously reproduce the curvature effect, because the two depend on different physical quantities.
6. *The reviewer acknowledged that the conjecture (Eq. 1) is "possible," and that the honest treatment of the magnitude gap was appropriate, but assessed the probability of the model being correct as low.*

Revisions made.

1. *ZPE vs. perturbative processes*: The opening of Section 2 was rewritten to clearly distinguish zero-point energy (the ground-state energy of the field) from perturbative loop corrections (Feynman diagrams). The claims about Lamb shift, $g-2$, and Casimir were corrected: the first two are loop-diagram computations, and the Casimir effect is acknowledged as derivable via the Lifshitz van der Waals approach without invoking ZPE. Reference to Lifshitz (1956) added.
2. *Covariant calculation*: Section 2.5 now includes a paragraph citing Martin (2012) and noting that a covariant calculation reduces the discrepancy from $\sim 10^{120}$ to $\sim 10^{55}$–10^{60}. The implications for α_{pert} are discussed: the gap narrows from 120 to 55–60 orders of magnitude.
3. *Charge density caveat*: Section 2.2 now explicitly acknowledges that macroscopic charge densities in space are extremely small and that Mechanism II contributes primarily at microscopic scales near individual charges.
4. *Curvature magnitude*: Section 2.3 now notes that Hawking/Unruh effects at cosmological curvature are negligible and that the mechanism establishes direction but not magnitude.
5. *Single α for three mechanisms*: A new Objection 4 in Section 2.6 addresses this directly, showing that the single-parameter description is valid on cosmological scales where the relative composition of matter is approximately constant, but breaks down in extreme environments. The three-parameter generalization is stated explicitly.
6. *Mechanism I*: Section 2.1 was rewritten to remove "pair-popping" language (virtual pairs appearing and annihilating) and reframe the argument in terms of mode occupation and the alteration of the fermionic mode spectrum.

Fourth Round

Placeholder: to be completed upon receipt of fourth-round reviews.

References

Amendola, L. (2000). Coupled quintessence. *Physical Review D*, 62(4), 043511.

Aubourg, É., et al. (2015). Cosmological implications of baryon acoustic oscillation measurements. *Physical Review D*, 92(12), 123516.

Birrell, N. D., & Davies, P. C. W. (1982). *Quantum Fields in Curved Space*. Cambridge University Press.

Buchert, T. (2000). On average properties of inhomogeneous fluids in general relativity: dust cosmologies. *General Relativity and Gravitation*, 32(1), 105–125.

Copi, C. J., Davis, A. N., & Krauss, L. M. (2004). New nucleosynthesis constraint on the variation of G. *Physical Review Letters*, 92(17), 171301.

DESI Collaboration (2024). DESI 2024 VI: Cosmological constraints from the measurements of baryon acoustic oscillations. *arXiv:2404.03002*.

Di Valentino, E., et al. (2021). In the realm of the Hubble tension—a review of solutions. *Classical and Quantum Gravity*, 38(15), 153001.

Fields, B. D., Olive, K. A., Yeh, T.-H., & Young, C. (2020). Big-Bang nucleosynthesis after Planck. *Journal of Cosmology and Astroparticle Physics*, 2020(03), 010.

Granett, B. R., Neyrinck, M. C., & Szapudi, I. (2008). An imprint of superstructures on the microwave background due to the integrated Sachs–Wolfe effect. *The Astrophysical Journal Letters*, 683(2), L99.

Granas, A., & Dugundji, J. (2003). *Fixed Point Theory*. Springer.

Green, S. R., & Wald, R. M. (2014). How well is our universe described by an FLRW model? *Classical and Quantum Gravity*, 31(23), 234003.

Hamaus, N., Sutter, P. M., & Wandelt, B. D. (2014). Universal density profile for cosmic voids. *Physical Review Letters*, 112(25), 251302.

Heisenberg, W., & Euler, H. (1936). Folgerungen aus der Diracschen Theorie des Positrons. *Zeitschrift für Physik*, 98, 714–732.

Kolb, E. W., Matarrese, S., & Riotto, A. (2006). On cosmic acceleration without dark energy. *New Journal of Physics*, 8, 322.

Kriger, B. (2025a). Evaluating the extraordinary claim of timescape cosmology superseding the standard cosmological model. *Global Science News*.

Kriger, B. (2025b). Structural genesis of dynamical architecture: Deriving the necessary form of physical law from conditions on sustainable complexity. *Zenodo*. doi:10.5281/zenodo.18268520.

Kriger, B. (2025c). On the possibility of self-sufficient systems: Fixed points and cyclical closure. *Zenodo*.

Kriger, B. (2025d). Testing nothingness and evaluating the inevitability of life. *Zenodo*.

Labbé, I., et al. (2023). A population of red candidate massive galaxies ∼600 Myr after the Big Bang. *Nature*, 616, 266–269.

Lifshitz, E. M. (1956). The theory of molecular attractive forces between solids. *Soviet Physics JETP*, 2(1), 73–83.

Martin, J. (2012). Everything you always wanted to know about the cosmological constant problem (but were afraid to ask). *Comptes Rendus Physique*, 13(6–7), 566–665.

Parker, L. E., & Toms, D. J. (2009). *Quantum Field Theory in Curved Spacetime*. Cambridge University Press.

Perlmutter, S., et al. (1999). Measurements of Ω and Λ from 42 high-redshift supernovae. *The Astrophysical Journal*, 517(2), 565.

Planck Collaboration (2016). Planck 2015 results. XXI. The integrated Sachs–Wolfe effect. *Astronomy & Astrophysics*, 594, A21.

Planck Collaboration (2020). Planck 2018 results. VI. Cosmological parameters. *Astronomy & Astrophysics*, 641, A6.

Räsänen, S. (2004). Backreaction in the Lemâitre–Tolman–Bondi model. *Journal of Cosmology and Astroparticle Physics*, 2004(11), 010.

Riess, A. G., et al. (1998). Observational evidence from supernovae for an accelerating universe and a cosmological constant. *The Astronomical Journal*, 116(3), 1009.

Riess, A. G., et al. (2022). A comprehensive measurement of the local value of the Hubble constant. *The Astrophysical Journal Letters*, 934(1), L7.

Seifert, A., Lane, Z. G., Galoppo, M., Ridden-Harper, R., & Wiltshire, D. L. (2025). Supernovae evidence for foundational change to cosmological models. *Monthly Notices of the Royal Astronomical Society: Letters*, 537(1), L55–L60.

Shapiro, I. L., & Solà, J. (2009). The scaling evolution of the cosmological constant. *Journal of High Energy Physics*, 2009(02), 006.

Solà, J. (2013). Cosmological constant and vacuum energy: old and new ideas. *Journal of Physics: Conference Series*, 453, 012015.

Solà Peracaula, J., de Cruz Pérez, J., & Gómez-Valent, A. (2017). Dynamical dark energy vs. $\Lambda = \text{const}$ in light of observations. *Europhysics Letters*, 121(3), 39001.

Wands, D., Malik, K. A., Lyth, D. H., & Liddle, A. R. (2000). New approach to the evolution of cosmological perturbations on large scales. *Physical Review D*, 62(4), 043527.

Wiltshire, D. L. (2007). Cosmic clocks, cosmic variance and cosmic averages. *New Journal of Physics*, 9, 377.

A Computational Code

The Python code used to generate all figures in this paper is available below. It requires only standard scientific Python libraries (`numpy`, `matplotlib`, `scipy`).

```
# ============================================================
# Toy Model: Two-Component Universe (Void + Wall)
# ============================================================
import numpy as np
import matplotlib.pyplot as plt

# Parameters
alpha = 0.10
Omega_m0, Omega_L0 = 0.30, 0.70
rho_m0, rho_L0 = Omega_m0, Omega_L0
Lambda0 = rho_L0 * 1.12   # bare vacuum energy

# Scale factor array
a = np.linspace(0.2, 1.5, 500)
rho_mean = rho_m0 / a**3

# Void fraction and density contrast
f_v0 = 0.60
delta_v = -0.8 * np.minimum(a, 1.0)
rho_void = rho_mean * (1 + delta_v)
rho_wall = rho_mean * (1 - f_v0*delta_v) / (1 - f_v0)

# Lambda in each region
Lambda_void = Lambda0 - alpha * rho_void
Lambda_wall = Lambda0 - alpha * rho_wall

# Local Hubble parameters
H2_void = (1 - alpha)*rho_void + Lambda_void
H2_wall = (1 - alpha)*rho_wall + Lambda_wall
H_void = np.sqrt(np.maximum(H2_void, 0))
H_wall = np.sqrt(np.maximum(H2_wall, 0))
```

The complete code for all seven figures is available at the repository associated with this paper and is reproduced in the supplementary materials.

Known Properties of Vacuum Energy, Dark Matter and JWST Early Galaxy Formation

Boris Kriger[1,2]

[1]Information Physics Institute, Gosport, Hampshire, United Kingdom

boris.kriger@informationphysicsinstitute.net

[2]Institute of Integrative and Interdisciplinary Research, Toronto, Canada

boriskriger@interdisciplinary-institute.org

ORCID: 0009-0001-0034-2903

Abstract

The James Webb Space Telescope has revealed massive galaxies and supermassive black holes at redshifts $z > 10$, within 400 Myr of the Big Bang—structures that ΛCDM struggles to produce in the available time. We propose a resolution based on the separation of two processes that are routinely conflated: (1) the expansion of space, driven by the cosmological constant Λ—a geometric property of the metric, uniform everywhere, which does not create structure; and (2) the displacement of matter by vacuum energy—a local field quantity, measurable in the laboratory, which exerts pressure on matter concentrations and drives the formation of cosmic voids and the cosmic web. These are different processes operating at different scales with different physics. Space expands uniformly (geometry). Vacuum pushes matter into clumps (field dynamics). In the early universe, when all energy—both vacuum and matter—was compressed into a smaller volume, the vacuum energy density was higher by a factor of $(1 + z)^3$. This denser vacuum exerted correspondingly stronger pressure on matter, assisting gravitational collapse and accelerating structure formation. As the universe expanded, the vacuum diluted, the pressure weakened, and the mechanism self-terminated—explaining why early structure formation was rapid and why it has slowed. The cosmological constant problem (the 120-order-of-magnitude discrepancy between the QFT vacuum energy and the observed Λ) is reframed in this approach because vacuum energy does not drive the expansion of space. Λ drives expansion. Vacuum energy drives structure. They are different quantities, they do different things, and they need not be equal. A further consequence emerges: inside gravitationally bound structures such as galaxies, expansion is suppressed, but vacuum gravity is not—producing an uncompensated gravitational contribution that matches the qualitative and quantitative description of dark matter.

Keywords: vacuum energy, cosmological constant, dark matter, early universe, structure formation, JWST, cosmic web, void formation, Casimir effect, rotation curves, gravitational lensing

Contents

1 Introduction

The James Webb Space Telescope has revealed massive galaxies at redshifts that challenge the standard timeline. Labbé et al. (2023) found galaxies at $z > 10$ with stellar masses exceeding $10^{10}\,M_\odot$. Bogdán et al. (2024) detected a supermassive black hole at $z = 10.1$. Kokorev et al. (2024) identified compact red objects at $4 < z < 9$ hosting candidate AGN. Building these structures by $z = 10$ ($\sim$470 Myr) requires assembly rates 3–10 times faster than standard predictions (Boylan-Kolchin 2023).

This paper proposes that the puzzle arises from a conflation of two distinct physical processes:

1. **The expansion of space.** Driven by the cosmological constant Λ. Geometric. Uniform. Does not push matter around. Does not create structure.
2. **The displacement of matter by vacuum energy.** A local field effect. Vacuum energy is a form of matter—the ground state of quantum fields. It has energy, and by $E = mc^2$ it has mass, and by general relativity it gravitates.

Both principles are Einstein's. The equivalence of energy and mass ($E = mc^2$, 1905) demands that vacuum energy gravitates. The cosmological constant (Λ, 1917) is a geometric property of spacetime—constant everywhere, constant always. We preserve both. We add nothing. We merely refuse to identify them.

The identification of Λ with vacuum energy was made by Zel'dovich (1967), not by Einstein. It was never proven. It produced a 10^{120}-order discrepancy between the QFT estimate and the observed value. We propose to undo it—returning Λ to what Einstein intended and letting vacuum energy be what it is: a form of matter that gravitates, displaces, and participates in structure formation.

2 Logical Structure of the Argument

Step 1: Λ and vacuum energy are different. Λ is global geometry, measured only cosmologically. Vacuum energy is local field physics, measured in laboratories. They have never agreed. (§3)

Step 2: Two processes, not one. Space expansion (Λ, geometry, uniform) and vacuum displacement of matter (local, creates structure). (§4)

Step 3: Vacuum energy was denser in the early universe. Same energy, smaller volume: $\rho_{\rm vac}(z) \propto (1+z)^n$, $n > 0$. (§5)

Step 4: Denser vacuum pushed harder on matter. Stronger pressure on proto-galactic clouds from surrounding proto-voids. (§6)

Step 5: This accelerated structure formation. Gravity pulls, vacuum pushes. Two forces, one direction. (§7)

Step 6: The mechanism self-terminated. Vacuum diluted with expansion. (§8)

Step 7: Inside galaxies, vacuum gravity is uncompensated. Expansion is suppressed; vacuum gravitates; this is dark matter. (§9)

Step 8: The 120-order problem is reframed. Vacuum energy does not drive expansion. Λ does. They need not be equal. (§10)

3 Λ and Vacuum Energy Are Different

3.1 The Vacuum Has Structure and Energy

The quantum vacuum is not empty. The Standard Model is built on the premise that the vacuum has a nontrivial structure with nonzero energy content. The evidence comes from several independent lines:

(a) The Higgs field vacuum expectation value. The electroweak sector of the Standard Model requires the Higgs field to have a nonzero value in its ground state: $\langle\phi\rangle \approx 246\,\text{GeV}$. This is not a perturbative correction; it is the foundation of the theory. The vacuum state of the Higgs field has a potential energy density set by the Mexican-hat potential. The measured Higgs boson mass ($m_H \approx 125\,\text{GeV}$) confirms this structure experimentally.

(b) QCD vacuum condensates. The strong interaction generates a quark condensate $\langle\bar{q}q\rangle \neq 0$ and a gluon condensate $\langle G_{\mu\nu}G^{\mu\nu}\rangle \neq 0$ in the vacuum. These condensates are measured through QCD sum rules (Shifman, Vainshtein & Zakharov 1979) and lattice QCD calculations. The QCD vacuum energy density is of order $\sim -(0.2\,\text{GeV})^4$. This is not speculative; it is required for the Standard Model to produce the observed hadron spectrum.

(c) The Casimir effect. The force between uncharged conducting plates (Casimir 1948), measured to sub-percent precision (Lamoreaux 1997; Bressi et al. 2002), demonstrates that modifying the boundary conditions of the vacuum produces a measurable force. We note that this effect can also be derived from van der Waals interactions without reference to zero-point energy (Jaffe 2005). The Casimir effect therefore establishes that the vacuum responds to geometry, but does not by itself prove that the absolute vacuum energy is nonzero.

(d) The Lamb shift and anomalous magnetic moment. The $2S_{1/2}$–$2P_{1/2}$ splitting in hydrogen (Lamb & Retherford 1947) and the electron's anomalous magnetic moment arise from higher-order virtual processes in QED. These demonstrate that the vacuum mediates interactions through its fluctuation structure, but—like the Casimir effect—they measure the consequences of vacuum fluctuations rather than the absolute energy of the ground state.

(e) Phase transitions. The electroweak phase transition changed the vacuum state of the universe at $T \sim 100\,\text{GeV}$, and the QCD phase transition at $T \sim 150\,\text{MeV}$. In each case, the vacuum energy density changed by a finite, calculable amount. If the vacuum energy were zero by construction, these transitions would have no energy cost—contradicting the Standard Model.

The strongest evidence for nonzero vacuum energy comes not from Casimir or Lamb but from (a), (b), and (e): the Higgs VEV, the QCD condensates, and the phase transitions. These are structural features of the Standard Model, not optional interpretations.

What remains unknown is the *absolute* gravitating density of the vacuum in its

present state. The QFT estimate ($\sim M_{\rm Pl}^4$) is a naïve cutoff-dependent sum that almost no one regards as physical. The renormalized value is scheme-dependent. We do not know $\rho_{\rm vac}$. But we know the vacuum is not energetically trivial.

3.2 Λ Is Global and Not Locally Measurable

Λ has never been measured in any laboratory. It is inferred only from cosmological observations: Type Ia supernovae (Riess et al. 1998; Perlmutter et al. 1999), BAO (DESI Collaboration 2024), and CMB (Planck Collaboration 2020). Every measurement of Λ is a measurement of global geometry. Einstein introduced it in 1917 without reference to quantum physics.

3.3 The 120-Order Discrepancy as Evidence of Non-Identity

If Λ and $\rho_{\rm vac}$ were the same, local measurements should give the global value. They do not: $\rho_{\rm vac}^{\rm QFT} \sim M_{\rm Pl}^4 \sim 10^{76}\,{\rm GeV}^4$, while $\rho_\Lambda^{\rm obs} \sim 10^{-47}\,{\rm GeV}^4$. A discrepancy of 10^{120}.

Standard interpretation: a theoretical crisis (Weinberg 1989).

Our interpretation: evidence that the two quantities are not the same. One is local. The other is global. They enter the Einstein equations at similar positions, which led to their identification by Zel'dovich (1967)—without proof. Weinberg (1989) framed the resulting discrepancy as the cosmological constant problem. Coleman (1988) and Kaloper & Padilla (2014) constructed mechanisms to decouple them. We argue the decoupling is the physically correct default.

Counterarguments and Responses

Objection: "In GR, any energy density gravitates. Vacuum energy must contribute to the Friedmann equation."

Response: In QFT, absolute vacuum energy is unobservable; only differences are measurable. Standard renormalization subtracts the vacuum contribution. If this extends to gravity (as the sequestering programme proposes), vacuum energy does not enter the Friedmann equation. What enters is Λ—a geometric constant—and deviations from vacuum (matter, radiation). This is a proposal, not a theorem.

4 Two Processes, Not One

The standard narrative says: "Dark energy expands the universe and fills the voids." We split this into two separate statements about two separate processes.

4.1 Process 1: Expansion of Space

Driven by Λ. Geometric. The metric itself stretches. This happens *everywhere uniformly*—inside galaxies, inside voids, inside atoms (though overwhelmed by local forces at small scales). It does not push matter around. It does not create structure. It does

not favor voids over walls. It is the property of the metric, not of anything *in* the metric.

4.2 Process 2: Vacuum Displaces Matter

Vacuum energy is a local field quantity: the energy of quantum field fluctuations in a given region. Where matter is present, the vacuum state is modified—Pauli blocking reduces fermionic modes, vacuum polarization alters the electromagnetic vacuum, curvature changes the mode spectrum (Kriger 2026). The vacuum energy density inside a matter concentration differs from that in the surrounding empty space.

The surrounding vacuum—unperturbed, at full energy density—exerts pressure on the matter concentration from all sides. This is the same physics as the Casimir effect: modified vacuum (between plates or inside matter) has different energy from unmodified vacuum (outside), and the energy difference produces a force. The force is directed inward: from high-vacuum-energy voids toward low-vacuum-energy matter concentrations.

This pressure pushes matter into clumps. The spaces left behind—emptied of matter—become voids. The voids are not "expanding" in the sense that Λ pushes them apart. They are *growing* because vacuum pressure continues to push residual matter toward the walls and filaments. The voids are filled with unperturbed vacuum, which is the energetically preferred state.

4.3 How Voids Grow: Two Contributions

A void grows for two reasons simultaneously:

1. **Space expansion.** Λ stretches the metric everywhere, including inside the void. This is geometric growth—the void gets bigger because space itself gets bigger.
2. **Vacuum displacement.** The vacuum pressure at the void–wall boundary pushes residual matter outward (from the void's perspective) into the walls. This is physical growth—the void gets emptier because matter is expelled.

These are additive but independent processes. Process 1 happens whether or not there is any vacuum energy. Process 2 happens whether or not space is expanding. In the real universe, both occur simultaneously.

Counterarguments and Responses

Objection: "This distinction is semantic. In the Einstein equations, Λ and vacuum energy enter identically."

Response: Mathematically, a constant $\Lambda\, g_{\mu\nu}$ on the left side and a constant $-\rho_{\text{vac}}\, g_{\mu\nu}$ on the right side produce the same equations. But ρ_{vac} is not constant—it depends on local conditions (Casimir effect). When the vacuum energy is inhomogeneous (because matter is inhomogeneous), its gradient produces forces that Λ cannot. The distinction is physical, not semantic: Λ has no gradient; $\rho_{\text{vac}}(\mathbf{x})$ does.

Section Result and Implications

Space expansion and vacuum displacement are different processes. Conflating them leads to confusion about what "dark energy does." Separating them clarifies: Λ expands; vacuum pushes.

5 Vacuum Energy in the Early Universe

If vacuum energy is a local quantity—the energy of field fluctuations in a given volume—then in a smaller universe, the same energy occupied a smaller volume and the density was higher.

The exact scaling depends on the field content and regularization. For a comoving momentum cutoff, massless fields give $\rho_{\rm vac} \propto a^{-4}$ (radiation-like), massive fields give $\propto a^{-3}$ (matter-like) (Parker & Toms 2009; Birrell & Davies 1982). We adopt $\rho_{\rm vac}(z) \propto (1+z)^n$ with $n \approx 3$ as an illustrative assumption. The qualitative conclusion—vacuum was denser at high z—holds for any $n > 0$.

Epoch	Redshift z	$(1+z)^3$	$\rho_{\rm vac}/\rho_{\rm vac,0}$
Today	0	1	1
Quasar peak	2	27	27
Cosmic web	5	216	216
JWST galaxies	12	2,197	$\sim$ 2,000
First stars	20	9,261	$\sim$ 9,000

Table 1: Vacuum energy density at selected epochs, assuming $n = 3$ scaling.

Does this vacuum energy enter the Friedmann equation? No—under our proposal. The Friedmann equation is driven by Λ (constant, geometric) and matter/radiation. The vacuum energy participates in *local* dynamics (pressure, displacement) but not in *global* expansion. This is the working hypothesis motivated by the sequestering programme (Kaloper & Padilla 2014). If this hypothesis is wrong, and vacuum energy with $w = 0$ does enter Friedmann, then Planck data require $\rho_{\rm vac,0} \ll \rho_\Lambda^{\rm obs}$, weakening the mechanism. We identify the CMB test as the highest-priority constraint.

Counterarguments and Responses

Objection: "The vacuum is Lorentz-invariant with $w = -1$. It cannot dilute."

Response: In flat Minkowski space, yes. In expanding FRW spacetime, Lorentz invariance is broken by the expansion; the mode spectrum evolves with $a(t)$ (Birrell & Davies 1982). The vacuum state at $a = 0.1$ differs from the state at $a = 1$. Assigning $w = 0$ is an effective description of this evolution.

Objection: "The $(1+z)^3$ scaling is assumed, not derived from the renormalized $\langle T_{\mu\nu} \rangle$."

Response: Correct. A rigorous derivation from the renormalized stress-energy tensor of the Standard Model fields in FRW spacetime is an open problem. Our estimate

is parametric; the qualitative conclusion (denser vacuum at higher z) holds for any $n > 0$.

6 Vacuum Pressure on Early Structures

In the early universe, a proto-galactic cloud was surrounded by proto-voids containing unperturbed vacuum at full density. The vacuum pressure at the cloud boundary was:

$$\Delta P_{\rm vac}(z) \sim \rho_{\rm vac}(z)\, c^2 \sim \rho_{\rm vac,0}\, (1+z)^3\, c^2\,. \tag{1}$$

At $z = 12$: $\Delta P_{\rm vac} \sim 2{,}000\, \rho_{\rm vac,0}\, c^2$.

Normalization caveat. The present vacuum energy density $\rho_{\rm vac,0}$ is unknown. If $\rho_{\rm vac,0} \sim \rho_\Lambda^{\rm obs} \sim 6 \times 10^{-27}$ kg m^{-3}, the pressure is dynamically significant ($\sim 10^{-12}$ Pa, exceeding the gravitational self-pressure of proto-galactic clouds). If $\rho_{\rm vac,0}$ is many orders of magnitude smaller, the effect is negligible. All quantitative estimates are conditional on $\rho_{\rm vac,0}$.

The mechanism works because the vacuum pressure is *anisotropic at the cloud boundary*: full vacuum pressure on the void side, modified (reduced) vacuum on the matter side. The gradient drives matter inward—from voids into clumps. This is the same mechanism as the Casimir effect, where modified vacuum between plates has lower energy than unmodified vacuum outside, producing a net inward force.

Counterarguments and Responses

Objection: "Isotropic pressure cancels. You need to demonstrate gradient formation from the stress-energy tensor, not by analogy."

Response: The pressure is isotropic within each region (void, cloud interior) but differs in magnitude between regions because the vacuum state differs. At the boundary, a pressure gradient exists—higher on the void side, lower inside. This is the same principle as atmospheric pressure acting on a vacuum chamber. The field-theoretic derivation of this gradient for realistic cosmological geometries is an open problem—the most important theoretical gap in this work.

7 Consequences for Early Structure Formation

At $z \sim 12$, a collapsing proto-galactic cloud experienced two inward-directed forces:

1. **Gravity.** Self-attraction of the matter cloud. Standard mechanism.
2. **Vacuum pressure.** External compression from the surrounding denser vacuum. $\sim 2{,}000\times$ stronger than today (conditional on normalization).

Both squeeze the cloud. The collapse was faster not because gravity was stronger, but because it had a partner.

Black hole seeds. Eddington-limited growth ($M \propto e^{t/t_{\rm Sal}}$, $t_{\rm Sal} \approx 45$ Myr; Salpeter 1964) is exponentially sensitive to when the first seeds form. If vacuum pressure caused the first massive halos to collapse 30–50 Myr earlier, the exponential amplifies this

into orders of magnitude in final mass. This is a sensitivity illustration; quantitative predictions require simulations.

Giant early stars. Low metallicity prevents fragmentation (Bromm & Larson 2004). Vacuum pressure provides additional external compression, potentially producing more massive stars and heavier remnants.

8 Why the Mechanism Is Inoperative Today

1. Vacuum energy density at $z = 0$ is $\sim$ 2,000$\times$ lower than at $z = 12$. Pressure proportionally weaker.
2. Present-day structures are far denser than the vacuum. Vacuum pressure is negligible compared to gravitational and gas forces.
3. The void–wall contrast in absolute terms is tiny because $\bar{\rho}_{m,0}$ is tiny.

This explains: no new giant galaxies forming today; declining quasar activity; no new supermassive black holes from scratch. The "second hand" has weakened below detectability.

Note: voids still grow today—but primarily through Process 1 (space expansion stretching them) rather than Process 2 (vacuum actively displacing matter). In the early universe, Process 2 was dominant.

9 Uncompensated Vacuum Gravity Inside Galaxies

The two-process framework leads to an unexpected consequence.

9.1 The Fundamental Observation

Every point in space contains energy. Energy is equivalent to mass ($E = mc^2$). Mass gravitates. This is general relativity, not a hypothesis.

The quantum vacuum has energy everywhere. Therefore it has mass everywhere. Therefore it gravitates everywhere. The question is not *whether* vacuum gravitates, but *whether its gravitation is observable.*

9.2 Two Phases of Vacuum

The answer depends on whether the vacuum is in the *expanding* phase or the *bound* phase:

Expanding phase (voids). In a void, the vacuum is uniform. There is no density gradient—no direction in which it can "fall." Vacuum cannot collapse onto itself because it is the same everywhere; there is no center of attraction. Additionally, Λ stretches the space, compensating the vacuum's gravitational self-attraction. The void is stable.

Bound phase (inside galaxies). Inside a gravitationally bound structure, the visible matter creates a potential well deep enough to prevent Λ from stretching the interior. Space inside a galaxy does not expand—this is standard physics (bound systems decouple from the Hubble flow). But the vacuum energy is still there, between

the stars, filling the vast empty spaces. And its gravity is no longer compensated by expansion, because there is no expansion here.

The vacuum inside the galaxy is *part of the galaxy.* It is gravitationally bound, just as the stars are. Its mass adds to the total. A star orbiting at the edge does not care whether the mass comes from stars or from vacuum. A photon being lensed does not care. Mass is mass.

9.3 The Phase Transition Boundary

The boundary between expanding and bound vacuum is the surface where the galaxy's gravitational potential can no longer overcome cosmic expansion. Inside: vacuum is bound, its gravity uncompensated, it is part of the galaxy. Outside: vacuum is free, expanding, its gravity compensated by Λ.

This boundary is the *dark matter halo edge.* Not an arbitrary cutoff but a physical phase transition. The boundary is smooth (the potential decreases gradually), producing a diffuse halo—exactly as observed.

And to infalling galaxy clusters, it does not matter what is inside the halo—stars, gas, or bound vacuum. They gravitate toward the total mass. Light bends around the total mass.

9.4 Order-of-Magnitude Estimate

A typical spiral galaxy has a visible (baryonic) mass of $M_{\rm bar} \sim 5 \times 10^{10}\, M_\odot$ and a dark matter halo mass of $M_{\rm DM} \sim 5 \times M_{\rm bar} \sim 2.5 \times 10^{11}\, M_\odot$, enclosed within a radius $R \sim 100$ kpc $\sim 3 \times 10^{21}$ m.

The volume of this region:

$$V = \frac{4}{3}\pi R^3 \approx 1.1 \times 10^{65}\,\mathrm{m}^3\,. \tag{2}$$

If the vacuum energy density is $\rho_{\rm vac,0}$ and it gravitates, the gravitating vacuum mass in this volume is:

$$M_{\rm vac} = \rho_{\rm vac,0}\, V\,. \tag{3}$$

For $M_{\rm vac}$ to match $M_{\rm DM}$:

$$\rho_{\rm vac,0} = \frac{M_{\rm DM}}{V} = \frac{2.5 \times 10^{11} \times 2 \times 10^{30}}{1.1 \times 10^{65}} \approx 4.5 \times 10^{-24}\,\mathrm{kg\,m^{-3}}\,. \tag{4}$$

Compare with the observed dark energy density: $\rho_\Lambda^{\rm obs} \approx 5.9 \times 10^{-27}\,\mathrm{kg\,m^{-3}}$. The required $\rho_{\rm vac,0}$ is ~ 800 times larger than $\rho_\Lambda^{\rm obs}$.

This is a discrepancy—but a discrepancy of a factor of 10^3, not 10^{120}. And the comparison is not with Λ (which is geometry, not vacuum energy) but with whatever the local vacuum energy density actually is. If $\rho_{\rm vac,0}$ is set by the physics of vacuum fluctuations rather than by Λ, there is no a priori reason it should equal $\rho_\Lambda^{\rm obs}$.

9.5 Rotation Curve Profile

The gravitating vacuum is uniformly distributed (it fills the volume between stars). A uniform mass density ρ_{vac} inside a sphere of radius r contributes:

$$M_{\text{vac}}(r) = \frac{4}{3}\pi\,\rho_{\text{vac}}\,r^3\,. \tag{5}$$

The circular velocity contribution from this uniform component:

$$v_{\text{vac}}(r) = \sqrt{\frac{G\,M_{\text{vac}}(r)}{r}} = \sqrt{\frac{4\pi G\,\rho_{\text{vac}}}{3}}\,r\,. \tag{6}$$

This rises linearly with r. Combined with the falling Keplerian contribution from the baryonic disk ($v_{\text{bar}} \propto r^{-1/2}$ at large r), the total rotation curve:

$$v_{\text{tot}}(r) = \sqrt{v_{\text{bar}}^2(r) + v_{\text{vac}}^2(r)} \tag{7}$$

transitions from rising (inner region, baryonic disk dominates) to approximately flat (outer region, rising vacuum contribution compensates falling baryonic contribution)—exactly as observed.

This is qualitatively the same as an NFW profile at intermediate radii. A detailed comparison with observed rotation curves for specific galaxies is beyond the scope of this paper but constitutes a concrete, falsifiable prediction.

9.6 Gravitational Lensing

A photon passing through a galaxy is deflected by the total gravitational mass, including the vacuum contribution. Since the vacuum mass is distributed more uniformly than the baryonic mass (which is concentrated in a disk and bulge), the lensing profile would differ from a point-mass prediction—stronger at large impact parameters than the visible mass alone would produce. This is consistent with the observed lensing signatures attributed to dark matter halos.

9.7 The Bullet Cluster

The Bullet Cluster (1E 0657-56) is often cited as the strongest evidence for particulate dark matter. Two galaxy clusters collided; the hot gas (detected in X-rays) was slowed by ram pressure and remains near the collision center, while the gravitational mass (detected by lensing) has passed through and is offset from the gas.

This observation is qualitatively consistent with gravitating vacuum. Gas is made of particles—it collides. Vacuum is a field—it cannot collide with itself. Two regions of vacuum simply overlap; there is no scattering cross-section, no ram pressure, no friction. When two clusters merge, their bound vacuum passes through the opposing bound vacuum without interaction, as the lensing data require.

However, a quantitative test is more demanding. If vacuum energy density depends on local curvature (as Section 9.5 requires for rotation curves), then during a cluster

merger the vacuum energy would need to track the evolving gravitational potential in a complex, geometry-dependent way. Whether this reproduces the observed lensing morphology—two distinct mass concentrations spatially offset from the gas—is an open question that requires detailed modelling. We note this as a necessary future test, not a confirmed prediction.

Counterarguments and Responses

Objection: "Dark matter must be cold and collisionless to reproduce the CMB power spectrum and the large-scale structure."

Response: The vacuum is "cold" in the sense that it has no bulk velocity (it fills space uniformly). It is "collisionless" in the sense that it does not scatter—it is a field, not particles. Both properties that CMB fits require of dark matter are automatically satisfied by gravitating vacuum. Whether the vacuum can reproduce the specific CMB acoustic peak ratios (which constrain $\Omega_{\rm DM}h^2$ to $\sim 1\%$) requires a detailed calculation that has not yet been performed.

Objection: "The required $\rho_{\rm vac,0}$ is $\sim 800\times$ the observed dark energy density. This is another fine-tuning."

Response: It is a discrepancy of $\sim 10^3$, not 10^{120}. And the comparison is illegitimate if $\Lambda \neq \rho_{\rm vac}$. The vacuum energy density is whatever it is; it need not equal $\Lambda/8\pi G$. Whether $\rho_{\rm vac,0} \sim 5 \times 10^{-24}\,{\rm kg\,m^{-3}}$ is a "natural" value depends on the underlying physics, which is currently unknown.

Objection: "If vacuum gravity explains dark matter, you have eliminated one mystery but created another: what sets $\rho_{\rm vac,0}$?"

Response: Correct. But the same objection applies to dark matter particles: what sets their mass and cross-section? Decades of direct detection experiments have failed to find them. We replace an undetected particle with a measured phenomenon (vacuum energy)—at the cost of not knowing its gravitating density.

Objection: "Vacuum energy is the same everywhere. How can it form a halo?"

Response: The vacuum energy density *is* the same everywhere. What differs is whether its gravity is compensated by expansion. Inside the bound phase: uncompensated, contributes to the gravitational mass. Outside: compensated by Λ, gravitationally invisible. The "halo" is not a concentration of vacuum—it is the region where vacuum gravity is uncompensated. Its edge is the phase transition between bound and expanding vacuum.

Section Result and Implications

If vacuum energy gravitates ($E = mc^2$, GR) and expansion is absent inside bound structures, the vacuum acts as a uniformly distributed, invisible, collisionless gravitating component—matching the description of dark matter. The halo boundary is a phase transition between bound and expanding vacuum. The required density ($\sim 5\times10^{-24}\,{\rm kg\,m^{-3}}$) is empirically testable. If confirmed, dark matter is not a particle—it is vacuum energy, gravitationally bound to the structures it helps hold together.

10 The 120-Order Problem Is Reframed

In this framework, the cosmological constant problem is reframed:

- Λ is a geometric property of spacetime. It drives expansion. Its value is $\rho_\Lambda^{\rm obs} \sim 10^{-47}$ GeV^4. This is a measured number.
- $\rho_{\rm vac}$ is the energy of quantum field fluctuations. It drives structure formation (via pressure and displacement). Its value is whatever QFT computes—possibly $\sim M_{\rm Pl}^4 \sim 10^{76}$ GeV^4.
- They do different things. They need not be equal. There is no problem.

The "problem" arose because in 1967 Zel'dovich identified $\rho_{\rm vac}$ with Λ. This identification was never proven. It was motivated by the mathematical observation that both enter the Einstein equations as terms proportional to $g_{\mu\nu}$. But this mathematical similarity does not imply physical identity, any more than two forces that both obey $F \propto 1/r^2$ are the same force.

The vacuum energy may be enormous. It may be 10^{120} times Λ. This is not a problem—it is simply two different quantities having different values. One of them (vacuum energy) pushes matter around locally and gravitates inside bound structures. The other (Λ) stretches space globally. Neither needs to explain the other.

In a sense, Einstein was right—twice. His $E = mc^2$ (1905) demands that vacuum energy gravitates. His Λ (1917) is a geometric constant of spacetime. Both stand. What does not stand is the identification $\Lambda = 8\pi G\rho_{\rm vac}$, introduced by Zel'dovich (1967), which was never a consequence of Einstein's theory but an additional assumption. The 120-order "crisis" is the result of this assumption. Remove it, and both of Einstein's results are preserved exactly as stated—and three major puzzles (early galaxies, dark matter, the cosmological constant problem) find a common resolution.

Counterarguments and Responses

Objection: "This doesn't *solve* the CC problem. It just refuses to acknowledge it."

Response: The CC problem as traditionally stated—why do Λ and $\rho_{\rm vac}$ disagree by 10^{120}?—exists only if $\Lambda = 8\pi G\rho_{\rm vac}$. If this identity is wrong, that specific question loses its force. However, the residual question—why doesn't the large vacuum energy dominate cosmological expansion?—remains. We do not solve this; we reframe it as a separate problem that may have a separate answer (e.g., vacuum sequestering: Kaloper & Padilla 2014). The reframing may or may not be productive, but the original identification was assumed without proof, and questioning it is legitimate.

11 Connections to Existing Work

11.1 Vacuum Sequestering

Weinberg (1989) surveyed mechanisms for neutralizing vacuum gravity. Coleman (1988) proposed wormhole-mediated cancellation. Kaloper & Padilla (2014) built Lagrangian-level sequestering. Our proposal is consistent with this tradition: vacuum energy does not enter the Friedmann equation.

11.2 Backreaction Programme

Buchert (2000) and Räsänen (2004) showed that averaging over inhomogeneities produces effective dark-energy-like terms. Wiltshire (2007) attributed apparent acceleration to differential expansion. Seifert et al. (2025) found evidence for this in supernova data. Our model differs: we do not derive effective dark energy from averaging. We propose that vacuum energy is a separate dynamical component that drives structure formation locally. The two approaches may be complementary.

11.3 Penrose and Ellis

Penrose's gravitational entropy programme (1979, 2004, 2010): the growth of structure corresponds to increasing Weyl curvature. Our mechanism provides a physical driver—vacuum pressure—for rapid early structure growth. Ellis's fitting problem (1984, 1987): if vacuum energy is local and inhomogeneous, fitting to a smooth Friedmann model introduces systematic errors. Both connections are qualitative.

11.4 Companion Paper

A companion paper (Kriger 2026) developed a parametric model of spatial vacuum energy variation: $\Lambda(\rho_m) = \Lambda_0 - \alpha\rho_m$, addressing the void-vs-wall contrast at a fixed epoch. The present paper addresses temporal evolution. The two approaches are complementary but independent.

12 Discussion

12.1 The Central Claim

If Λ and ρ_{vac} are different, three things follow immediately:

1. Vacuum energy was denser in the past (it dilutes; Λ does not).
2. Vacuum pressure on matter was stronger in the early universe.
3. The 120-order problem is reframed (it ceases to be a comparison of two supposedly identical quantities).

If $\Lambda = \rho_{\text{vac}}$, the model fails entirely.

12.2 The Normalization Problem

$\rho_{\text{vac},0}$ is unknown. If comparable to $\rho_\Lambda^{\text{obs}}$, the vacuum pressure was dynamically significant. If much smaller, the effect is negligible. This is the model's largest uncertainty—spanning potentially many orders of magnitude. Determining $\rho_{\text{vac},0}$ independently (perhaps through precision Casimir measurements of absolute vacuum energy, or through lattice QFT calculations) would test the model.

12.3 The CMB Test

Compatibility with the CMB is not an optional follow-up; it is a prerequisite for viability. The baryon-to-dark-matter ratio at recombination is measured to high precision by Planck ($\Omega_{\rm DM}h^2 = 0.120 \pm 0.001$). Dark matter must behave as a pressureless, clustering component before decoupling. If vacuum energy with $w \approx 0$ enters the Friedmann equation, Planck data require $\rho_{\rm vac,0} \ll \rho_\Lambda^{\rm obs}$, severely weakening the mechanism. Under the sequestering hypothesis, vacuum energy is gravitationally inert at the global level and no CMB conflict arises—but this hypothesis must be tested. Albareti & Maroto (2014) showed that vacuum energy of massive fields can scale as nonrelativistic matter and that vacuum density perturbations grow on sub-Hubble scales; whether this extends to the full Standard Model field content is unknown. A rigorous MCMC analysis is the highest priority for future work and could be decisive.

13 Limitations

1. The separation of Λ and $\rho_{\rm vac}$ is a proposal, not a proven fact.
2. The scaling $\rho_{\rm vac} \propto (1+z)^n$ is parametric; n is model-dependent.
3. $\rho_{\rm vac,0}$ is unknown. Quantitative predictions are conditional.
4. The pressure gradient mechanism is Casimir-motivated, not derived from the stress-energy tensor in cosmological geometry.
5. If vacuum energy enters Friedmann, Planck constraints may be severe.
6. No simulations performed.
7. Hawking radiation is theoretical, not directly observed.
8. Connections to Penrose/Ellis/backreaction are qualitative.

14 Future Directions

1. Derivation of $\langle T_{\mu\nu} \rangle_{\rm ren}$ in FRW for Standard Model fields.
2. Hydrodynamic simulations with vacuum pressure.
3. MCMC fit to Planck with diluting vacuum component.
4. Independent determination of $\rho_{\rm vac,0}$.
5. Modified Press–Schechter with vacuum pressure.
6. Lagrangian formulation of the two-process separation.

15 Conclusions

We have proposed that three major puzzles in cosmology—early galaxy formation, dark matter, and the cosmological constant problem—share a common origin: the conflation of two distinct quantities (Λ and $\rho_{\rm vac}$) and two distinct processes (space expansion and vacuum displacement of matter).

Λ is global geometry. It stretches space uniformly. It is constant everywhere and always—exactly as Einstein intended in 1917.

Vacuum energy is local field physics. It has mass ($E = mc^2$). It gravitates. It pushes matter into clumps, forming the cosmic web. In the early universe, it was $\sim$ 2,000 times denser and pushed $\sim$ 2,000 times harder, accelerating structure formation. As the universe expanded, it diluted and the mechanism turned off.

Inside galaxies, where expansion is suppressed by gravitational binding, vacuum gravity is uncompensated—producing the invisible, collisionless, uniformly distributed gravitating component we call dark matter. The dark matter halo boundary is a phase transition between bound and expanding vacuum. Dark matter "passes through itself" (Bullet Cluster) because fields superpose—they do not collide.

The 120-order problem is reframed: if vacuum energy and Λ are different quantities with different roles, they need not be equal.

The model is falsifiable: if $\Lambda = \rho_{\rm vac}$ can be demonstrated, it fails. If simulations cannot reproduce observed rotation curves with uniform vacuum density, it fails. If the required $\rho_{\rm vac,0} \sim 5 \times 10^{-24}\,\mathrm{kg\,m^{-3}}$ is excluded by independent measurement, it fails.

16 Peer Reviews and Revision History

First Round

Reviewer assessment (multiple reviewers). The paper was found to be bold, clearly written, and to address timely issues. Major concerns raised: (1) the $(1+z)^3$ scaling is assumed, not derived from the renormalized $\langle T_{\mu\nu} \rangle$; (2) the normalization $\rho_{\rm vac,0}$ is unknown, making all quantitative estimates conditional; (3) CMB compatibility is a prerequisite, not an optional test; (4) the vacuum pressure gradient is motivated by Casimir analogy but not derived from the stress-energy tensor in cosmological geometry; (5) claiming the CC problem "dissolves" overclaims; (6) the Bullet Cluster argument was too casual; (7) self-citation balance. Verdict: major revisions.

Response. (1) The scaling is now explicitly labeled as a parametric assumption with model-dependent exponent n; qualitative conclusions hold for any $n > 0$. (2) The normalization uncertainty is emphasized throughout as the single largest uncertainty. (3) The CMB section has been rewritten to state that compatibility is a prerequisite, not a follow-up, and cites Albareti & Maroto (2014) on vacuum energy behaving as nonrelativistic matter. (4) The pressure gradient is acknowledged as the most important theoretical gap; we do not claim a derivation. (5) "Dissolves" has been replaced by "is reframed," with explicit discussion of the residual question. (6) The Bullet Cluster section now acknowledges that a quantitative lensing model is needed. (7) The companion paper citation has been toned down.

References

Albareti, F. D., & Maroto, A. L. (2014). Vacuum energy as dark matter. *Phys. Rev. D*, 90, 123509.

Bahcall, J. N., & Pinsonneault, M. H. (2004). What do we (not) know theoretically about solar neutrino fluxes? *Phys. Rev. Lett.*, 92, 121301.

Birrell, N. D., & Davies, P. C. W. (1982). *Quantum Fields in Curved Space*. Cambridge Univ. Press.

Bogdán, Á., et al. (2024). Evidence for heavy-seed origin of early supermassive black holes. *Nat. Astron.*, 8, 126–133.

Boylan-Kolchin, M. (2023). Stress testing ΛCDM with high-redshift galaxy candidates. *Nat. Astron.*, 7, 731–735.

Bressi, G., et al. (2002). Measurement of the Casimir force. *Phys. Rev. Lett.*, 88, 041804.

Bromm, V., & Larson, R. B. (2004). The first stars. *Ann. Rev. Astron. Astrophys.*, 42, 79–118.

Buchert, T. (2000). On average properties of inhomogeneous fluids in general relativity. *Gen. Rel. Grav.*, 32, 105–125.

Casimir, H. B. G. (1948). On the attraction between two perfectly conducting plates. *Proc. Kon. Ned. Akad. Wet.*, 51, 793–795.

Coleman, S. (1988). Why there is nothing rather than something. *Nucl. Phys. B*, 310, 643–668.

DESI Collaboration (2024). DESI 2024 VI: Cosmological constraints from BAO. arXiv:2404.03002.

Ellis, G. F. R. (1984). Relativistic cosmology: its nature, aims and problems. In *Gen. Rel. Grav.* (pp. 215–288). Reidel.

Ellis, G. F. R. (1987). The fitting problem in cosmology. In *Gen. Rel. Grav.* (pp. 337–347). Plenum.

Hawking, S. W. (1974). Black hole explosions? *Nature*, 248, 30–31.

Hawking, S. W. (1975). Particle creation by black holes. *Commun. Math. Phys.*, 43, 199–220.

Jaffe, R. L. (2005). Casimir effect and the quantum vacuum. *Phys. Rev. D*, 72, 021301.

Kaloper, N., & Padilla, A. (2014). Sequestering the standard model vacuum energy. *Phys. Rev. Lett.*, 112, 091304.

Kokorev, V., et al. (2024). A census of photometrically selected little red dots at $4 < z < 9$. *ApJ*, 968, 38.

Kriger, B. (2026). Matter-dependent vacuum energy density and inhomogeneous cosmic expansion. Information Physics Institute. doi:10.5281/zenodo.18896536.

Labbé, I., et al. (2023). A population of red candidate massive galaxies ∼600 Myr after the Big Bang. *Nature*, 616, 266–269.

Lamb, W.E., Jr., & Retherford, R.C. (1947). Fine structure of the hydrogen atom. *Phys. Rev.*, 72, 241–243.

Lamoreaux, S.K. (1997). Demonstration of the Casimir force. *Phys. Rev. Lett.*, 78, 5–8.

Parker, L.E., & Toms, D.J. (2009). *Quantum Field Theory in Curved Spacetime*. Cambridge Univ. Press.

Penrose, R. (1979). Singularities and time-asymmetry. In *Gen. Rel.: An Einstein Centenary Survey* (pp. 581–638). Cambridge Univ. Press.

Penrose, R. (2004). *The Road to Reality*. Jonathan Cape.

Penrose, R. (2010). *Cycles of Time*. Bodley Head.

Perlmutter, S., et al. (1999). Measurements of Ω and Λ from 42 high-redshift supernovae. *ApJ*, 517, 565.

Planck Collaboration (2020). Planck 2018 results. VI. Cosmological parameters. *A&A*, 641, A6.

Räsänen, S. (2004). Backreaction in the LTB model. *JCAP*, 2004(11), 010.

Riess, A.G., et al. (1998). Observational evidence from supernovae for an accelerating universe. *Astron. J.*, 116, 1009.

Salpeter, E.E. (1964). Accretion of interstellar matter by massive objects. *ApJ*, 140, 796–800.

Seifert, A., et al. (2025). Supernovae evidence for foundational change to cosmological models. *MNRAS Lett.*, 537, L55–L60.

Shifman, M.A., Vainshtein, A.I., & Zakharov, V.I. (1979). QCD and resonance physics. *Nucl. Phys. B*, 147, 385–447.

Solà, J. (2013). Cosmological constant and vacuum energy: old and new ideas. *J. Phys.: Conf. Ser.*, 453, 012015.

Solà Peracaula, J., et al. (2017). Dynamical dark energy vs. Λ = const. *Europhys. Lett.*, 121, 39001.

Volonteri, M. (2010). Formation of the first massive black holes. *Astron. Astrophys. Rev.*, 18, 279–315.

Weinberg, S. (1989). The cosmological constant problem. *Rev. Mod. Phys.*, 61, 1–23.

Wiltshire, D. L. (2007). Cosmic clocks, cosmic variance and cosmic averages. *New J. Phys.*, 9, 377.

Zel'dovich, Ya. B. (1967). Cosmological constant and elementary particles. *JETP Letters*, 6, 316–317.

A Computational Code

```
import numpy as np

rho_vac_0 = 5.9e-27  # kg/m^3 (illustrative: ~ rho_Lambda_obs)
c = 3e8               # m/s
G = 6.674e-11         # m^3 kg^-1 s^-2

def rho_vac(z, n=3):
    return rho_vac_0 * (1+z)**n

def P_vac(z, n=3):
    return rho_vac(z, n) * c**2

# Table
print(f"{'z':>5} {'rho/rho0':>12} {'P_vac (Pa)':>12}")
for z in [0, 2, 5, 12, 20]:
    print(f"{z:5d} {(1+z)**3:12.0f} {P_vac(z):12.2e}")

# Comparison at z=12
rho_cloud = 100 * 2000 * 2.7e-27  # 100x overdensity at z=12
R = 3e19  # 1 kpc
P_grav = G * rho_cloud**2 * R**2
P_v = P_vac(12)
print(f"\nz=12: P_vac={P_v:.2e} Pa, P_grav={P_grav:.2e} Pa")
print(f"Ratio: {P_v/P_grav:.0f}")
print("(Conditional on rho_vac_0 ~ rho_Lambda_obs)")
```

Two Pathways of Primordial Cloud Collapse:

Fragmentation versus Direct Collapse under Enhanced Vacuum Energy

Boris Kriger[1,2]

[1] Information Physics Institute, Gosport, Hampshire, United Kingdom
boris.kriger@informationphysicsinstitute.net

[2] Institute of Integrative and Interdisciplinary Research, Toronto, Canada
boriskriger@interdisciplinary-institute.org

ORCID: 0009-0001-0034-2903

Abstract

We explore the consequences of a specific hypothetical scenario for primordial cloud collapse. The scenario rests on three conditional premises: (1) that the cosmological constant Λ and the quantum vacuum energy density $\rho_{\rm vac}$ are physically distinct quantities; (2) that if they are distinct, $\rho_{\rm vac}$ was denser in the early universe by a factor $(1+z)^3$; and (3) that if such a denser vacuum existed, there is a mechanism by which it exerts net inward pressure on matter concentrations. None of these premises is established. Each may be wrong. We do not claim to prove them. We ask: *if all three hold*, what happens to a primordial gas cloud?

We trace the evolution of a single cloud ($M \sim 10^5\ M_\odot$, $T \sim 10^4$ K, $z \sim 12$) under three sets of conditions. In Scenario A (trace metallicity, standard vacuum), dust-induced cooling triggers fragmentation into a stellar cluster with remnant black holes of $\sim$ 10–100 $M_\odot$. In Scenario B (zero metallicity, standard vacuum), the well-established direct-collapse pathway produces a supermassive star and a $\sim 10^4$–$10^5\ M_\odot$ seed—but requires a fine-tuned Lyman–Werner radiation source. In Scenario C (zero metallicity, enhanced vacuum pressure), the hypothetical vacuum confinement provides an additional, isotropic compression mechanism that may reduce the Lyman–Werner requirement and accelerate the collapse timescale. Scenario C is the new contribution. Scenarios A and B are well-established control cases drawn from the existing literature.

The comparison is a thought experiment grounded in standard collapse physics (Jeans instability, Bonnor–Ebert stability, Salpeter accretion), applied under a hypothetical boundary condition (enhanced external vacuum pressure) whose physical reality remains to be demonstrated. The value of the exercise is that *if* the premises hold, the resulting mechanism is universal (no fine-tuning), self-terminating (dilutes with expansion), and produces the heavy seeds that JWST observations appear to demand.

Keywords: vacuum energy, direct collapse black hole, primordial gas cloud, Jeans instability, Bonnor–Ebert mass, supermassive star, early universe, JWST, structure formation, fragmentation, conditional model

Contents

1 Introduction

The James Webb Space Telescope has revealed massive galaxies and supermassive black holes at redshifts that challenge the standard cosmological timeline. Labbé et al. (2023) found candidate massive galaxies with stellar masses exceeding 10^{10} $M_\odot$ at $z > 10$, within ~ 400 Myr of the Big Bang. Bogdán et al. (2024) detected a supermassive black hole at $z = 10.1$ consistent with a heavy-seed origin. Maiolino et al. (2024) confirmed an AGN at $z \approx 8.7$ with a black-hole-to-stellar-mass ratio exceeding local scaling relations by two orders of magnitude. Boylan-Kolchin (2023) demonstrated formally that these discoveries require assembly rates 3–10 times faster than ΛCDM predictions.

The timescale problem is acute. Growing stellar-mass seeds ($\sim$ 10–100 $M_\odot$; Bromm & Larson 2004) to $\sim 10^9$ $M_\odot$ by $z \sim 6$ via Eddington-limited accretion ($M \propto e^{t/t_{\rm Sal}}$, $t_{\rm Sal} \approx 45$ Myr; Salpeter 1964) requires nearly continuous accretion over $\sim$ 800 Myr (Inayoshi et al., 2020; Volonteri, 2010). The direct-collapse black hole (DCBH) scenario (Bromm & Loeb, 2003; Lodato & Natarajan, 2006) circumvents this by producing seeds of 10^4–10^6 $M_\odot$, but requires two restrictive conditions: zero metallicity ($Z < 10^{-5}$ $Z_\odot$; Omukai et al. 2008) and intense Lyman–Werner UV radiation ($J_{21} \gtrsim 10^3$; Omukai 2001). The LW requirement confines DCBH formation to rare "synchronized pairs" of halos (Inayoshi et al., 2020), producing an abundance of seeds that may be too low for the observed population of early massive black holes.

This paper explores whether a third ingredient—external vacuum pressure—could relax the LW requirement and make direct collapse more common. The exploration is conditional. It rests on three premises, each of which is a hypothesis:

P1: Separation: The cosmological constant Λ and the quantum vacuum energy density $\rho_{\rm vac}$ are physically distinct quantities. Λ is a geometric property of spacetime; $\rho_{\rm vac}$ is a local field quantity. This is not established. The identification $\Lambda = 8\pi G\rho_{\rm vac}$ by Zel'dovich (1967) was assumed, not derived, but it has not been disproven either.

P2: Dilution: If $\rho_{\rm vac}$ is a local quantity distinct from Λ, it need not be constant. We assume it dilutes with expansion as $\rho_{\rm vac}(z) = \rho_{\rm vac}[0]\,(1+z)^3$, making the vacuum $\sim$ 2,000 times denser at $z = 12$. The exponent $n = 3$ is motivated by self-consistency requirements of the matter-dependent ansatz $\rho_{\rm vac}(\rho_m) = \rho_{\rm vac}[\text{bare}] - \alpha\,\rho_m$ developed in Kriger (2026d) and Kriger (2026c), but is not derived from the renormalized stress-energy tensor and may be wrong.

P3: Pressure mechanism: If a denser vacuum surrounds a matter concentration, there exists a mechanism by which the energy-density contrast at the cloud bound-

ary produces a net inward pressure. We motivate this by analogy with the Casimir effect (energy-density contrast between regions with different boundary conditions produces a force), but we acknowledge explicitly that the Casimir analogy involves conducting plates at microscopic separations, not diffuse gas clouds at kiloparsec scales. The extrapolation has not been derived from the stress-energy tensor in cosmological geometry.

What this paper does: We take P1–P3 as given and ask what follows for primordial cloud collapse, using only standard physics (Jeans instability, Bonnor–Ebert stability, Salpeter accretion) under this hypothetical boundary condition.

What this paper does not do: We do not prove P1, P2, or P3. We do not claim that vacuum energy is the source of the pressure. We do not claim this model is correct. We explore its consequences and identify what would need to be true—and what could be tested—for it to work.

The paper is organized as follows. Section 2 maps the logical structure. Section 3 reviews established collapse physics. Section 4 develops the conditional framework. Section 5 presents the mathematical development with three scenarios. Section 6 compares growth histories quantitatively. Sections 7–9 discuss implications, limitations, and future tests.

2 Logical Structure of the Argument

The reasoning is a conditional chain: *if P1, P2, P3 hold, then the following consequences follow.*

1. **Metallicity determines fragmentation** (§3). Below $Z_{\rm cr} \sim 10^{-5}$–$10^{-6}\ Z_\odot$, clouds do not fragment (Omukai et al., 2005, 2008). Above $Z_{\rm cr}$, dust cooling drives fragmentation. This is established physics.
2. **External pressure modifies the critical mass for collapse** (§3). The Bonnor–Ebert critical mass $M_{\rm BE} \propto T^2/P_{\rm ext}^{1/2}$ (Bonnor, 1956; Ebert, 1955). Higher external pressure lowers $M_{\rm BE}$. This is established physics.
3. **Premise P1–P3 supply a hypothetical external pressure** (§4). If the vacuum at $z \sim 12$ was $\sim 2{,}000\times$ denser, and if a pressure mechanism exists, this pressure enters the Bonnor–Ebert problem as an additional confining term. *This step is conditional.*
4. **Three scenarios are compared** (§5).
   A: Metals + standard vacuum → fragmentation → stellar cluster.
   B: No metals + standard vacuum → standard DCBH (requires LW fine-tuning).

C: No metals + enhanced vacuum pressure → DCBH with relaxed LW requirement.

Scenarios A and B are established. Scenario C is the conditional prediction.

5. **Growth comparison** (§6). The mass advantage of heavy seeds is quantified via Salpeter growth. This is standard physics applied to the different seed masses.
6. **The mechanism would be universal and self-terminating** (§7). If P1–P3 hold, vacuum pressure acts isotropically (no LW fine-tuning) and dilutes with expansion (self-terminates).

Steps 1, 2, 4 (Scenarios A and B), and 5 involve only established physics. Step 3 and Scenario C are conditional on P1–P3.

3 Background and Related Work

3.1 Thermal Evolution of Collapsing Primordial Gas

The fate of a collapsing gas cloud is governed by the temperature–density relation during collapse. Omukai (2001) showed that in metal-free gas with suppressed H_2 cooling, the gas cools only via Lyα emission, maintaining $T \approx 8{,}000$ K throughout collapse. The Jeans mass at this temperature is

$$M_{\rm J} = \frac{\pi^{5/2}}{6} \frac{c_s^3}{G^{3/2}\,\rho^{1/2}} \approx 7.6 \times 10^4\ M_\odot \quad (\text{at } T = 8{,}000\ \text{K},\ n = 10^4\ \text{cm}^{-3})\,, \tag{1}$$

preventing fragmentation.

Omukai et al. (2005) mapped the full metallicity range. Omukai et al. (2008) established the critical metallicity: $Z_{\rm cr} \sim 10^{-5}$–$10^{-6}\ Z_\odot$. Below this threshold, direct collapse proceeds; above it, dust cooling triggers fragmentation into sub-solar-mass clumps. Recent 3D simulations by Chon et al. (2025) confirm this threshold.

3.2 The Standard DCBH Pathway

The DCBH scenario (Bromm & Loeb, 2003; Lodato & Natarajan, 2006; Begelman et al., 2006) requires:

1. Metal-free gas ($Z < Z_{\rm cr}$).
2. Suppressed H_2 cooling, typically via an external LW flux $J_{21} \gtrsim 10^2$–10^3.
3. An atomic-cooling halo ($T_{\rm vir} \gtrsim 10^4$ K).

Under these conditions, the gas collapses isothermally at $\sim 8{,}000$ K with accretion rates $\dot{M} \sim c_s^3/G \sim 0.1$–$1\ M_\odot\,{\rm yr}^{-1}$ (Shu, 1977). Rapid accretion inflates the protostar,

suppressing UV feedback (Hosokawa et al., 2012, 2013), allowing growth to $\sim 10^5\ M_\odot$ before collapse via GR instability.

The LW requirement is the key bottleneck. It restricts DCBH formation to the vicinity of star-forming galaxies, yielding predicted number densities of $\sim 10^{-6}$–10^{-4} Mpc^{-3} (Inayoshi et al., 2020)—possibly insufficient for the JWST population. Wise et al. (2019) showed that cold turbulent accretion flows can bypass the LW requirement in rare halo configurations, but this pathway is also cosmologically infrequent.

3.3 External Pressure in Cloud Stability

The Bonnor–Ebert mass (Bonnor, 1956; Ebert, 1955) defines the maximum mass stable against collapse under external pressure:

$$M_{\rm BE} = 1.18\,\frac{c_s^4}{G^{3/2}\,P_{\rm ext}^{1/2}}\,. \tag{2}$$

Higher $P_{\rm ext}$ lowers $M_{\rm BE}$: external compression destabilizes clouds. Zier et al. (2021) showed quantitatively that increased external pressure from stellar winds can trigger Bonnor–Ebert collapse. This is the established physics we will apply under the hypothetical vacuum pressure boundary condition.

Section Result and Implications

The physics of metallicity-dependent fragmentation, isothermal DCBH collapse, and pressure-modified stability is well established. What is not established is whether vacuum energy provides a relevant external pressure. Everything in this section is standard; everything conditional enters in the next section.

4 Conceptual Framework: The Conditional Premises

This section states the three premises explicitly and examines what each would imply if true. We emphasize: these are hypotheses, not results.

4.1 Premise P1: $\Lambda \neq 8\pi G\,\rho_{\rm vac}$

The identification of Λ with $\rho_{\rm vac}$ was proposed by Zel'dovich (1967). It produced the 10^{120}-order discrepancy (Weinberg, 1989). Several programmes have explored their decoupling: Coleman (1988) proposed wormhole-mediated cancellation; Kaloper &

Padilla (2014) built a Lagrangian-level sequestering mechanism. Kriger (2026a,b,c) developed the specific framework we explore here.

Status: P1 is a legitimate open question in theoretical physics. It has not been confirmed or excluded by any experiment. The 10^{120} discrepancy can be read as evidence for separation, but this reading is not forced.

4.2 Premise P2: $\rho_{\rm vac}(z) = \rho_{\rm vac}[0]\,(1+z)^3$

If $\rho_{\rm vac}$ is distinct from Λ, its evolution depends on the physics of the vacuum in expanding spacetime. In flat Minkowski space, the vacuum is Lorentz-invariant with $w = -1$. In FRW spacetime, the mode spectrum evolves with $a(t)$ (Birrell & Davies, 1982), and the effective equation of state depends on the field content.

Critical point regarding observational constraints: A vacuum component with $w = 0$ and density comparable to or exceeding the cosmological constant would be catastrophically inconsistent with CMB, BAO, and supernova data—*if it entered the Friedmann equation.* The companion framework (Kriger, 2026c) proposes that $\rho_{\rm vac}$ is sequestered from cosmological dynamics: it gravitates locally inside bound structures but does not drive expansion. Under this hypothesis, the Friedmann equation contains Λ (geometric, small, constant) plus matter and radiation—but not $\rho_{\rm vac}$. If this sequestering fails, P2 is observationally excluded.

Important clarification regarding sequestering. The mechanism proposed in the companion framework is *not* identical to the Kaloper & Padilla (2014) vacuum sequestering. Kaloper & Padilla construct a Lagrangian-level mechanism that cancels the vacuum energy's contribution to *both* local and global gravity—their mechanism removes vacuum energy from gravitational dynamics entirely. The companion framework requires something different and more demanding: a mechanism that removes vacuum energy from the Friedmann equation (global expansion) while preserving its gravitational effect inside bound structures (local dynamics). This requires the gravitational coupling of $\rho_{\rm vac}$ to be *scale-dependent*: inactive on cosmological (Hubble) scales but active on galactic scales where expansion is suppressed. In standard general relativity, the equivalence principle ties local and global gravitational effects together, making such scale-dependent coupling difficult to achieve.

We do not have a Lagrangian derivation of this selective sequestering. The companion framework motivates it by analogy with the well-established fact that bound systems (galaxies, clusters) decouple from the Hubble flow (Carrera & Giulini, 2010): inside a gravitationally bound structure, expansion is suppressed and the vacuum's

gravity is uncompensated, while outside, expansion compensates the vacuum's self-gravitation. Whether this physical picture can be elevated to a rigorous field-theoretic mechanism is an open question. Until it is, P2 rests on an assumed (not derived) scale-dependent coupling. The sequestering hypothesis has not been tested against Planck data via MCMC analysis, and we identify this as the most important quantitative test (Section 9).

Status: P2 depends on P1 and on an untested sequestering mechanism. It is speculative.

4.3 Premise P3: Vacuum Energy Exerts Net Pressure on Matter

If the vacuum energy density differs between regions (higher in voids, lower inside matter concentrations due to mode-spectrum modification), the gradient produces a net force. This is motivated by analogy with the Casimir effect (Casimir, 1948): different boundary conditions produce different vacuum energies, and the difference generates a measurable force (Lamoreaux, 1997).

The analogy's limitations: The Casimir effect involves conducting plates separated by sub-micrometer distances, where the mode spectrum is sharply modified by metallic boundary conditions. A diffuse gas cloud at kiloparsec scales with density $n \sim 10^4$ cm^{-3} presents a qualitatively different situation. The mode-spectrum modification inside such a cloud—due to Pauli blocking of fermionic modes, vacuum polarization by the electromagnetic field, and curvature modification of the fluctuation spectrum—has not been computed from the stress-energy tensor in cosmological geometry.

What would need to be true: For P3 to work, the vacuum energy inside a matter concentration must be measurably lower than outside, and the transition must occur over a scale comparable to the cloud radius, producing a pressure differential at the boundary. Whether this happens is an open question in quantum field theory in curved spacetime.

Status: P3 is the weakest premise. It is motivated but not derived. The paper acknowledges this explicitly and treats all results conditioned on P3 as hypothetical.

Counterarguments and Responses

Objection: If P1–P3 are all unproven, why write the paper?

Response: Because the consequences are specific, quantitative, and testable. If the premises are wrong, the consequences will not match observation, and the premises can be discarded. If they are right, the model predicts a universal mechanism for heavy seed formation that resolves a real observational puzzle. The paper's value lies not in asserting that the premises hold, but in deriving what would follow if they did—and in identifying the tests that could confirm or refute them.

Objection: A paper built on three unproven premises is speculation, not physics.

Response: Much of theoretical cosmology explores consequences of hypotheses. Dark matter particle models are built on the unproven premise that such particles exist. Modified gravity theories rest on unproven modifications to GR. The standard DCBH model itself rests on the premise that sufficiently strong LW radiation exists near pristine halos—a condition that is posited, not observed directly. What matters is whether the hypothesis leads to testable predictions and whether those predictions are novel. This paper provides both.

Section Result and Implications

Three conditional premises have been stated, with their status assessed honestly. P1 is a legitimate open question; P2 depends on untested sequestering; P3 is the weakest link, motivated but not derived. All quantitative results in subsequent sections are explicitly conditioned on P1–P3.

5 Mathematical Development

5.1 Initial Conditions (Shared Across All Scenarios)

Definition 5.1 (Reference Cloud)**.** *The reference cloud has the following properties at the onset of collapse:*

- *Total mass:* $M_{\rm cloud} = 10^5\ M_\odot$
- *Initial temperature:* $T_0 = 10^4$ K
- *Mean molecular weight:* $\mu = 1.22$ *(neutral primordial gas)*
- *Initial hydrogen number density:* $n_0 = 10^4\ {\rm cm}^{-3}$
- *Redshift:* $z = 12$
- *Halo virial temperature:* $T_{\rm vir} \approx 10^4$ K *(atomic-cooling halo)*

The isothermal sound speed at $T = 8{,}000$ K (the atomic-cooling floor relevant to

Scenarios B and C):

$$c_s = \sqrt{\frac{k_B T}{\mu\, m_H}} = \sqrt{\frac{1.38 \times 10^{-23} \times 8000}{1.22 \times 1.67 \times 10^{-27}}} \approx 7.4\ \mathrm{km\,s^{-1}}\,. \tag{3}$$

The thermal pressure of the cloud at $n_0 = 10^4$ cm^{-3}, $T = 8{,}000$ K:

$$P_{\rm cloud} = n_0\, k_B\, T = 10^{10}\ \mathrm{m^{-3}} \times 1.38 \times 10^{-23}\ \mathrm{J\,K^{-1}} \times 8000\ \mathrm{K} = 1.1 \times 10^{-9}\ \mathrm{Pa}\,. \tag{4}$$

This is the correct scale against which any additional external pressure should be compared—not the gravitational self-pressure, which describes the weight of the cloud per unit area, but the thermal pressure, which is what actually supports the cloud against collapse.

The standard free-fall time at this density:

$$t_{\rm ff} = \sqrt{\frac{3\pi}{32\, G\, \rho_0}} = \sqrt{\frac{3\pi}{32 \times 6.674 \times 10^{-11} \times 2.04 \times 10^{-17}}} \approx 4.7 \times 10^{13}\ \mathrm{s} \approx 1.5\ \mathrm{Myr}\,. \tag{5}$$

5.2 Scenario A: Fragmentation (Metals + Standard Vacuum)

Proposition 5.2 (Fragmentation Outcome)**.** *A cloud with $Z \gtrsim 10^{-5}\ Z_\odot$ and standard vacuum evolves as follows:*

1. *Isothermal collapse at $T \sim 8{,}000$–$10{,}000$ K (atomic cooling).*
2. *Molecular cooling (H_2, HD) reduces T to ~ 200–500 K at $n \sim 10^4$–10^8 cm^{-3}.*
3. *Dust cooling at $n \gtrsim 10^{10}$ cm^{-3} drives $\gamma_{\rm eff} < 1$.*
4. *Jeans mass drops to $M_{\rm J} \sim 0.01$–$1\ M_\odot$.*
5. *Cloud fragments into $\sim 10^2$–10^3 stars.*
6. *Massive stars produce BH remnants of ~ 10–$100\ M_\odot$ (Heger et al., 2003).*

Calculation. At the dust-cooling temperature $T \approx 200$ K and $n = 10^{12}$ cm^{-3}: $c_s = 7.4 \times (200/8000)^{1/2} = 1.17$ km s^{-1}. $\rho = 1.22 \times 1.67 \times 10^{-27} \times 10^{18} = 2.04 \times 10^{-9}$ kg m^{-3}. $M_{\rm J} \approx 1.0 \times 10^{29}$ kg $\approx 0.05\ M_\odot$. This is confirmed by Omukai et al. (2005), Omukai et al. (2008), and simulations by Chon & Omukai (2020); Chon et al. (2025); Machida et al. (2009).

5.3 Scenario B: Standard DCBH (No Metals + Standard Vacuum)

This is the well-established DCBH pathway, included as a control.

Proposition 5.3 (Standard DCBH Outcome)**.** *A cloud with $Z = 0$, standard vacuum, and a strong LW background ($J_{21} \gtrsim 10^3$) evolves as follows:*

1. *Isothermal collapse at $T \approx 8{,}000$ K (Lyα cooling; H_2 suppressed by LW).*
2. *$M_{\rm J} \sim 7.6 \times 10^4\ M_\odot$ throughout collapse.*
3. *No fragmentation.*
4. *Accretion rate $\dot{M} \sim c_s^3/G \sim 0.3\ M_\odot\,{\rm yr}^{-1}$.*
5. *SMS of $\sim 10^4$–$10^5\ M_\odot$ forms; collapses into DCBH seed.*

Calculation. $\dot{M} = 0.975\, c_s^3/G = 0.975 \times (7.4 \times 10^3)^3/(6.674 \times 10^{-11}) = 5.9 \times 10^{21}\ {\rm kg\,s^{-1}} \approx 0.3\ M_\odot\,{\rm yr}^{-1}$. This matches Inayoshi et al. (2014) and Latif et al. (2013).

Key limitation: This pathway requires a nearby star-forming galaxy providing $J_{21} \gtrsim 10^2$–10^3. The probability of the required "synchronized pair" is low, yielding predicted DCBH number densities of $\sim 10^{-6}$–$10^{-4}\ {\rm Mpc}^{-3}$ (Inayoshi et al., 2020).

5.4 Scenario C: Vacuum-Enhanced DCBH (No Metals + Enhanced Vacuum)

This is the new, conditional scenario. **Everything below is conditioned on P1–P3.**

Definition 5.4 (Hypothetical Vacuum Pressure at $z = 12$)**.** *If P1–P3 hold, the vacuum pressure on the cloud boundary is*

$$\Delta P_{\rm vac}(z) = \rho_{\rm vac}[0]\,(1+z)^3\,c^2\,. \tag{6}$$

At $z = 12$: $\Delta P_{\rm vac}(12) = 2{,}197\ \rho_{\rm vac}[0]\,c^2 \approx 2{,}000\ \rho_{\rm vac}[0]\,c^2$.

The normalization question. The magnitude of $\Delta P_{\rm vac}$ depends entirely on the unknown $\rho_{\rm vac}[0]$. We parametrize the results in terms of the dimensionless ratio

$$\eta(z) \equiv \frac{\Delta P_{\rm vac}(z)}{P_{\rm cloud}} = \frac{\rho_{\rm vac}[0]\,(1+z)^3\,c^2}{P_{\rm cloud}}\,, \tag{7}$$

where $P_{\rm cloud} = 1.1 \times 10^{-9}$ Pa is the cloud's thermal pressure from Eq. (4). At $z = 12$: $\eta(12) \approx 2{,}000\ \rho_{\rm vac}[0]\,c^2/P_{\rm cloud}$. The redshift dependence of $\eta(z)$ is central to the self-termination argument (Section 7): as the universe expands, η decreases as $(1+z)^3$.

Three regimes:

- $\eta \ll 1$: vacuum pressure is negligible. The cloud evolves as in Scenario B (standard DCBH).
- $\eta \sim 0.1$–1: vacuum pressure is a significant perturbation. It supplements gravity, deepens the potential well, and may modestly accelerate collapse.

- $\eta \gg 1$: vacuum pressure dominates. The quasi-static Bonnor–Ebert framework breaks down; the cloud undergoes pressure-driven implosion on a timescale shorter than the free-fall time. This regime would require a fully dynamical treatment beyond the scope of this paper.

For the illustrative value $\rho_{\rm vac}[0] = \rho_\Lambda^{\rm obs} \approx 5.9 \times 10^{-27}\ {\rm kg\,m^{-3}}$:

$$\Delta P_{\rm vac}(12) \approx 2{,}000 \times 5.9 \times 10^{-27} \times (3 \times 10^8)^2 = 1.1 \times 10^{-6}\ {\rm Pa}\,, \tag{8}$$

giving $\eta \approx 10^3$. This places the system firmly in the $\eta \gg 1$ regime, where vacuum pressure overwhelms thermal pressure and the Bonnor–Ebert framework is inapplicable in its standard form. This is an important result: *if* $\rho_{\rm vac}[0] \sim \rho_\Lambda^{\rm obs}$, the vacuum pressure is not a gentle perturbation—it is an overwhelming compression that would require dynamical simulation to model correctly.

For the vacuum pressure to act as a *modest* enhancement ($\eta \sim 0.1$–1), the present-day vacuum energy density would need to be

$$\rho_{\rm vac}[0] \sim \frac{P_{\rm cloud}}{2{,}000\,c^2} \sim \frac{1.1 \times 10^{-9}}{2{,}000 \times 9 \times 10^{16}} \sim 6 \times 10^{-30}\ {\rm kg\,m^{-3}}\,, \tag{9}$$

which is $\sim 10^{-3}\,\rho_\Lambda^{\rm obs}$—far below the observed dark energy density.

The honest conclusion: Either (a) $\rho_{\rm vac}[0]$ is far smaller than $\rho_\Lambda^{\rm obs}$ and the effect is a gentle perturbation within the Bonnor–Ebert framework; (b) $\rho_{\rm vac}[0] \sim \rho_\Lambda^{\rm obs}$ and the effect is overwhelming, requiring dynamical simulation; or (c) the pressure mechanism (P3) is far less efficient than a simple energy-density contrast would suggest. All three possibilities are open. The paper proceeds with parametric results expressed in terms of η.

Confrontation with the companion framework's own prediction. The companion papers (Kriger, 2026c) propose that dark matter is gravitationally bound vacuum energy, requiring $\rho_{\rm vac}[0] \sim 4.5 \times 10^{-24}\ {\rm kg\,m^{-3}} \approx 800\,\rho_\Lambda^{\rm obs}$. At $z = 12$, this gives $\eta \approx 800 \times 10^3 \approx 10^6$. We state this plainly: *the companion framework's own predicted value of* $\rho_{\rm vac}[0]$ *places the system six orders of magnitude above the regime where the Bonnor–Ebert analysis presented in this paper is valid.* At $\eta \sim 10^6$, the vacuum pressure exceeds the cloud's thermal pressure by a factor of one million, and the cloud would undergo pressure-driven implosion on a timescale of $t_{\rm ff}/(10^6)^{1/2} \sim 1.5$ yr—effectively instantaneous compared with any astrophysical process.

This means one of the following must be true:

(a) The pressure mechanism (P3) is far less efficient than a direct energy-density

contrast suggests. Perhaps the vacuum modification inside a diffuse cloud is not $\sim 100\%$ suppression (as assumed by $\Delta P_{\rm vac} \sim \rho_{\rm vac}\, c^2$) but a fractional suppression of $\sim 10^{-6}$ or less, yielding a net pressure far below $\rho_{\rm vac}\, c^2$. This would bring η into the tractable range but requires a specific model of the mode-spectrum modification.

(b) The spatial scale over which the vacuum transitions from "suppressed" to "unsuppressed" is much larger than the cloud radius, producing a gradient that is too shallow to compress the cloud effectively.

(c) The companion framework's value of $\rho_{\rm vac}[0]$ is wrong, and the actual vacuum energy density is far smaller.

Possibility (a) is the most physically plausible and has an established parallel: the Casimir force between plates at separation d is not $\sim \rho_{\rm vac}\, c^2\, d^2$ (which would be enormous) but is suppressed by $\sim (\hbar c/d^4)$ factors that reflect the specific mode-spectrum modification. The actual vacuum pressure at cloud boundaries may be similarly suppressed relative to the naive estimate $\rho_{\rm vac}\, c^2$. Determining the suppression factor requires a full QFT-in-curved-spacetime calculation that has not been performed.

This is a fundamental limitation of the present paper. We can parametrize results in terms of η, but we cannot determine η from the premises alone. The paper's quantitative Bonnor–Ebert results apply only in the $\eta \sim 0.1$–10 regime. Whether the actual physical system falls in this regime is unknown.

Proposition 5.5 (Modified Bonnor–Ebert Mass (Conditional on P1–P3))**.** *If vacuum pressure $\Delta P_{\rm vac}$ supplements the confining pressure, the Bonnor–Ebert critical mass is*

$$M_{\rm BE}^{\rm mod} = 1.18\, \frac{c_s^4}{G^{3/2}\,(P_{\rm thermal} + \Delta P_{\rm vac})^{1/2}}\,, \tag{10}$$

reduced from the standard value by a factor $(1+\eta)^{-1/2}$.

Calculation. $M_{\rm BE}^{\rm mod}/M_{\rm BE}^{\rm standard} = (1+\eta)^{-1/2}$. For $\eta = 0.5$: reduction by 18%. For $\eta = 1$: reduction by 29%. For $\eta = 10$: reduction by 70%.

Proposition 5.6 (H_2 Formation vs. Compression Timescale (Conditional on P1–P3))**.** *The LW requirement can be relaxed if the compression timescale is shorter than the H_2 formation timescale, preventing H_2 from accumulating sufficiently to cool the gas below* $\sim 8{,}000$ K.

Timescale estimate. The H_2 formation timescale in primordial gas at $n \sim 10^4$ cm^{-3}

and $T \sim 8{,}000$ K is (Inayoshi et al., 2020):

$$t_{\mathrm{H}_2} \sim \frac{1}{k_{\mathrm{H}^-}\, n_e\, n_H} \sim 10^5\text{–}10^6 \text{ yr}\,, \tag{11}$$

where k_{H^-} is the H^- route rate coefficient and $n_e/n_H \sim 10^{-4}$ is the residual electron fraction. The standard free-fall time at this density is $t_{\mathrm{ff}} \approx 1.5$ Myr (Eq. 5).

If vacuum pressure reduces the effective compression time by a factor $(1+\eta)^{1/2}$, then for $\eta \sim 1$: $t_{\mathrm{compress}} \sim 1$ Myr, comparable to t_{H_2}. For $\eta \sim 10$: $t_{\mathrm{compress}} \sim 0.45$ Myr, shorter than t_{H_2}. In this regime, the gas collapses before H_2 can accumulate to the level needed for significant cooling, even without LW radiation.

This is the physical mechanism by which vacuum pressure could relax the LW requirement: not by destroying H_2, but by compressing the gas faster than H_2 can form.

Counterarguments and Responses

Objection: At higher densities (as the cloud compresses), t_{H_2} decreases because n_e and n_H both increase. The race between compression and H_2 formation is not obviously won by compression.

Response: Correct. The H_2 formation rate scales as n^2, while the compression rate under external pressure scales as $n^{1/2}$ (free-fall). At sufficiently high density, H_2 formation wins. However, what matters is whether H_2 accumulates to a fractional abundance $x_{\mathrm{H}_2} \gtrsim 10^{-4}$ sufficient for significant cooling (Omukai, 2001). The critical question is whether the cloud reaches the density at which atomic cooling becomes the sole effective coolant (the "loitering point" at $n \sim 10^4$ cm^{-3}, $T \sim 8{,}000$ K) before x_{H_2} exceeds the critical threshold. A rigorous answer requires a chemical network coupled to the hydrodynamic simulation—this is identified as the highest-priority future calculation.

Section Result and Implications

Three scenarios have been formally compared using the same initial cloud. Scenarios A and B reproduce well-established results. Scenario C introduces vacuum pressure as a conditional, parametric addition. The results are expressed in terms of $\eta = \Delta P_{\mathrm{vac}}/P_{\mathrm{cloud}}$, making the dependence on the unknown $\rho_{\mathrm{vac}}[0]$ transparent. For $\eta \sim 1$, the effect is a significant perturbation; for $\eta \gg 1$, the Bonnor–Ebert framework breaks down.

6 Empirical and Data-Grounded Illustrations

6.1 Growth Comparison: Salpeter Timescale

This comparison uses only standard accretion physics. The results are independent of P1–P3; they simply show the consequence of different seed masses and formation times.

Proposition 6.1 (Mass Amplification from Earlier, Heavier Seeding)**.** *If Scenario B or C produces a DCBH seed at time t_0 and Scenario A produces a stellar remnant at time $t_0 + \Delta t$, the mass advantage is*

$$\frac{M_{\rm heavy}(t)}{M_{\rm light}(t)} = \frac{M_{\rm seed}^{\rm heavy}}{M_{\rm seed}^{\rm light}} \exp\left(\frac{\Delta t}{t_{\rm Sal}}\right) . \tag{12}$$

Calculation. Direct substitution into $M(t) = M_{\rm seed}\, e^{t/t_{\rm Sal}}$.

Origin of the head start Δt. The head start has two components:

(i) Stellar evolution delay. In Scenario A, star formation must proceed before BH remnants appear: the cloud fragments, protostars form ($\sim 10^5$ yr), massive stars evolve ($\sim$ 3–10 Myr), and supernovae or direct collapses produce remnant BHs. The total delay from cloud collapse to the first $\sim 100\ M_\odot$ BH is $\sim$ 10–15 Myr.

(ii) Prior enrichment delay. Scenario A requires metallicity $Z \gtrsim 10^{-5}\ Z_\odot$, which means the halo must have experienced prior star formation—it is a *second-generation* system. The first generation of stars must have formed, evolved, and enriched the medium to $Z > Z_{\rm cr}$ before Scenario A can begin. Population III stars in minihalos at $z \sim$ 20–30 evolve on timescales of $\sim$ 3–10 Myr, but the enriched ejecta must mix with the surrounding gas and be incorporated into a new collapsing halo, which requires an additional $\sim$ 50–100 Myr (Bromm & Larson, 2004; Inayoshi et al., 2020). Scenarios B and C require *pristine* gas, which is available in first-generation halos that collapse at earlier redshifts.

The total head start of Scenarios B/C over Scenario A is therefore

$$\Delta t_{\rm B/C\,vs.\,A} \approx (50\text{–}100) + (10\text{–}15) \approx 60\text{–}115\ {\rm Myr}\,, \tag{13}$$

with the prior enrichment delay being the dominant component. For the Table, we adopt a conservative estimate of $\Delta t \approx 65$ Myr.

Table 1: Growth comparison for Scenarios A, B, and C. Scenario A forms in a second-generation halo (requiring prior enrichment); B and C form in pristine first-generation halos.

Parameter	Scenario A	Scenario B	Scenario C
Seed mass	100 $M_\odot$	10^5 $M_\odot$	10^5 $M_\odot$
Halo type	2nd generation	1st generation	1st generation
Halo collapse (after BB)	$\sim$ 420 Myr	$\sim$ 340 Myr	$\sim$ 340 Myr
Delay to seed formation	15 Myr	2 Myr	2 Myr
Seed formation (after BB)	435 Myr	342 Myr	342 Myr
Δt vs. Scenario A	—	93 Myr	93 Myr
Seed mass ratio vs. A	—	10^3	10^3
$\exp(\Delta t/t_{\rm Sal})$	—	7.9	7.9
Combined advantage vs. A	—	$\sim$ 8,000$\times$	$\sim$ 8,000$\times$
e-folds to 10^9 $M_\odot$	16.1	9.2	9.2
Time to 10^9 $M_\odot$	725 Myr	414 Myr	414 Myr
LW requirement	N/A	$J_{21} \gtrsim 10^3$	Reduced (P1–P3)
Cosmological abundance	Common	Rare	Common (P1–P3)

Key observation: The growth advantage of Scenarios B and C over Scenario A is identical—it comes from three factors, all standard DCBH physics: (1) the $10^3\times$ heavier seed, (2) the $\sim$ 13 Myr stellar evolution delay, and (3) the $\sim$ 80 Myr prior enrichment delay before Scenario A's halo can even begin to collapse with the required metallicity. The prior enrichment delay—often overlooked in simple comparisons—is the dominant component, contributing $\exp(80/45) \approx 5.9$ of the $7.9\times$ exponential factor. The unique contribution of Scenario C is not faster growth, but *higher abundance*: if vacuum pressure relaxes the LW requirement, more halos can undergo direct collapse, increasing the comoving density of heavy seeds from $\sim 10^{-4}$ Mpc^{-3} (Scenario B) toward $\sim$ 1–10 Mpc^{-3} (the density of pristine atomic-cooling halos at $z \sim 15$).

Counterarguments and Responses

Objection: If Scenarios B and C produce identical seeds, Scenario C adds nothing to the growth calculation. The only claim is about abundance, which is not quantified.

Response: This is precisely correct, and it represents the honest assessment. Scenario C does not make seeds heavier or faster-growing. It makes them *more numerous*—if P1–P3 hold. The abundance gain is not quantified because it requires radiation-hydrodynamic simulations with vacuum pressure that have not been performed.

Objection: The 8,000$\times$ combined advantage includes the enrichment delay, which is a property of Scenario A's requirements (needing metals), not a property of vacuum

pressure.

Response: Correct. The enrichment delay is a feature of any comparison between first-generation (metal-free) and second-generation (metal-enriched) collapse pathways. It applies equally to Scenarios B and C. We include it because a fair comparison between the fragmentation and direct-collapse pathways must account for the different halo generations, but we emphasize that this timing advantage is standard DCBH physics, not a contribution of the vacuum mechanism.

6.2 Comparison with JWST Observations

Starting from a $10^5\ M_\odot$ seed at $z \sim 15$ ($t_{\rm age} \approx 270$ Myr):

$$M(z = 10.1) \approx 10^5 \exp\left(\frac{200}{45}\right) \approx 8 \times 10^6\ M_\odot\,, \tag{14}$$

$$M(z = 8.7) \approx 10^5 \exp\left(\frac{330}{45}\right) \approx 1.5 \times 10^8\ M_\odot\,. \tag{15}$$

These are consistent with Bogdán et al. (2024) ($z = 10.1$) and Maiolino et al. (2024) ($z \approx 8.7$). But this is a property of *all* DCBH scenarios (B and C alike), not specific to the vacuum mechanism.

Section Result and Implications

The $\sim$ 8,000$\times$ mass advantage of DCBH seeds (B or C) over stellar remnants (A)—arising from the $10^3\times$ heavier seed, the stellar evolution delay, and the prior enrichment delay—is standard DCBH physics. The specific contribution of Scenario C is the potential for higher DCBH abundance through LW relaxation—a qualitative prediction that requires simulation to quantify.

7 Discussion

7.1 What Scenario C Adds to the Existing Literature

The standard DCBH literature (Scenarios A and B) is mature: the physics is well understood, the simulations are detailed, and the bottleneck is clearly identified as the LW fine-tuning. Several mechanisms have been proposed to relax this bottleneck, each using only standard physics:

- **Cold turbulent accretion flows** (Wise et al., 2019): At the convergence of strong, cold filamentary accretion flows, turbulence in the halo suppresses star formation and prevents H_2 cooling, enabling massive seed formation without an external LW background. This mechanism is cosmologically rare: it requires a specific halo configuration at the intersection of multiple accretion streams.
- **Baryon streaming motions** (Inayoshi et al., 2020): Relative velocities between baryons and dark matter inherited from the pre-recombination era can suppress H_2 formation by preventing gas from settling into minihalos. This delays star formation, keeping gas pristine until it enters atomic-cooling halos. The effect is modest ($v_{\rm stream} \sim 30\ {\rm km\,s^{-1}}$ at recombination, decaying as $(1+z)$) and patchy.
- **Dynamical heating**: Rapid halo assembly through major mergers can heat the gas above the H_2 cooling threshold, temporarily maintaining isothermal conditions. This is stochastic and depends on the merger history.
- **Super-Eddington accretion** (Inayoshi et al., 2020): Rather than producing heavier seeds, this approach allows lighter seeds ($\sim$ 10–100 $M_\odot$) to grow faster. Radiatively inefficient accretion flows or photon trapping in dense gas envelopes can sustain $\dot{M} \gg \dot{M}_{\rm Edd}$ for limited periods. This relaxes the seed mass requirement but requires specific accretion geometries.

Scenario C proposes a qualitatively different mechanism: external pressure from a denser high-z vacuum. Its distinguishing feature—if P1–P3 hold—is *universality*: it acts on every cloud at a given epoch, regardless of local environment. Cold accretion flows, streaming motions, and dynamical heating are all stochastic, depending on specific halo properties. Vacuum pressure (if it exists) is isotropic and epoch-dependent.

However, the comparison reveals an uncomfortable asymmetry: the standard mechanisms (Wise, streaming, dynamical heating) require only established physics and have been confirmed or constrained by detailed simulations, while Scenario C requires three unproven premises and has not been simulated. The standard mechanisms produce quantitative predictions of DCBH abundance; Scenario C produces a qualitative prediction contingent on unknowns. Until the premises are tested and simulations performed, Scenario C's advantage in universality remains hypothetical.

7.2 Self-Termination

If $\rho_{\rm vac}(z) \propto (1+z)^3$, the vacuum pressure weakens with expansion:

- $z = 12$: $\rho_{\rm vac}/\rho_{\rm vac}[0] \approx 2{,}000$.
- $z = 2$: $\rho_{\rm vac}/\rho_{\rm vac}[0] = 27$.

- $z = 0$: $\rho_{\rm vac}/\rho_{\rm vac}[0] = 1$.

This would explain why massive seed formation was rapid at $z > 10$ and has since ceased.

7.3 Connection to Companion Papers

The companion papers develop the Λ–$\rho_{\rm vac}$ separation framework across several dimensions: the foundational question of vacuum energy and missing mass (Kriger, 2026a); the connection to JWST early galaxy formation and dark matter (Kriger, 2026b); the full reinterpretation of ΛCDM including the three-component galactic mass model, the $\Lambda(\rho_m)$ ansatz, and CMB compatibility (Kriger, 2026c); the parametric model of spatially varying vacuum energy density and inhomogeneous cosmic expansion (Kriger, 2026d); and the observational consequences of temporal resolution limits on cosmological measurement (Kriger, 2026e). The present paper uses one consequence of that framework (enhanced vacuum density at high redshift) to explore a specific astrophysical application. The present paper stands or falls with the companion framework: if $\Lambda = 8\pi G\,\rho_{\rm vac}$, the premises fail and Scenario C reduces to Scenario B.

Section Result and Implications

Scenario C is a conditional prediction embedded in a larger framework. Its unique contribution is the proposal that vacuum pressure can relax the LW bottleneck, increasing DCBH abundance. This prediction is testable by simulation and may be falsifiable by observation.

8 Limitations

1. **P1 (Separation) is unproven.** The identification $\Lambda = 8\pi G\,\rho_{\rm vac}$ has not been confirmed, but neither has its negation.
2. **P2 (Dilution) depends on untested sequestering.** If $\rho_{\rm vac}$ enters the Friedmann equation with $w = 0$ and $\rho_{\rm vac}[0] \sim \rho_\Lambda^{\rm obs}$, it is excluded by CMB, BAO, and SN data. The proposed sequestering requires scale-dependent gravitational coupling (active locally, inactive globally), which differs from the Kaloper & Padilla (2014) mechanism and has no Lagrangian derivation. The sequestering hypothesis has not been tested against Planck 2018, DESI BAO, or Pantheon+ data.
3. **P3 (Pressure mechanism) is the weakest premise.** It is motivated by Casimir analogy but not derived from the stress-energy tensor at cosmological

scales.

4. **The normalization $\rho_{\rm vac}[0]$ is unknown.** All quantitative results are parametric.
5. **No simulations have been performed.** The Bonnor–Ebert and Jeans analyses are approximate.
6. **The LW relaxation is estimated, not computed.** A rigorous answer requires a chemical-hydrodynamic simulation.
7. **The $\eta \gg 1$ regime is not modeled.** If vacuum pressure dominates thermal pressure, the quasi-static framework is invalid. The companion framework's own predicted $\rho_{\rm vac}[0] \sim 800\,\rho_\Lambda^{\rm obs}$ gives $\eta(z{=}12) \sim 10^6$, placing the system far outside the regime where this paper's Bonnor–Ebert analysis applies. The paper's quantitative results are valid only for $\eta \sim 0.1$–10, which requires either $\rho_{\rm vac}[0] \ll \rho_\Lambda^{\rm obs}$ or an efficient suppression of the pressure mechanism relative to the naive $\rho_{\rm vac}\,c^2$ estimate.
8. **The companion papers are archived on Zenodo but not independently peer-reviewed in established journals.** This weakens the evidential basis for P1–P3.

9 Future Directions

1. **Radiation-hydrodynamic simulations with enhanced external pressure.** Embed a parametric external pressure term in ENZO or AREPO and compare collapse outcome with and without it. This tests whether external compression relaxes the LW requirement quantitatively.
2. **CMB MCMC analysis.** Fit a sequestered vacuum component to Planck data. If the sequestering hypothesis fails, P2 is excluded.
3. **Chemical network calculation.** Couple H_2 formation kinetics to a modified collapse timescale and determine the minimum η needed to suppress H_2 below the cooling threshold without LW radiation.
4. **Stress-energy tensor derivation.** Compute $\langle T_{\mu\nu} \rangle_{\rm ren}$ inside a matter overdensity in FRW spacetime and determine whether a pressure gradient at the boundary exists. This would promote P3 from analogy to derivation.
5. **Independent peer review of companion papers.** The companion papers (Kriger, 2026a,b,c,d,e) are archived on Zenodo with DOIs but have not undergone independent peer review in established journals. Submission to journals with established referee processes would strengthen the evidential basis for P1–P3.

10 Conclusions

We have explored the consequences of three conditional premises (P1: $\Lambda \neq 8\pi G\,\rho_{\rm vac}$; P2: $\rho_{\rm vac} \propto (1+z)^3$; P3: vacuum exerts net pressure on matter) for primordial cloud collapse.

Established results (Scenarios A and B): A trace-metallicity cloud fragments into a stellar cluster (Scenario A). A zero-metallicity cloud with a strong LW background collapses monolithically into a DCBH seed (Scenario B). These results are due to Omukai (2001); Omukai et al. (2005, 2008); Bromm & Loeb (2003); Inayoshi et al. (2020) and are not new.

Conditional result (Scenario C): If P1–P3 hold, vacuum pressure provides an additional, isotropic confining mechanism at $z \sim 12$ that may accelerate collapse and suppress H_2 formation, relaxing the LW requirement. This would increase the cosmological abundance of DCBH seeds, potentially resolving the tension between the observed population of early massive black holes and the rarity of standard DCBH formation sites.

What we claim: The conditional chain P1+P2+P3 $\Rightarrow$ enhanced DCBH abundance is internally consistent and leads to testable predictions.

What we do not claim: That P1, P2, or P3 are correct. That vacuum pressure is the explanation for early massive black holes. That this model supersedes the established DCBH literature.

The model is falsifiable: if the sequestering hypothesis is excluded by CMB data, if simulations show external pressure does not relax the LW requirement, or if $\rho_{\rm vac}[0]$ is independently measured and found to be too small, the conditional prediction of Scenario C fails. The value of the exercise lies in mapping out the consequences of a specific set of hypotheses, identifying quantitative tests, and providing a target for future simulation.

Bibliography

Albareti, F. D. & Maroto, A. L. (2014). Vacuum energy as dark matter. *Phys. Rev. D*, 90, 123509.

Begelman, M. C., Volonteri, M. & Rees, M. J. (2006). Formation of supermassive black holes by direct collapse in pre-galactic haloes. *MNRAS*, 370, 289–298.

Birrell, N. D. & Davies, P. C. W. (1982). *Quantum Fields in Curved Space*. Cambridge University Press.

Bogdán, Á. et al. (2024). Evidence for heavy-seed origin of early supermassive black holes from a z ≈ 10 X-ray quasar. *Nature Astronomy*, 8, 126–133.

Bonnor, W. B. (1956). Boyle's law and gravitational instability. *MNRAS*, 116, 351–359.

Boylan-Kolchin, M. (2023). Stress testing ΛCDM with high-redshift galaxy candidates. *Nature Astronomy*, 7, 731–735.

Bromm, V. & Larson, R. B. (2004). The First Stars. *Ann. Rev. Astron. Astrophys.*, 42, 79–118.

Bromm, V. & Loeb, A. (2003). Formation of the First Supermassive Black Holes. *ApJ*, 596, 34–46.

Casimir, H. B. G. (1948). On the attraction between two perfectly conducting plates. *Proc. Kon. Ned. Akad. Wet.*, 51, 793–795.

Carrera, M. & Giulini, D. (2010). Influence of global cosmological expansion on local dynamics and kinematics. *Rev. Mod. Phys.*, 82, 169–208.

Chon, S. & Omukai, K. (2020). Supermassive star formation via super competitive accretion in slightly metal-enriched clouds. *MNRAS*, 494, 2851–2860.

Chon, S., Omukai, K. & Schneider, R. (2025). Formation of supermassive stars and dense star clusters in metal-poor clouds exposed to strong FUV radiation. *MNRAS*, 539, 2561–2578.

Coleman, S. (1988). Why there is nothing rather than something: A theory of the cosmological constant. *Nucl. Phys. B*, 310, 643–668.

Ebert, R. (1955). Über die Verdichtung von H I-Gebieten. *Zeitschrift für Astrophysik*, 37, 217–232.

Heger, A. et al. (2003). How Massive Single Stars End Their Lives. *ApJ*, 591, 288–300.

Hosokawa, T., Omukai, K., Yoshida, N. & Yorke, H. W. (2011). Protostellar Feedback Halts the Growth of the First Stars in the Universe. *Science*, 334, 1250–1253.

Hosokawa, T. et al. (2013). Formation of Massive Primordial Stars: Intermittent UV Feedback with Episodic Mass Accretion. *ApJ*, 778, 178.

Inayoshi, K., Omukai, K. & Tasker, E. (2014). On the minimum mass of supermassive black holes and their seeds. *MNRAS*, 445, L109–L113.

Inayoshi, K., Visbal, E. & Haiman, Z. (2020). The Assembly of the First Massive Black Holes. *Ann. Rev. Astron. Astrophys.*, 58, 27–97.

Kaloper, N. & Padilla, A. (2014). Sequestering the Standard Model Vacuum Energy. *Phys. Rev. Lett.*, 112, 091304.

Kriger, B. (2026). On Quantum Vacuum Energy, Cosmological Constant and Missing Mass. Zenodo. *Preprint.* doi:10.5281/zenodo.18943014.

Kriger, B. (2026). Known Properties of Vacuum Energy, Dark Matter and JWST Early Galaxy Formation. Zenodo. *Preprint.* doi:10.5281/zenodo.18942968.

Kriger, B. (2026). What If the Vacuum Gravitates? A Reinterpretation of ΛCDM That Might Resolve Its Paradoxes. Information Physics Institute. Zenodo. *Preprint.* doi:10.5281/zenodo.18946637.

Kriger, B. (2026). Matter-Dependent Vacuum Energy Density and Inhomogeneous Cosmic Expansion. Information Physics Institute, Department of Cosmology. Zenodo. *Preprint.* doi:10.5281/zenodo.18896536.

Kriger, B. (2026). The Frozen Universe Illusion: Temporal Resolution as a Fundamental Limit on Cosmological Observation and SETI. Information Physics Institute, Department of Cosmology. Zenodo. *Preprint.* doi:10.5281/zenodo.18901492.

Labbé, I. et al. (2023). A population of red candidate massive galaxies ∼600 Myr after the Big Bang. *Nature*, 616, 266–269.

Lamb, W. E., Jr. & Retherford, R. C. (1947). Fine Structure of the Hydrogen Atom by a Microwave Method. *Phys. Rev.*, 72, 241–243.

Lamoreaux, S. K. (1997). Demonstration of the Casimir Force in the 0.6 to 6 μm Range. *Phys. Rev. Lett.*, 78, 5–8.

Latif, M. A. et al. (2013). Black hole formation in the early Universe. *MNRAS*, 433, 1607–1618.

Lodato, G. & Natarajan, P. (2006). Supermassive black hole formation during the assembly of pre-galactic discs. *MNRAS*, 371, 1813–1823.

Machida, M. N., Omukai, K., Matsumoto, T. & Inutsuka, S. (2009). Binary formation with different metallicities: dependence on initial conditions. *MNRAS*, 399, 1255–1263.

Maiolino, R. et al. (2024). A small and vigorous black hole in the early Universe. *Nature*, 627, 59–63.

Omukai, K. (2001). Primordial Star Formation under Far-Ultraviolet Radiation. *ApJ*, 546, 635–651.

Omukai, K., Tsuribe, T., Schneider, R. & Ferrara, A. (2005). Thermal and Fragmentation Properties of Star-forming Clouds in Low-Metallicity Environments. *ApJ*, 626, 627–643.

Omukai, K., Schneider, R. & Haiman, Z. (2008). Can Supermassive Black Holes Form in Metal-Enriched High-Redshift Protogalaxies? *ApJ*, 686, 801–814.

Salpeter, E. E. (1964). Accretion of Interstellar Matter by Massive Objects. *ApJ*, 140, 796–800.

Shu, F. H. (1977). Self-similar collapse of isothermal spheres and star formation. *ApJ*, 214, 488–497.

Solà Peracaula, J., de Cruz Pérez, J. & Gómez-Valent, A. (2017). Dynamical dark energy vs. Λ = const in light of observations. *Europhys. Lett.*, 121, 39001.

Volonteri, M. (2010). Formation of the First Massive Black Holes. *Astron. Astrophys. Rev.*, 18, 279–315.

Weinberg, S. (1989). The cosmological constant problem. *Rev. Mod. Phys.*, 61, 1–23.

Wise, J. H. et al. (2019). Formation of massive black holes in rapidly growing pre-galactic gas clouds. *Nature*, 566, 85–88.

Zel'dovich, Ya. B. (1967). Cosmological constant and elementary particles. *JETP Letters*, 6, 316–317.

Zier, O., Burkert, A. & Alig, C. (2021). On the Interaction of a Bonnor–Ebert Sphere with a Stellar Wind. *ApJ*, 915, 7.

A Computational Code

```
import numpy as np

# Constants (SI)
G = 6.674e-11       # m^3 kg^-1 s^-2
c = 3e8             # m/s
kB = 1.38e-23       # J/K
mH = 1.67e-27       # kg
Msun = 2e30         # kg
Myr = 3.156e13      # seconds
yr = 3.156e7        # seconds
mu = 1.22           # mean molecular weight (neutral primordial)

def cs(T):
    """Isothermal sound speed [m/s]."""
    return np.sqrt(kB * T / (mu * mH))

def M_Jeans(T, n_cm3):
    """Jeans mass [Msun]. n_cm3 in cm^{-3}."""
    rho = mu * mH * n_cm3 * 1e6  # kg/m^3
    c_s = cs(T)
    MJ = (np.pi**(5./2.) / 6.) * c_s**3 / (G**1.5 * rho**0.5)
    return MJ / Msun

def P_thermal(T, n_cm3):
    """Thermal pressure [Pa]. n_cm3 in cm^{-3}."""
    return n_cm3 * 1e6 * kB * T

def P_vac(z, rho_vac_0=5.9e-27):
    """Vacuum pressure [Pa] at redshift z."""
    return rho_vac_0 * (1 + z)**3 * c**2

def t_ff(n_cm3):
    """Free-fall time [Myr]."""
    rho = mu * mH * n_cm3 * 1e6
```

```
    return np.sqrt(3 * np.pi / (32 * G * rho)) / Myr

def M_BH(M_seed, t_growth_Myr, t_Sal=45):
    """BH mass after Salpeter growth [Msun]."""
    return M_seed * np.exp(t_growth_Myr / t_Sal)

# === Results ===
print("=== Jeans Mass ===")
print(f"  T=8000 K, n=1e4 cm^-3: M_J = {M_Jeans(8000, 1e4):.1e} Msun")
print(f"  T=200 K, n=1e12 cm^-3: M_J = {M_Jeans(200, 1e12):.2e} Msun")

print("\n=== Thermal Pressure ===")
P_cloud = P_thermal(8000, 1e4)
print(f"  P_cloud(T=8000K, n=1e4) = {P_cloud:.2e} Pa")

print("\n=== Vacuum Pressure ===")
for z in [0, 2, 5, 12, 20]:
    Pv = P_vac(z)
    eta = Pv / P_cloud if P_cloud > 0 else 0
    print(f"  z={z:2d}: P_vac = {Pv:.2e} Pa, "
          f"eta = P_vac/P_cloud = {eta:.1e}")

print("\n=== Free-fall Time ===")
print(f"  n=1e4 cm^-3: t_ff = {t_ff(1e4):.1f} Myr")

print("\n=== Salpeter Growth (Table 2, corrected) ===")
# Scenario A: 2nd-gen halo collapse at 420 Myr + 15 Myr delay
# Scenarios B,C: 1st-gen halo collapse at 340 Myr + 2 Myr delay
for label, M_seed, t_seed in [("A", 100, 435),
                              ("B", 1e5, 342),
                              ("C", 1e5, 342)]:
    for z_obs, t_obs in [(10.1, 470), (8.7, 600), (6, 930)]:
        t_grow = max(t_obs - t_seed, 0)
        M = M_BH(M_seed, t_grow)
        print(f"  Scenario {label}, z~{z_obs}: "
              f"M = {M:.1e} Msun (t_grow={t_grow} Myr)")
```

```
print("\n=== Eta parametric (Item 10) ===")
print("rho_vac[0] / rho_Lambda_obs | eta(z=12) | regime")
for factor in [1e-3, 1e-2, 0.1, 1, 10, 100, 800]:
    rho_v0 = factor * 5.9e-27
    Pv = rho_v0 * (1+12)**3 * c**2
    eta_val = Pv / P_cloud
    regime = ("negligible" if eta_val < 0.1 else
              "perturbative" if eta_val < 10 else
              "BE breakdown")
    print(f"  {factor:>10.3f}               | "
          f"{eta_val:>9.1e} | {regime}")

print("\n=== Eta as function of z (for rho_vac[0] = rho_Lambda) ===")
for z in [0, 2, 5, 10, 12, 15, 20]:
    Pv_z = 5.9e-27 * (1+z)**3 * c**2
    eta_z = Pv_z / P_cloud
    print(f"  z={z:2d}: eta = {eta_z:.1e}")
```

Peer Reviews and Revision History

First Round

Reviewer assessment. The reviewer found the paper clearly written and addressing a timely problem, but raised five major concerns: (1) the central hypothesis is underdeveloped and lacks independent support; (2) the vacuum pressure mechanism lacks a rigorous derivation; (3) the original two-scenario comparison conflated metallicity and vacuum effects; (4) quantitative estimates of vacuum pressure vs. gravitational self-pressure were internally inconsistent; (5) the LW relaxation claim was not quantified. Minor concerns included notation inconsistency, misleading "proof" labels, unsubstantiated seed formation timing, and concentrated self-citations. Verdict: major revision.

Revisions made. (1) The paper has been reframed as a conditional exploration. Three explicit premises (P1, P2, P3) are stated in the Introduction and Section 4, each with its status assessed honestly. The paper now states clearly: "We do not claim to prove them. We ask: if all three hold, what happens?" (2) The Casimir analogy limitations are now stated explicitly. P3 is identified as the weakest premise. The paper acknowledges that the pressure mechanism is "motivated but not derived" and identifies the stress-energy tensor derivation as a future direction. (3) A third scenario (B: zero metallicity, standard vacuum) has been added as a control, cleanly isolating the vacuum effect. Table 2 now shows all three scenarios side by side. The unique contribution of Scenario C is identified as abundance enhancement, not growth advantage. (4) The pressure comparison has been corrected. The cloud's *thermal pressure* ($P_{\rm cloud} = 1.1 \times 10^{-9}$ Pa), not its gravitational self-pressure, is now used as the comparison scale. The dimensionless ratio $\eta = \Delta P_{\rm vac}/P_{\rm cloud}$ parametrizes results. Three regimes ($\eta \ll 1$, $\eta \sim 1$, $\eta \gg 1$) are discussed, with honest acknowledgment that for $\rho_{\rm vac}[0] \sim \rho_\Lambda^{\rm obs}$, the system is in the $\eta \gg 1$ regime where the Bonnor–Ebert framework breaks down. (5) The LW relaxation is now estimated via a timescale comparison (H_2 formation time vs. compression time, Proposition 5.6), with explicit acknowledgment that a rigorous answer requires chemical-hydrodynamic simulation. (6) "Proof" labels have been changed to "Calculation." (7) The 40 Myr head start has been replaced with a derived 13 Myr based on the stellar evolution delay in Scenario A. (8) Companion papers are labeled as preprints with Zenodo DOIs provided.

Second Round

Reviewer assessment. The reviewer found the revised manuscript substantially improved, with the conditional framing (P1–P3), three-scenario comparison, and η parametrization praised as significant advances. The pressure inconsistency resolution was called "illuminating" and the honest confrontation with $\eta \gg 1$ described as "a remarkable piece of self-criticism." Five remaining concerns were raised: (1) the narrowed scope may be insufficient for a full PRD article; (2) the companion framework's predicted $\rho_{\rm vac}[0] \sim 800\,\rho_\Lambda^{\rm obs}$ gives $\eta \sim 10^6$, placing the system far outside the regime where the Bonnor–Ebert analysis applies; (3) the sequestering mechanism differs from Kaloper & Padilla (2014) in a critical way—it requires scale-dependent gravitational coupling, which is difficult to achieve under the equivalence principle; (4) the head-start calculation omitted the prior enrichment delay (Scenario A requires a second-generation halo); (5) alternative standard-physics LW-bypass mechanisms deserved fuller comparison. Minor concerns included removing the journal recommendation section, removing empty placeholder sections, providing companion paper availability information, generalizing η as a function of redshift, and adding parametric η values to the code. Verdict: minor revision.

Revisions made. (1) Noted. The paper is structured as a thought experiment with a clear conditional framework; the scope is narrow but the predictions are specific and testable. The author acknowledges that a shorter-format venue (PRD Letter, JCAP Letter) may be more appropriate and defers to editorial judgment. (2) A new subsection in Section 5.4 now confronts the companion framework's $\rho_{\rm vac}[0] \sim 800\,\rho_\Lambda^{\rm obs}$ explicitly, computing $\eta \sim 10^6$ and stating plainly that the Bonnor–Ebert analysis is inapplicable at this value. Three possibilities are discussed: (a) the pressure mechanism (P3) is far less efficient than a naive energy-density contrast suggests, analogous to the Casimir force being suppressed relative to a naive vacuum-energy estimate; (b) the transition scale is too large for effective compression; (c) the companion framework's $\rho_{\rm vac}[0]$ is wrong. (3) Section 4.2 now clarifies that the proposed sequestering is *not* the Kaloper & Padilla mechanism: their mechanism cancels vacuum gravity both locally and globally, while the companion framework requires scale-dependent coupling (active locally, inactive globally). The difficulty of achieving this under the equivalence principle is stated explicitly. The mechanism is motivated by the physical picture that bound systems decouple from the Hubble flow (Carrera & Giulini, 2010), but this is acknowledged as a physical analogy, not a field-theoretic derivation. (4) The head-start calculation now includes the prior enrichment delay ($\sim$ 50–100 Myr) required for Sce-

nario A's second-generation halo. Table 2 reflects the updated timing, with the total head start of $\sim$ 93 Myr and combined advantage of $\sim$ 8,000×. (5) Section 7.1 now provides a structured comparison with four standard LW-bypass mechanisms (cold accretion flows, baryon streaming, dynamical heating, super-Eddington accretion), noting their stochastic character versus Scenario C's hypothetical universality, and acknowledging the uncomfortable asymmetry that the standard mechanisms are simulated while Scenario C is not. (6) The journal recommendation section has been removed (it is a cover-letter matter). (7) Empty placeholder sections removed. (8) Companion paper bibliography entries now include Zenodo DOIs. Two additional companion papers—on matter-dependent vacuum energy density (Kriger, 2026d) and temporal resolution limits on cosmological observation (Kriger, 2026e)—have been added to the reference list. (9) η is now defined as $\eta(z)$, a function of redshift. (10) Appendix code updated with η parametric values.